NUREG/CR-3145
Vol. 10

Geophysical Investigations of the Western Ohio-Indiana Region

Final Report
October 1986 – September 1992

Prepared by
L. Ruff, R. LaForge, R. Thorson, T. Wagner, F. Goudaen

Department of Geological Sciences
The University of Michigan

Prepared for
U.S. Nuclear Regulatory Commission

AVAILABILITY NOTICE

Availability of Reference Materials Cited in NRC Publications

Most documents cited in NRC publications will be available from one of the following sources:

1. The NRC Public Document Room, 2120 L Street, NW., Lower Level, Washington, DC 20555-0001

2. The Superintendent of Documents, U.S. Government Printing Office, Mail Stop SSOP, Washington, DC 20402-9328

3. The National Technical Information Service, Springfield, VA 22161

Although the listing that follows represents the majority of documents cited in NRC publications, it is not intended to be exhaustive.

Referenced documents available for inspection and copying for a fee from the NRC Public Document Room include NRC correspondence and internal NRC memoranda; NRC bulletins, circulars, information notices, inspection and investigation notices; licensee event reports; vendor reports and correspondence; Commission papers; and applicant and licensee documents and correspondence.

The following documents in the NUREG series are available for purchase from the GPO Sales Program: formal NRC staff and contractor reports, NRC-sponsored conference proceedings, international agreement reports, grant publications, and NRC booklets and brochures. Also available are regulatory guides, NRC regulations in the *Code of Federal Regulations*, and *Nuclear Regulatory Commission Issuances*.

Documents available from the National Technical Information Service include NUREG-series reports and technical reports prepared by other Federal agencies and reports prepared by the Atomic Energy Commission, forerunner agency to the Nuclear Regulatory Commission.

Documents available from public and special technical libraries include all open literature items, such as books, journal articles, and transactions. *Federal Register* notices, Federal and State legislation, and congressional reports can usually be obtained from these libraries.

Documents such as theses, dissertations, foreign reports and translations, and non-NRC conference proceedings are available for purchase from the organization sponsoring the publication cited.

Single copies of NRC draft reports are available free, to the extent of supply, upon written request to the Office of Administration, Distribution and Mail Services Section, U.S. Nuclear Regulatory Commission, Washington, DC 20555-0001.

Copies of industry codes and standards used in a substantive manner in the NRC regulatory process are maintained at the NRC Library, 7920 Norfolk Avenue, Bethesda, Maryland, for use by the public. Codes and standards are usually copyrighted and may be purchased from the originating organization or, if they are American National Standards, from the American National Standards Institute, 1430 Broadway, New York, NY 10018.

DISCLAIMER NOTICE

This report was prepared as an account of work sponsored by an agency of the United States Government. Neither the United States Government nor any agency thereof, or any of their employees, makes any warranty, expressed or implied, or assumes any legal liability of responsibility for any third party's use, or the results of such use, of any information, apparatus, product or process disclosed in this report, or represents that its use by such third party would not infringe privately owned rights.

NUREG/CR-3145
Vol. 10

Geophysical Investigations of the Western Ohio-Indiana Region

Final Report
October 1986 – September 1992

Prepared by
L. Ruff, R. LaForge, R. Thorson, T. Wagner, F. Goudaen

Department of Geological Sciences
The University of Michigan

Prepared for
U.S. Nuclear Regulatory Commission

AVAILABILITY NOTICE

Availability of Reference Materials Cited in NRC Publications

Most documents cited in NRC publications will be available from one of the following sources:

1. The NRC Public Document Room, 2120 L Street, NW., Lower Level, Washington, DC 20555-0001

2. The Superintendent of Documents, U.S. Government Printing Office, Mail Stop SSOP, Washington, DC 20402-9328

3. The National Technical Information Service, Springfield, VA 22161

Although the listing that follows represents the majority of documents cited in NRC publications, it is not intended to be exhaustive.

Referenced documents available for inspection and copying for a fee from the NRC Public Document Room include NRC correspondence and internal NRC memoranda; NRC bulletins, circulars, information notices, inspection and investigation notices; licensee event reports; vendor reports and correspondence; Commission papers; and applicant and licensee documents and correspondence.

The following documents in the NUREG series are available for purchase from the GPO Sales Program: formal NRC staff and contractor reports, NRC-sponsored conference proceedings, international agreement reports, grant publications, and NRC booklets and brochures. Also available are regulatory guides, NRC regulations in the *Code of Federal Regulations*, and *Nuclear Regulatory Commission Issuances*.

Documents available from the National Technical Information Service include NUREG-series reports and technical reports prepared by other Federal agencies and reports prepared by the Atomic Energy Commission, forerunner agency to the Nuclear Regulatory Commission.

Documents available from public and special technical libraries include all open literature items, such as books, journal articles, and transactions. *Federal Register* notices, Federal and State legislation, and congressional reports can usually be obtained from these libraries.

Documents such as theses, dissertations, foreign reports and translations, and non-NRC conference proceedings are available for purchase from the organization sponsoring the publication cited.

Single copies of NRC draft reports are available free, to the extent of supply, upon written request to the Office of Administration, Distribution and Mail Services Section, U.S. Nuclear Regulatory Commission, Washington, DC 20555-0001.

Copies of industry codes and standards used in a substantive manner in the NRC regulatory process are maintained at the NRC Library, 7920 Norfolk Avenue, Bethesda, Maryland, for use by the public. Codes and standards are usually copyrighted and may be purchased from the originating organization or, if they are American National Standards, from the American National Standards Institute, 1430 Broadway, New York, NY 10018.

NUREG/CR-3145
Vol. 10
RA

Geophysical Investigations of the Western Ohio-Indiana Region

Final Report
October 1986 – September 1992

Manuscript Completed: December 1993
Date Published: January 1994

Prepared by
L. Ruff, R. LaForge, R. Thorson, T. Wagner, F. Goudaen

Department of Geological Sciences
The University of Michigan
Ann Arbor, MI 48109

Prepared for
Division of Engineering
Office of Nuclear Regulatory Research
U.S. Nuclear Regulatory Commission
Washington, DC 20555–0001
NRC FIN D1695
Under Contract No. NRC–04–86–122

Previous Reports

Four major reports concerning this investigation were published under previous contract NRC 04-76-192:

Mauk, F.J., D. Coupland, D. Christensen, J. Kimball, P. Ford, 1979, Geophysical Investigations of the Anna, Ohio, Earthquake Zone: Annual Progress Report for the U. S. Nuclear Regulatory Commission, July 1978-July 1979, NUREG/CR-1065.
Mauk, F.J., S.G. Henry, D.H. Christensen, J. Sauber, C. Lanford, W. Meerschaert, J.K. Kimball, 1980, Geophysical Investigations of the Anna, Ohio, Earthquake Zone: Annual Progress Report for the U. S. Nuclear Regulatory Commission, July 1979-1980, NUREG/CR-1649.
Mauk, F.J., D.H. Christensen, 1980, A Probabilistic Evaluation of Earthquake Detection and Location Capability for Illinois, Indiana, Kentucky, Ohio and West Virginia: Report for the U. S. Nuclear Regulatory Commission, September 1980, NUREG/CR-1648.
Jackson, P.L., D.H. Christensen, F.J. Mauk, 1982, Geophysical Investigations of the Western Ohio - Indiana Region: Final Report for the U. S. Nuclear Regulatory Commission, November 1975-September 1981, NUREG/CR-2484.

Five reports were published under contract NRC-04-81-195-04:

Christensen, D.H., M.G. Wiedenbeck, P.L. Jackson, 1983, Geophysical Investigations of the Western Ohio - Indiana Region: Annual Report for the U. S. Nuclear Regulatory Commission, October 1981-September 1982, NUREG/CR-3145, Vol.1.
Pollack, H.N., D.H. Christensen, 1984, Geophysical Investigations of the Western Ohio - Indiana Region: Annual Report for the U. S. Nuclear Regulatory Commission, October 1982-September 1983, NUREG/CR-3145, Vol. 2.
Pollack, H.N., D.H. Christensen, 1985, Geophysical Investigations of the Western Ohio - Indiana Region: Annual Report for the U. S. Nuclear Regulatory Commission, October 1983-September 1984, NUREG/CR-3145, Vol. 3.
Pollack, H.N., D.H. Christensen, J. Welc, 1986, Geophysical Investigations of the Western Ohio - Indiana Region: Annual Report for the U. S. Nuclear Regulatory Commission, October 1984-September 1985, NUREG/CR-3145, Vol. 4.
Christensen, D.H., H.N. Pollack, T. Lay, S.Y. Schwartz, 1987, Geophysical Investigations of the Western Ohio - Indiana Region: Final Report for the U. S. Nuclear Regulatory Commission, October 1981-September 1986, NUREG/CR-3145, Vol. 5.

Four reports were published under contract NRC-04-86-122:

Schwartz, S.Y., D.H. Christensen, T. Lay, B.P. Cohee, 1988, Geophysical Investigations of the Western Ohio-Indiana Region: Annual Report for the U.S. Nuclear Regulatory Commission, October 1986-September 1987, NUREG/CR-3145, Vol. 6.
Schwartz, S.Y., T. Lay, C.J. Young, 1988, Geophysical Investigations of the Western Ohio-Indiana Region: Annual Report for the U.S. Nuclear Regulatory Commission, October 1987-September 1988, NUREG/CR-3145, Vol. 7.
Young, C.J., T. Lay, J. Jacobson, 1990, Geophysical Investigations of the Western Ohio-Indiana Region: Annual Report for the U.S. Nuclear Regulatory Commission, October 1988-September 1989, NUREG/CR-3145, Vol. 8.
J. Meert, L. Ruff, R. LaForge, C. Young, Geophysical Investigations of the Western Ohio-Indiana Region: Annual Report for the U.S. Nuclear Regulatory Commission, October 1989-September 1990, NUREG/CR-3145, Vol. 9.

Abstract

Earthquake activity in the Western Ohio - Indiana region has been monitored with a short-period vertical-component seismograph network consisting of nine stations located in west-central Ohio and four stations located in Indiana. A total of six local and regional earthquakes have been recorded during the past two year (October 1990 to September 1992), with magnitudes ranging from 0.6 to 5.0. A total of 36 local and regional earthquakes have been detected and recorded in the past six-year period (October 1986 to September 1992). Overall, a total of 78 local and regional earthquakes have been recorded since the network went into operation in 1977. There was a peak in seismicity in 1986, including the July 12, 1986 St. Marys event (mb=4.5). This activity was followed by an anomalously low level of seismicity for about two years. Then, the seismicity returned to a more typical level of activity. The most unusual feature of the seismicity in the past year is the occurrence of three earthquakes in Indiana. The locations of these felt earthquakes are scattered across central Indiana; an area that had been aseismic. This is a very surprising result, and this activity should be monitored in the future.

This final report also includes a comprehensive analysis of the arrival time data accumulated over the past 14 years. The most important conclusion is that the crustal velocity structure is different between the Anna region and central Indiana. Furthermore, the Anna region crustal structure is "slower" than the average mid-continent crustal structure; one implication of this result is that the proposed Keewenawan rift in the Anna region must have a different structure than found in other Keewenawan rifts in the mid-continent.

Summary

During the period from October, 1989 through September, 1990 the Western Ohio - Indiana network has been operational an average of 69% of the time. This represents a 12% decrease from the past annual period, primarily due to aging of equipment in the field and telephone line transmission problems.

Four local and two near-regional earthquakes have been well recorded during the past two years (October 1990 to September 1992). The two regional events occurred in previously-recognized seismic area. Three of the four local events were located across central Indiana, and the fourth event is close to the Ohio-Indiana border. This pattern of occurrence is quite unusual. An important question is whether this change in local seismicity is just a one-year aberration, or does it represent the beginning of a new phase of activity in Indiana?

The two largest earthquakes in Ohio over the last two decades are the July 12, 1986 St. Marys earthquake in the Anna zone and the January 31, 1986 Perry event in the Cleveland area. Focal mechanisms for these two events are essentially identical strike-slip mechanisms with an east-northeast striking compressional axis. There is weak evidence that focal mechanisms of Indiana earthquakes might be different. Fourteen years of seismic monitoring at Anna has found: 34 events in western and central Ohio; 5 events in northeastern Ohio; 1 event in Michigan; and 7 events in Indiana. Of the 34 events in western and central Ohio, 21 are within the Anna sub-network. The most notable spatial clustering of events is the cluster of 12 events just five kilometers southeast of station AN1. Hypocentral depth analysis of these earthquakes shows that they could all be at the same depth of 5 km below the top of the Pg layer, or 6 km below the surface (top of the Paleozoic rocks). Since the Paleozoic sedimentary section is less than 1 km thick in the Anna zone, these earthquakes are clearly within the pre-Cambrian basement.

P wave arrival times clearly show that crustal structure is different beneath the Anna and Indiana sub-networks. It appears that a "typical" mid-continent crustal model is allowed by the Indiana sub-network data, but the Anna zone has anomalous crustal structure. However, if we allow the maximum thickness of a P* layer (velocity of 6.63 km/s) beneath the Anna zone; then the Anna Pg layer is 20 km thick versus 15 km for "typical" mid-continent, and the P* layer is 24 km thick versus 26.5 km for "typical" mid-continent, and the total Anna crustal thickness is 43.3 km versus 41.5 km for "typical" mid-continent. The Anna crustal thickness is still less than values found in the Lake Superior region. Vertical travel times can be calculated for the various crustal structures. The difference between Anna and Indiana vertical travel times is roughly consistent with the teleseismic observations. The crustal structure determined for the Anna zone implies that the "felsic" rocks are anomalously thick compared to the "typical" mid-continent velocity model.

Table of Contents

Figures

Tables

PREFACE

This is the fifth annual and final report (Parts I and II) of the special additonal year (Oct. 1991 to Sept. 1992) under the contract NRC-04-86-122, a continuation of the effort funded under contracts NRC-04-76-192 and NRC-04-81-195-04. The contract includes maintenance and systematic processing of a nine station seismic array in Western Ohio initiated in 1976, and the subsequent expansion in 1981 to include a four-station array in Indiana. Portions of this report have been taken directly from earlier reports for completeness. We wish to express our appreciation to Scott Baird for keeping a wide range of instruments and computer peripherals in working condition.

1. Introduction

The mid-continent of North America, between the Appalachian and Rocky Mountains, has not been the site of significant plate boundary processes since the Mesozoic. However, large earthquakes have occurred in several locations. The New Madrid zone is the site of the largest earthquakes, but several other places also have a history of significant earthquakes. A seismicity map of larger earthquakes shows several distinct clusters of earthquakes that trend northeast from the New Madrid zone to the St. Lawrence River zone in Canada. The first distinct cluster of significant earthquakes northeast of the New Madrid region is known as the Anna, Ohio seismic zone (see Figure 1, which shows all the known earthquakes). The history of felt earthquakes in the Anna zone dates back to the late 1700's (Bradley & Bennett, 1965). A revised catalog of Anna earthquakes (Nuttli & Herrman, 1978; Nuttli & Brill, 1981) indicates that several events of magnitude 5 or so have occurred in the Anna zone. In addition, many other earthquakes have occurred in scattered locations in western and northern Ohio. Three large earthquakes occurred in the Anna seismic zone in the 1930's: 20 Sept 1931, 2 Mar 1937, and 9 Mar 1937. The 9 Mar 1937 earthquake and an event in 18 June 1875 are thought to be the two largest events in the Anna zone. Isoseismal maps for the two events of March 1937 show a maximum intensity of VII, and shaking with intensity IV extends from Cincinnati and Indianapolis to Toledo and Detroit (Figure 2). The possibility of future occurrence of large earthquakes in and around the Anna zone presents significant earthquake hazards to millions of people.

A program to monitor the seismicity in the Anna zone and the surrounding region of Ohio, Indiana, and Michigan began in 1977. The catalog of local events detected and located includes 33 earthquakes within the Anna zone, plus 47 other events in the surrounding region. Many other regional earthquakes have occurred to the south in Kentucky, to the southwest in Illinois and the New Madrid zone, and further to the northeast beyond Lake Erie. The two largest earthquakes that have occurred in the Ohio-Indiana-Michigan region since 1977 are the 31 Jan 1986 Leroy earthquake (in the Cleveland area) with m_b of 5.0, and the 12 July 1986 St. Marys earthquake (within the Anna seismic zone) with m_b of 4.5 (see Schwartz & Christensen, 1987). Isoseismal maps for these two earthquakes are shown in Figure 3. The maximum intensity is VI for both earthquakes, but the region of intensity IV shaking extended from Buffalo, New York to the Detroit metropolitan area for the Leroy earthquake, while the intensity IV shaking was mostly confined to western Ohio for the St. Marys earthquake. The Leroy and St. Marys earthquakes are recent reminders that damaging earthquakes occur in this region.

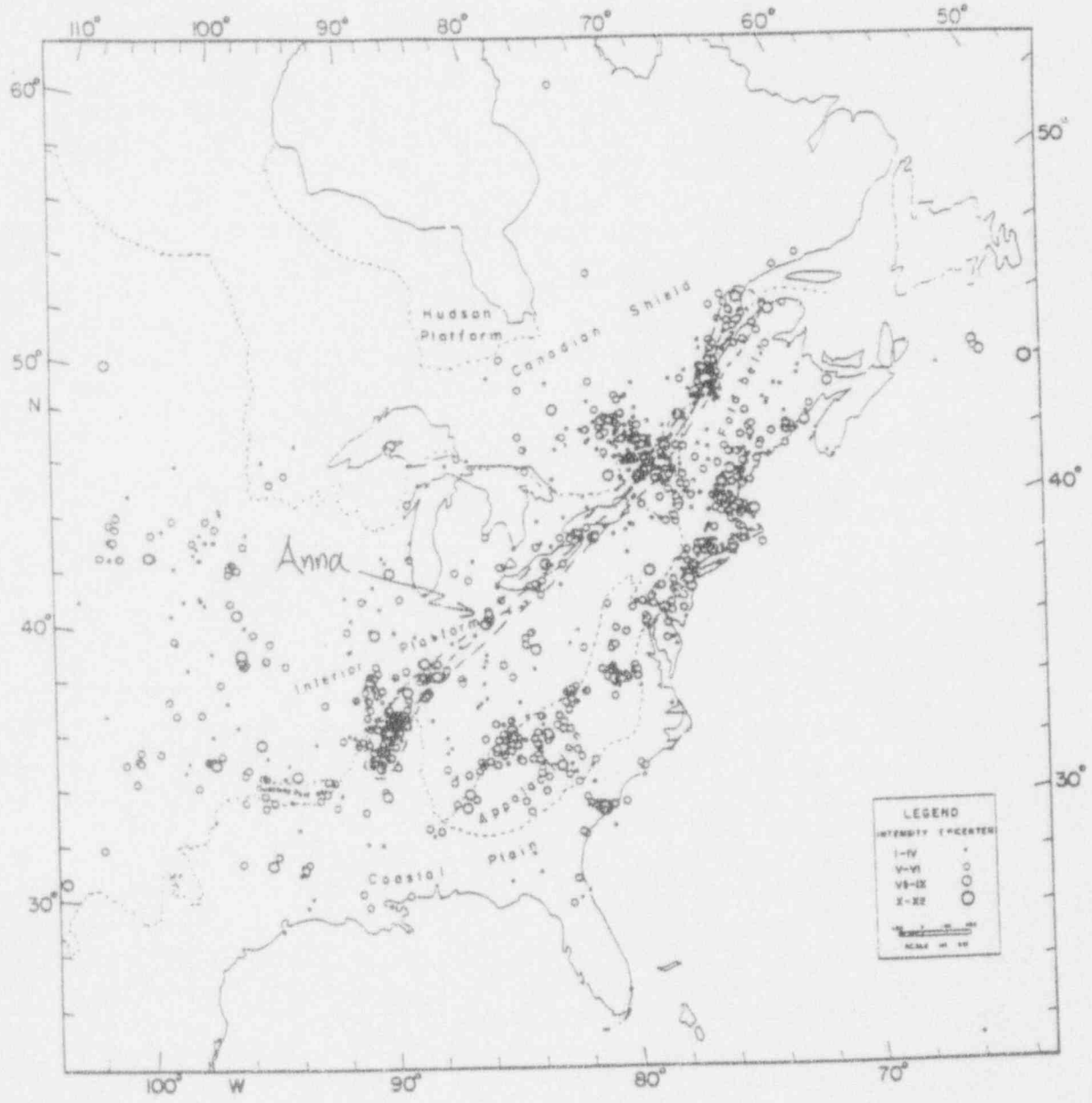

Figure 1. Map of seismicity in the eastern United States.

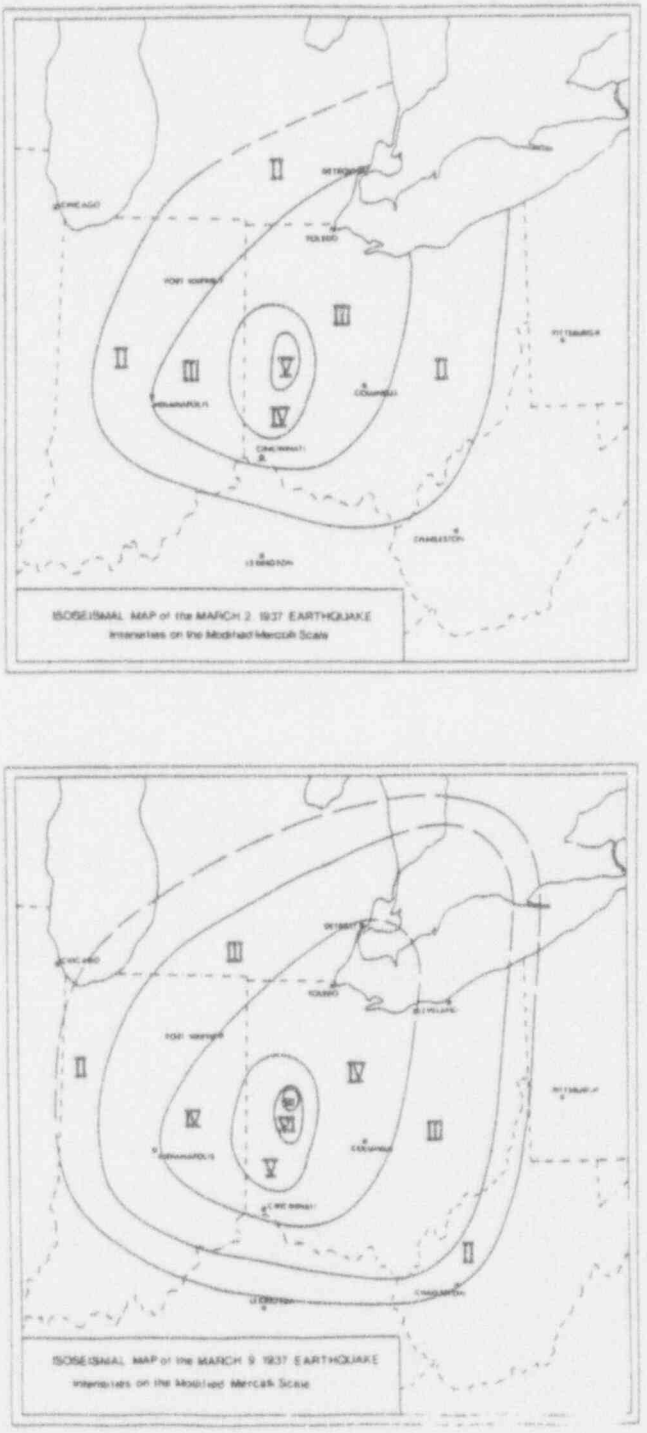

Figure 2. Isoseismal maps for the March 2, 1937 (upper) and the March 9, 1937 (lower) earthquakes.

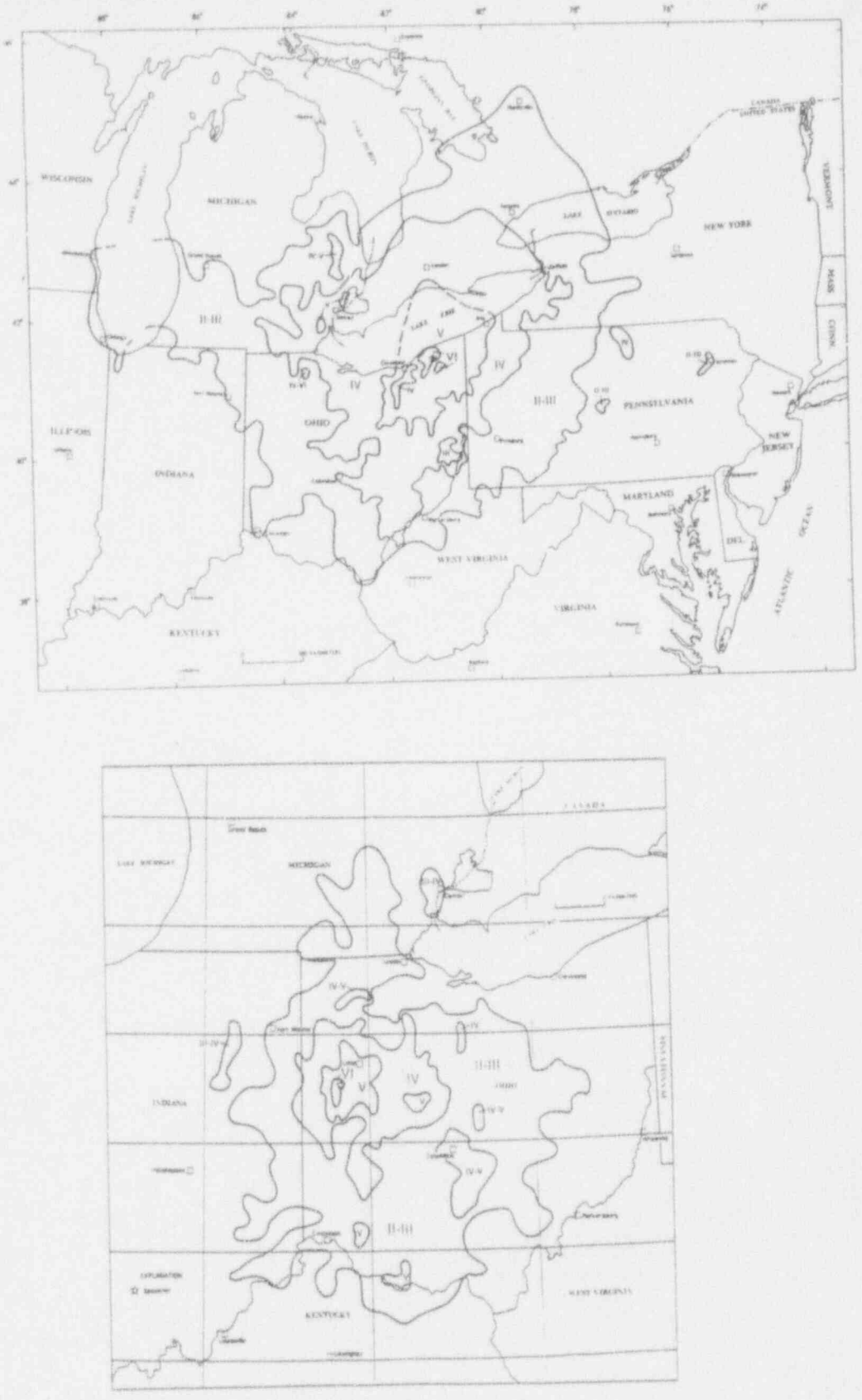

Figure 3. Isoseismal maps for the January 31, 1986 (upper) and July 12, 1986 (lower) Ohio earthquakes.

1.1 Regional Geology & Structure

Mid-continent earthquakes represent a scientific challenge. We cannot call upon plate boundary motions as the direct cause of mid-continent seismicity. Thus, why mid-continent earthquakes occur where they do, and do not, is a difficult question to answer. This question can be approached from a continent-wide perspective, as in Sykes, 1978, or by focussing on the immediate structural control of seismicity. Many years of comprehensive research in the New Madrid zone show that the seismicity may be controlled by a reactivated graben at the northern end of the Mississippi embayment structural feature (Braile et al., 1982). Thus, one aspect of our study of the Anna seismic zone is to investigate any possible association between the earthquakes and crustal structural features. The regional geology in and around the Anna seismic zone can be characterized by a variable thickness of Paleozoic sediments on a pre-Cambrian basement, and mostly covered by a thin veneer of glacial deposits. There are several significant features in the pre-Cambrian basement. The following brief description of the regional geology and structural features will start at the surface in the Anna seismic zone and proceed down and out.

The topography throughout western Ohio is best characterized as flat and level with small-scale topographic relief associated with glacial deposits. The elevation of the seismic stations varies between 226 and 346 m. Thickness of the glacial deposits varies between just a few meters to 150 meters, and they lie upon Paleozoic sedimentary rocks. If we remove the glacial deposits, the topographic features are mostly related to the pre-glacial Teays River, which was about the same size as the present-day Ohio River. The main channel of the Teays River trends SE-NW (Figure 4), and the Anna-Champaign Fault may align with this trend (Figure 5a). Three faults have been postulated to occur in the Anna region, though none have a clear surface expression. Various interpretations of basement faulting are described in several reports and abstracts (Stead (1975), Kiefer & Trapp (1975), McQuire (1975), and Thompson et al., 1976) and are summarized in the report by Christensen et al. (1986). The best studied fault is the Anna-Champaign fault (Figure 5a) which shows up to 30 m of vertical offset from gravity and proprietary seismic reflection surveys. The Logan-Harding fault is inferred from seismic and well-log data, and it is postulated to be the extension of the N-S trending Bowling Green fault which is exposed to the north (Stead, 1975).The postulated Auglaize fault is based just on well-log data. Figure 5 also shows prominent lineaments found in LANDSAT images by Jackson et al., 1981. It is curious that these lineaments seen in the present-day surface approximately coincide with the inferred faults in the underlying Paleozoic rocks.

Thickness of the Paleozoic rock section is about 700 m in the Anna seismic zone and increases greatly in the Michigan basin to the north and the Appalachian Basin to the east. As seen in Figure 5b, the Anna seismic zone is near the center of the Indiana-Ohio Platform. These structures are defined by the top of the pre-Cambrian surface. Three

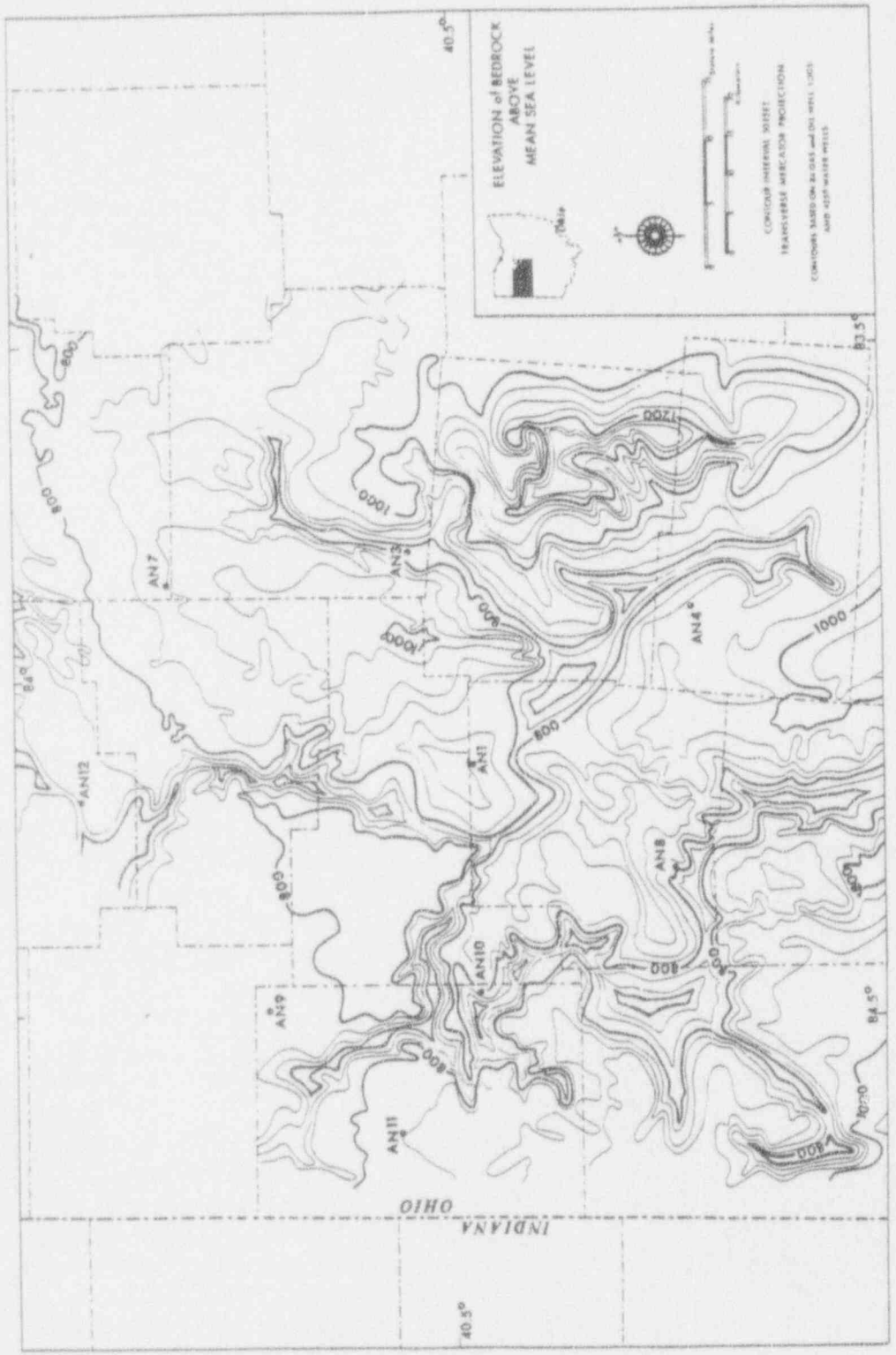

Figure 4. Contours of bedrock elevation beneath the Anna region. The ancient Teays River channel runs from southeast to northwest through the Anna region (after Christensen et al. 1986).

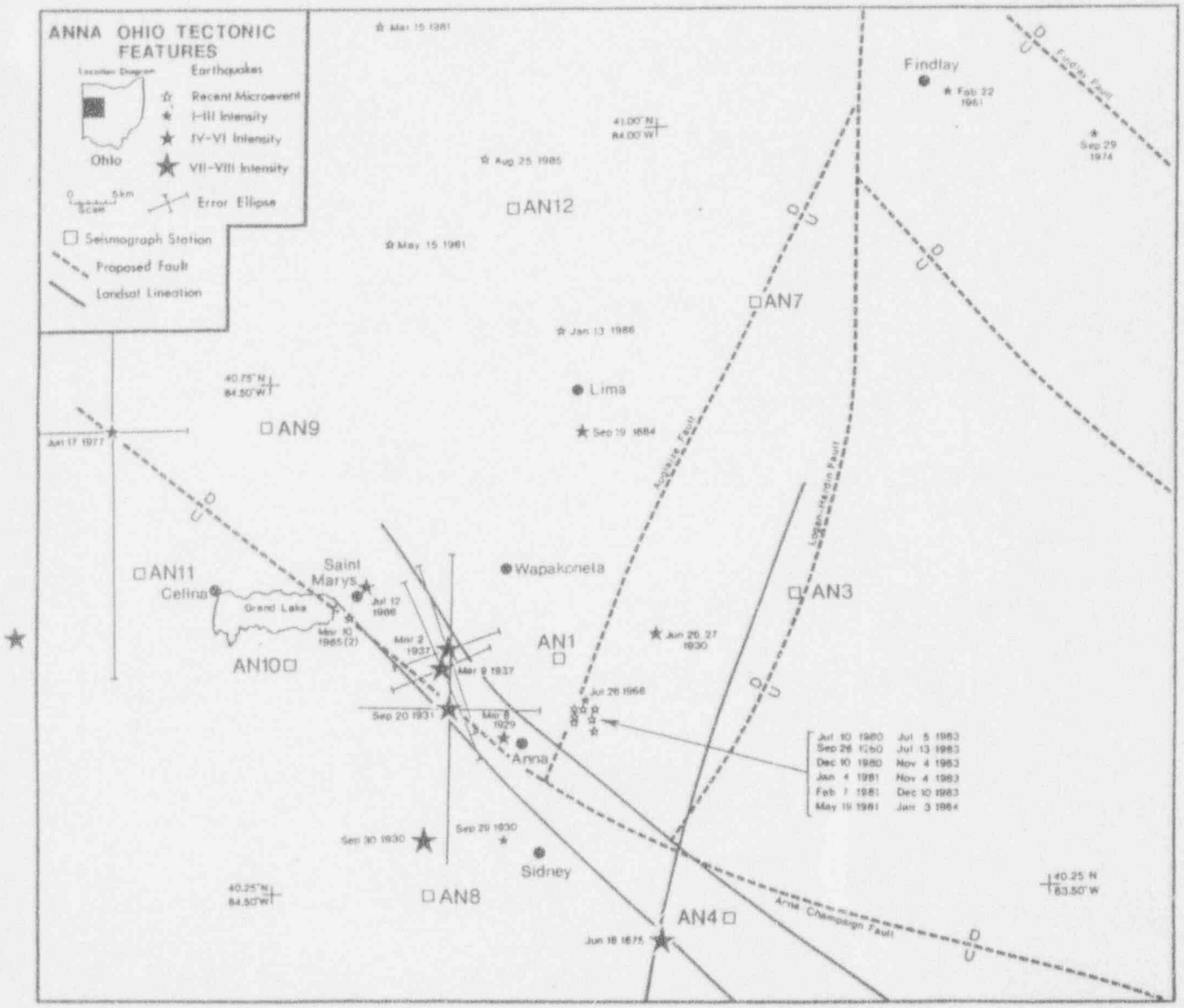

Figure 5a. Proposed faults and structural lineaments in the Anna seismic region, with locations of historical earthquakes and recent microseismicity (after Christensen et al., 1986).

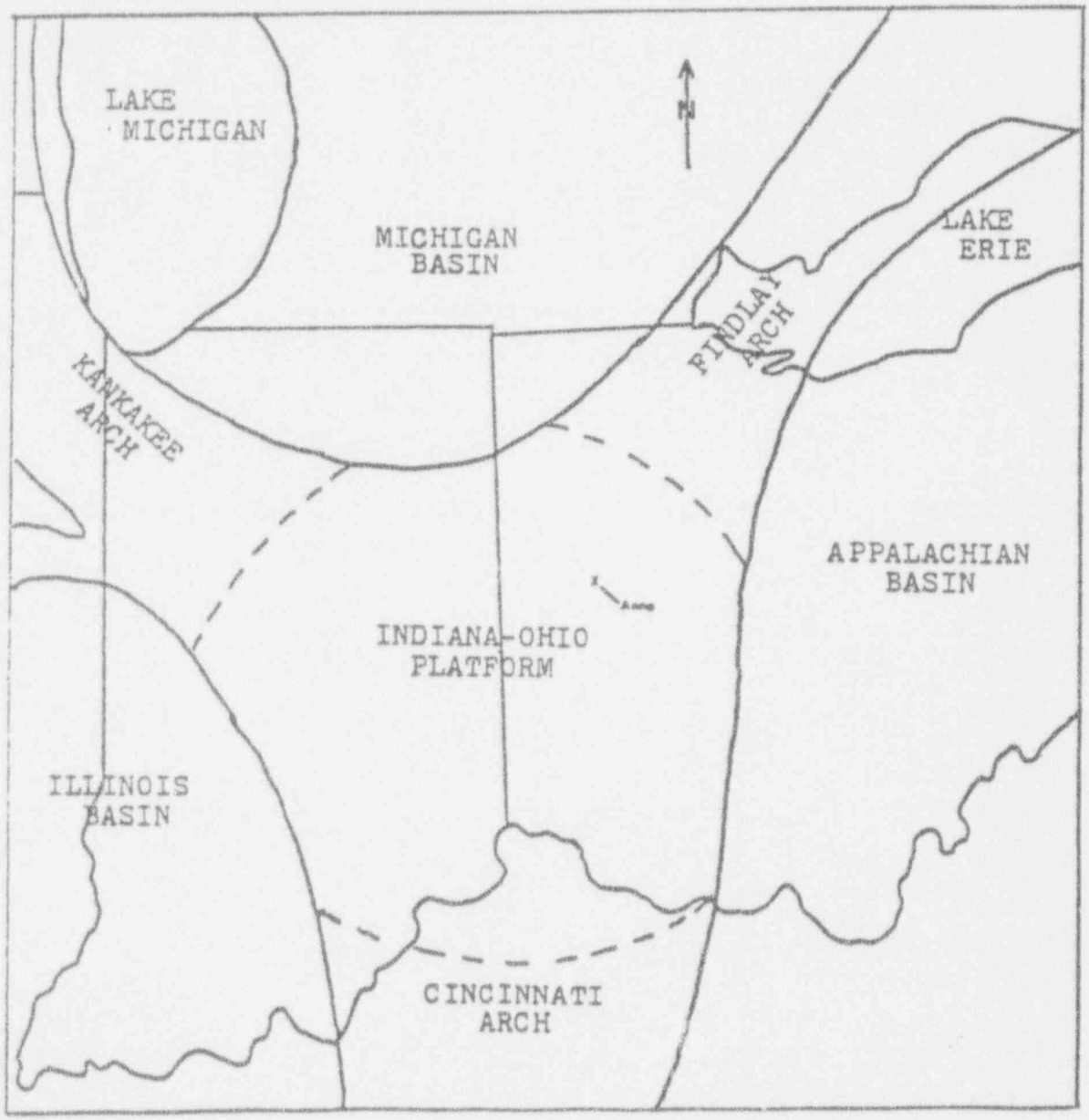

Figure 5b. The basin and arch structure in the Ohio-Indiana-Michigan region. The Anna seismic zone is located on a broad basement high.

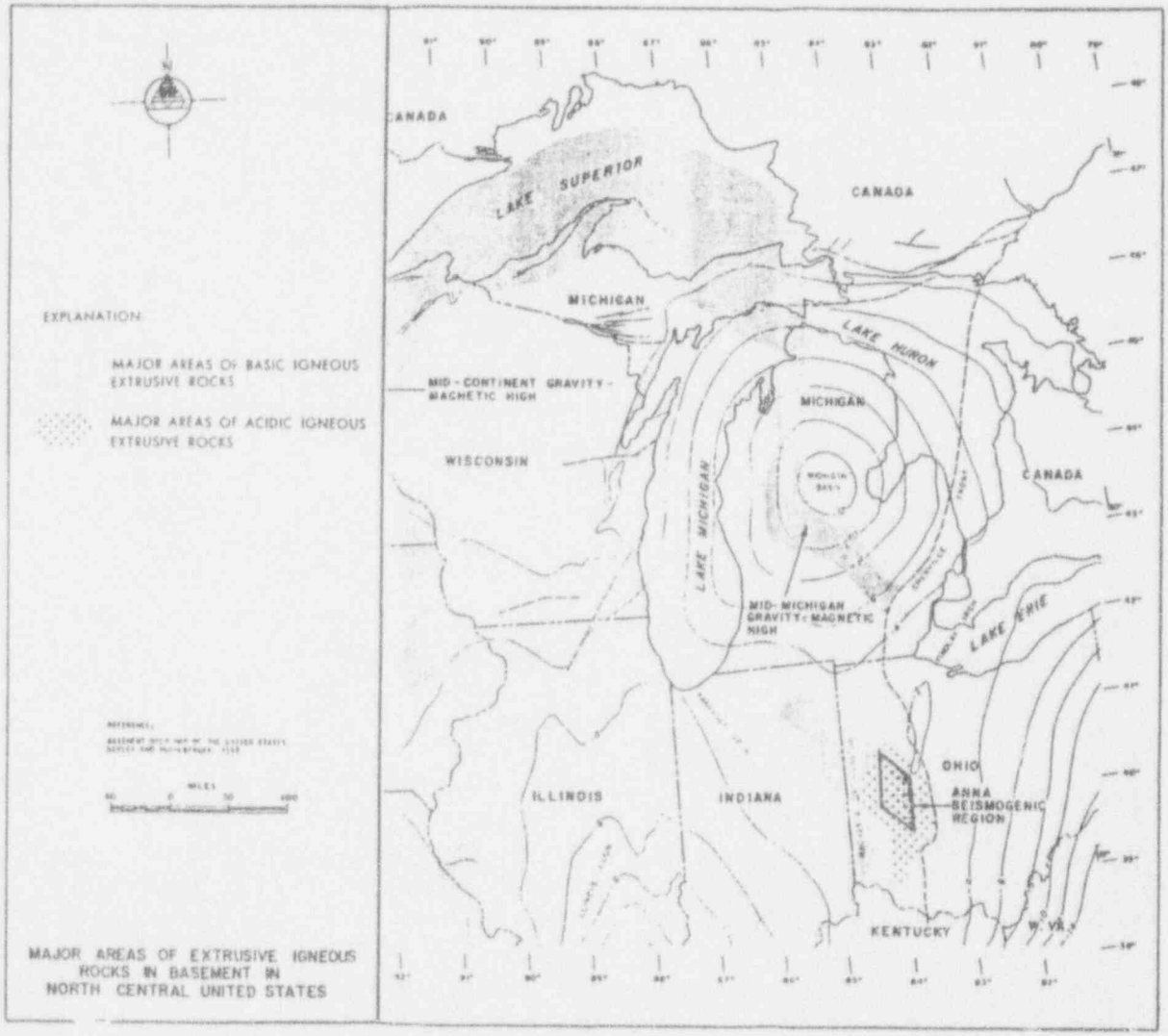

Figure 5c. Major structures in the crust in the north central United States (from Bayley and Muehlberger, 1968). The Grenville Front runs just to the east of the Anna seismogenic zone.

arches radiate away from the Indiana-Ohio platform to separate the Michigan, Appalachian, and Illinois Basins. While the formation of the Appalachian Basin can be related to the tectonics of the Appalachian orogeny, the formation of basins such as the Michigan and Illinois is more mysterious and contentious.

Since the Paleozoic sediments are only 700 km thick in the Anna seismic zone, it is likely that the seismicity is occurring within the pre-Cambrian basement. There are many significant features in the pre-Cambrian in the Ohio-Indiana-Michigan region. The Grenville front is a major boundary that separates the Grenville province to the east from somewhat older pre-Cambrian terranes to the west. The Grenville province is characterized by highly metamorphosed rocks, while the rocks to the west are slightly older in age and less altered; sedimentary and volcanic rocks and structures are well preserved. The Grenville front outcrops in Canada, where it has been extensively mapped and studied. The proposed extension of the Grenville front through Michigan and Ohio lies just 50 km to the east of the Anna seismic zone (Figure 5c).

There are rift events in the pre-Cambrian terranes to the west of the Grenville front. Lake Superior, far to the north, is the site of the Keewenaw rift event at about 1.1 billion years ago. The Mid-Michigan geophysical anomaly trends NW-SE near the center of the Michigan basin, and is thought to also represent Keewenaw rifting (see Hinze et al., 1975). The Mid-Michigan anomaly terminates at the Grenville Front in the vicinity of present-day Ann Arbor. It also appears that a Keewenawan rift also occurs in northeastern Indiana and western Ohio. The primary evidence for this rift is: rocks recovered from deep wells that sample the top of the pre-Cambrian rocks; and positive gravity and magnetic anomalies in northeastern Indiana, as extended into western Ohio (see Lucius & Von Frese, 1988). The Grenville front in Ohio is defined by the westernmost extent of highly metamorphosed rocks. In the Central Province to the west, many different rocks have been found. The proposed Keewenawan rift trends NW-SE, and its northeastern edge is approximately defined by the appearance of a metasedimentary and rhyolitic rocks (see most recent discussion in Lucius & Von Frese, 1988). Mafic rocks occur immediately to the southeast and northwest of the Anna zone. Thus, it appears that the Anna seismic zone occurs within or near to a proposed Keewenawan rift, just to the west of the intersection of this rift with the Grenville front.

An east-west COCORP seismic reflection profile was run across Ohio in 1987 (Pratt et al., 1989). This profile passed through the Anna seismic network. Figure 6 is shows the main features of this profile. The Paleozoic sediments are seen as the reflections for two-way times of about half a second. The strongest features in the pre-Cambrian basement are the east-dipping reflectors that are associated with the the Grenville front; these structures are clearly to the east of the Anna seismic zone. Moho is not seen in this profile, but is probably "deeper" than 13 to 15 s two-way time. There is a fairly strong reflector at the

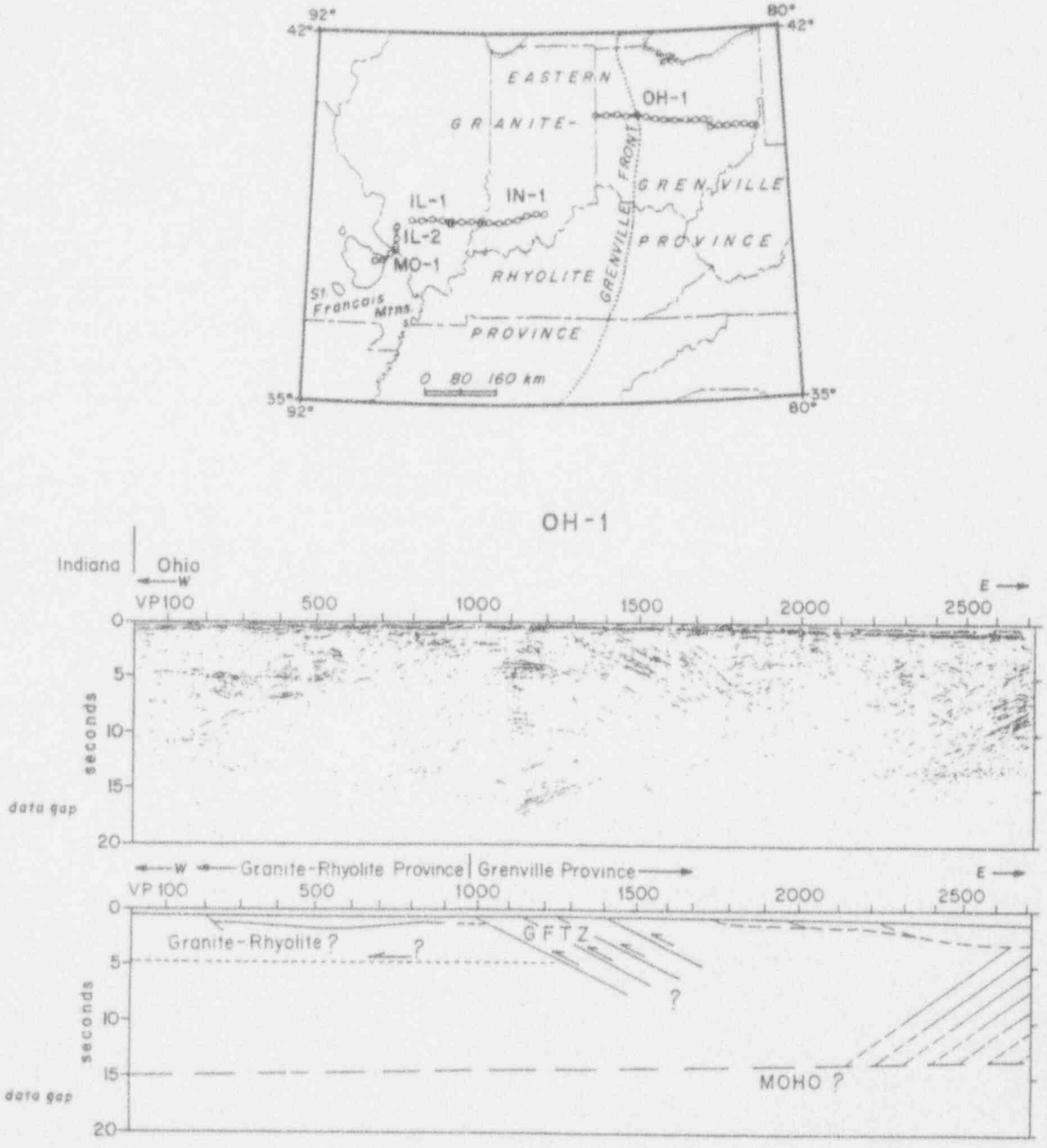

Figure 6. Some upper crustal features from the COCORP line that crosses the Anna seismogenic zone (from Pratt et al. 1989). The Anna zone is located to the west of the major features of the Grenville front. It appears that a strong reflector terminates just at the edge of the Anna zone

Ohio-Indiana border at 5 s two-way time, but this reflector disappears near the edge of the Anna seismic zone. One speculative interpretation might be that this mid-crustal reflector is truncated by the Keewenawan rift; we shall return to this question later after consideration of crustal structure.

1.2 The Ohio-Indiana-Michigan Seismic Network

The U.S. Nuclear Regulatory Commission sponsored the installation and operation of a local seismic network from 1976 to 1992. Fifteen short-period vertical-component stations have been recorded at the University of Michigan in Ann Arbor over this time period. The original nine stations of the Anna network became fully operational in June, 1978. The network was extended into Indiana with the installation of four widely scattered stations in February, 1981. In addition, two stations in southern Michigan have been recorded at various times. The original nine stations of the Anna sub-network span a maximum distance of about 80 km, while the four Indiana stations span 160 km. Station information is listed in Table 1. Several changes in seismometers, field equipment, and telemetry have been made over the years. These changes are well documented in the final reports of Jackson et al., 1981, Christensen et al., 1986. The network configuration has been stable since 1986, and we briefly describe the most recent network characteristics. The seismometers are Teledyne S-500 1 hz vertical components, with Teledyne 42.50-1 and 46.22 VCOs. The nine stations of the Anna sub-network use radio telemetry to transmit the signals to a central radio tower in Wapakoneta, Ohio. The batteries of the Anna stations are recharged by solar panels. The four stations of the Indiana sub-network are transmitted by leased telephone lines to the central facility in Wapakoneta, Ohio. At this central facility, signals from the thirteen stations are multiplexed onto three telephone lines and are received by the Seismological Observatory at the University of Michigan. Signals from the two Michigan stations, ACM in western Michigan and AAM in the vault of the WWSSN station in Ann Arbor, have been intermittently received by telephone line and direct radio telemetry, respectively.

The seismic stations are mostly located in rural settings where the cultural noise is mainly due to agricultural activities. Only the station at AAM has a controlled environment for the seismometer and system electronics; the Ohio and Indiana seismometers are shallowly buried and the electronics are in sheltered enclosures at the surface. The environmental conditions are characterized by below-freezing temperatures in the winter and numerous strong thunderstorms in the summer. The network has been operated at an annual up-time percentage (percentage of station-days with useful recordings with respect to the product of number of stations and days in the year) between 80% and 90% for most years (e.g., Table 2). The up-time percentage has been lower in recent years; this is largely due to increases in field equipment failures, e.g. electronic enclosures that leak water during thunderstorms, weakened support wires for solar

TABLE 1

STATION CHARACTERISTICS OF THE OHIO-INDIANA SEISMIC ARRAY

Station Code	Lat.°N	Long.°W	Elevation (Feet)	Displacement Gain (Peak)	Carrier (MHz) (x1000)	Subcarrier (Hz)
AN1	40.4792	84.1309	1003.	246.7	164.0093	1700
AN3	40.5489	83.8121	1070.	246.7	165.8093	1400
AN4	40.2222	83.8978	1134.	493.5	173.1940	1400
AN7	40.8235	83.8602	922.	493.5	171.4060	1700
AN8	40.2441	84.2860	992.	246.7	166.4218	680
AN9	40.7118	84.4967	835.	246.7	167.8090	2040
AN10	40.4729	84.4700	901.	246.7	167.1937	1020
AN11	40.5638	84.6804	895.	246.7	166.6565	1020
AN12	40.9217	84.1823	741.	493.5	163.7937	2040
IN1	40.542	85.894	837.	342.6	phone line	680
IN2	39.939	86.783	872.	342.6	phone line	1020
IN3	39.265	85.785	722.	342.6	phone line	1400
IN4	39.570	84.903	1025.	342.6	phone line	1700
ACM	42.6475	85.8517	880.	342.6	phone line	1700
AAM	42.2997	83.6561	817.	12.5	direct recording	

TABLE 2

STATION RELIABILITY DATA (%)

Monthly Summary	Stations AN1	AN3	AN4	AN7	AN8	AN9	AN10	AN11	AN12	IN1	IN2	IN3	IN4	ACM	Monthly Total
OCT 1990	100	100	0	100	90	100	90	90	100	100	100	100	10	0	77
NOV 1990	95	95	0	100	80	100	85	65	100	100	100	100	0	0	72
DEC 1990	100	100	0	100	100	100	95	95	100	100	0	90	0	0	70
JAN 1991	100	100	0	100	90	100	90	70	90	100	0	50	0	0	64
FEB 1991	100	100	0	100	80	100	95	95	100	100	20	100	0	0	71
MAR 1991	100	100	12	100	100	100	95	100	100	95	0	95	0	0	71
APR 1991	95	95	70	95	95	100	95	95	95	50	0	0	0	0	63
MAY 1991	95	95	10	100	100	100	80	80	90	70	0	10	0	0	59
JUN 1991	100	100	10	100	100	100	100	100	100	40	0	0	0	0	61
JUL 1991	100	100	100	100	100	100	100	100	100	90	90	30	100	0	86
AUG 1991	100	100	100	100	100	80	100	100	100	70	40	40	40	0	76
SEP 1991	100	100	100	100	95	0	90	100	100	20	0	0	0	0	58
Averages	99	99	33	100	94	90	93	91	98	78	29	51	13	0	69

panels and radio antennas, and decreased efficiency of solar panels and batteries. Typical field maintenance trips consist of replacing weakened batteries and VCOs that have suffered environmental damage.

The signals have always been recorded in analog fashion by an ink pen and paper drum system. The full system response curves are shown in Figure 7, these are based on the S-500 and L-4C seismometers for the Ohio and Indiana stations and a 12.5 hz low-pass filter used in the recording system. The magnification varies between stations and day to day, but typically falls in the range from 200,000 to 400,000. Time is kept by a Teledyne Geotech TG-120 clock which is corrected daily by WWV as received by a Kinemetrics radio, model WVTR Mark IV.

The network has also been digitally recorded in two different episodes. In the early 1980's, a PDP 11 computer with analog-to-digital conversion was used to record the signals. Due to the combination of cumbersome software, low capacity disk storage, and low rates of seismicity in the mid-Continent region, this digital system did not become part of routine operations. In the brief operational phase of this early system, the incoming electronic signals would be continuously recorded on analog magnetic tape, which would be played back through the digital system only when an event was detected on the ink pen seismograms. This operational style was reasonable given the small number of earthquakes to be analyzed each year. Figure 8a shows an example of digital seismograms from this system. The digital recordings improve the reliability of arrival times and first motion polarities.

The second episode of digital recording commenced in the summer of 1991. This new system is based on the software package developed over many years by Dr. W. Lee and colleagues which is distributed by the Seismological Society of America and IASPEI. The hardware consists of two AT-class PCs (on-line and off-line machines) connected by a LAN, and the on-line machine uses a Data Translation A-D board to digitize the analog signals and time code. The software package includes a flexible on-line program with graphical display, and various off-line programs for seismogram display and processing. Figure 8b shows seismograms from a local event recorded by this system. In addition to the desire to produce higher quality recordings, other motivations to use this digital system include reduction of long-term operational expense and acquisition of operational experience to possibly continue operation of the Anna network with on-site digital recording. Support of the Anna network by the NRC will end in 1992 as the USGS-sponsored USN becomes operational. While the USN should provide good regional coverage in the mid-Continent area, there is a strong desire by some persons in the State of Ohio and companies that own deep injection wells to continue operation of a local network in and around the Anna zone.

Response Curve	Pen Amplifier Setting	Peak Magnification
(a)	100 mv/mm	493.5k
(b)	100 mv/mm	342.6k

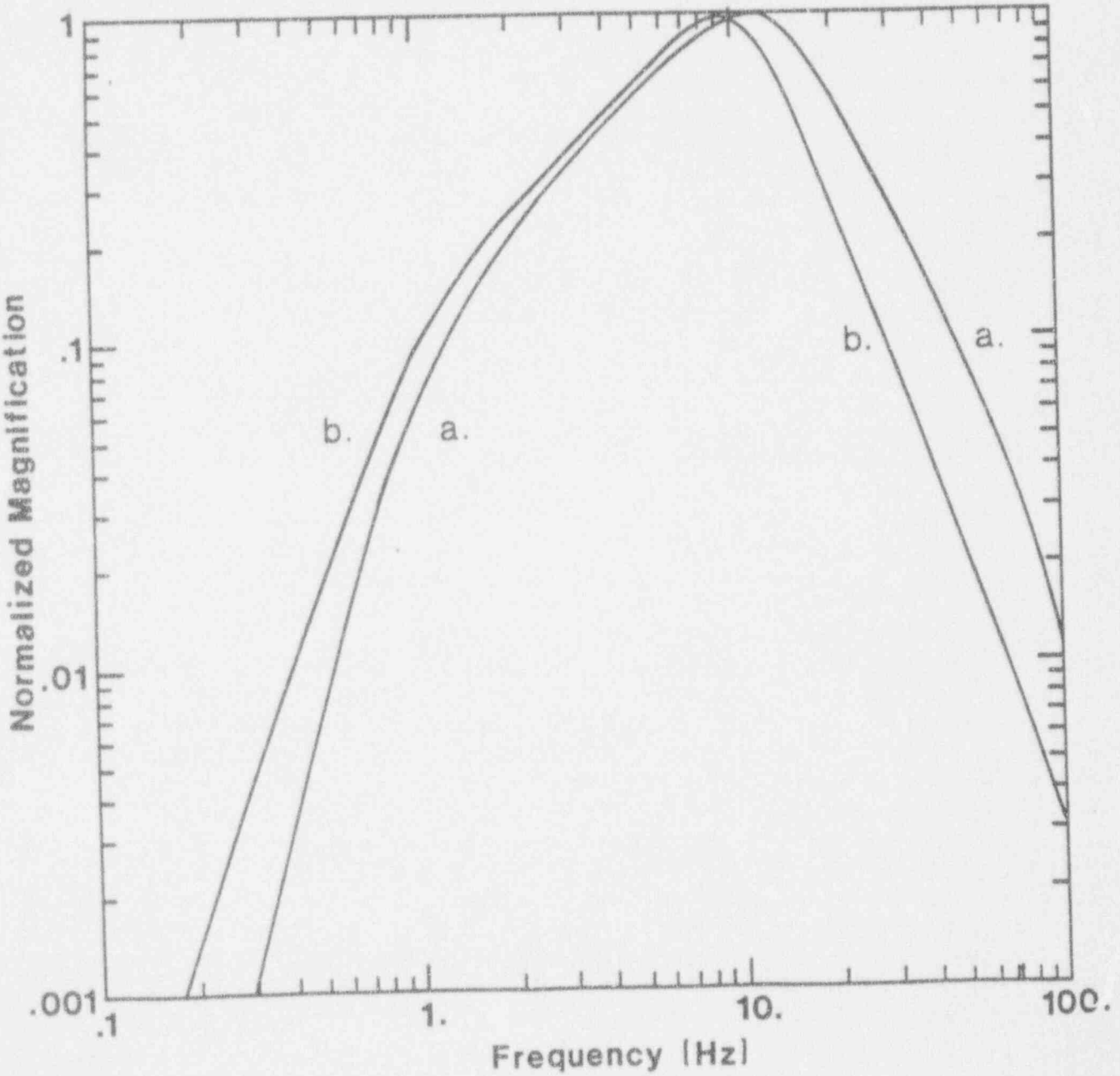

Figure 7. Normalized system frequency response curves for the: (a) Ohio stations (with S-500 seismometers), and (b) Indiana stations (with L-4C seismometers).

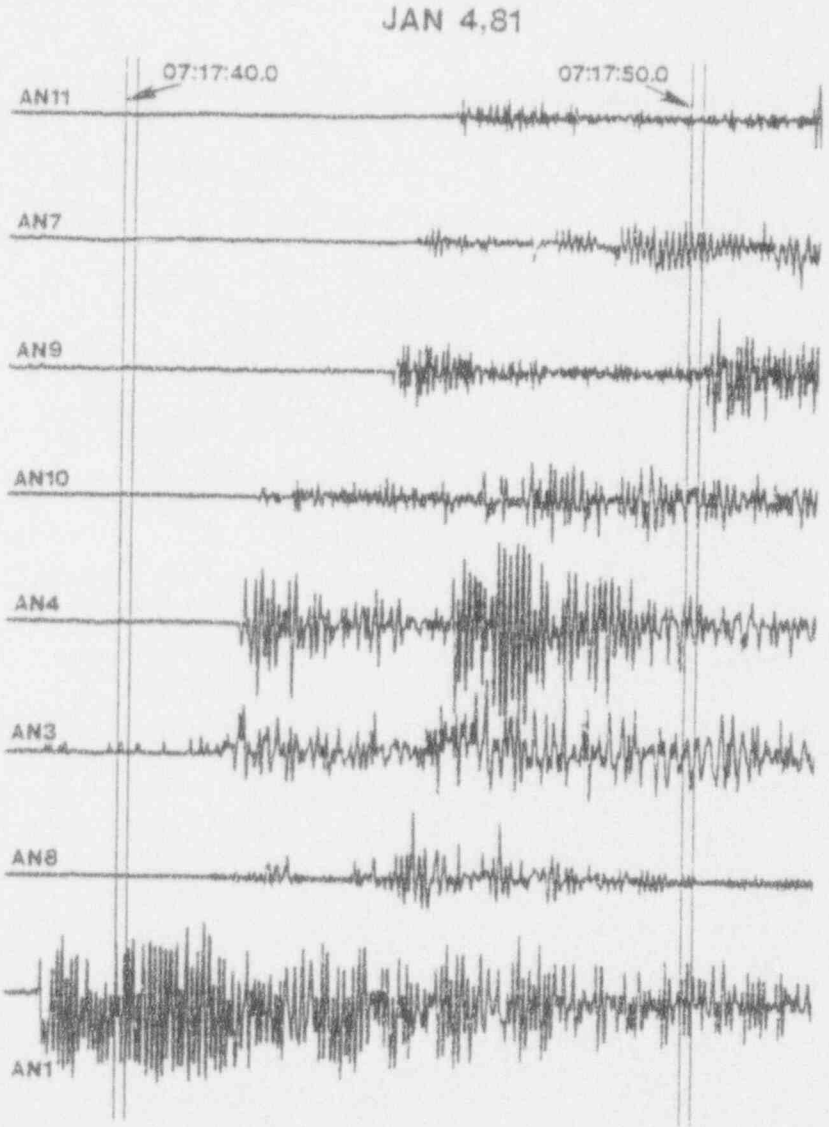

Figure 8a. Example of a local earthquake recorded digitally with the old system.

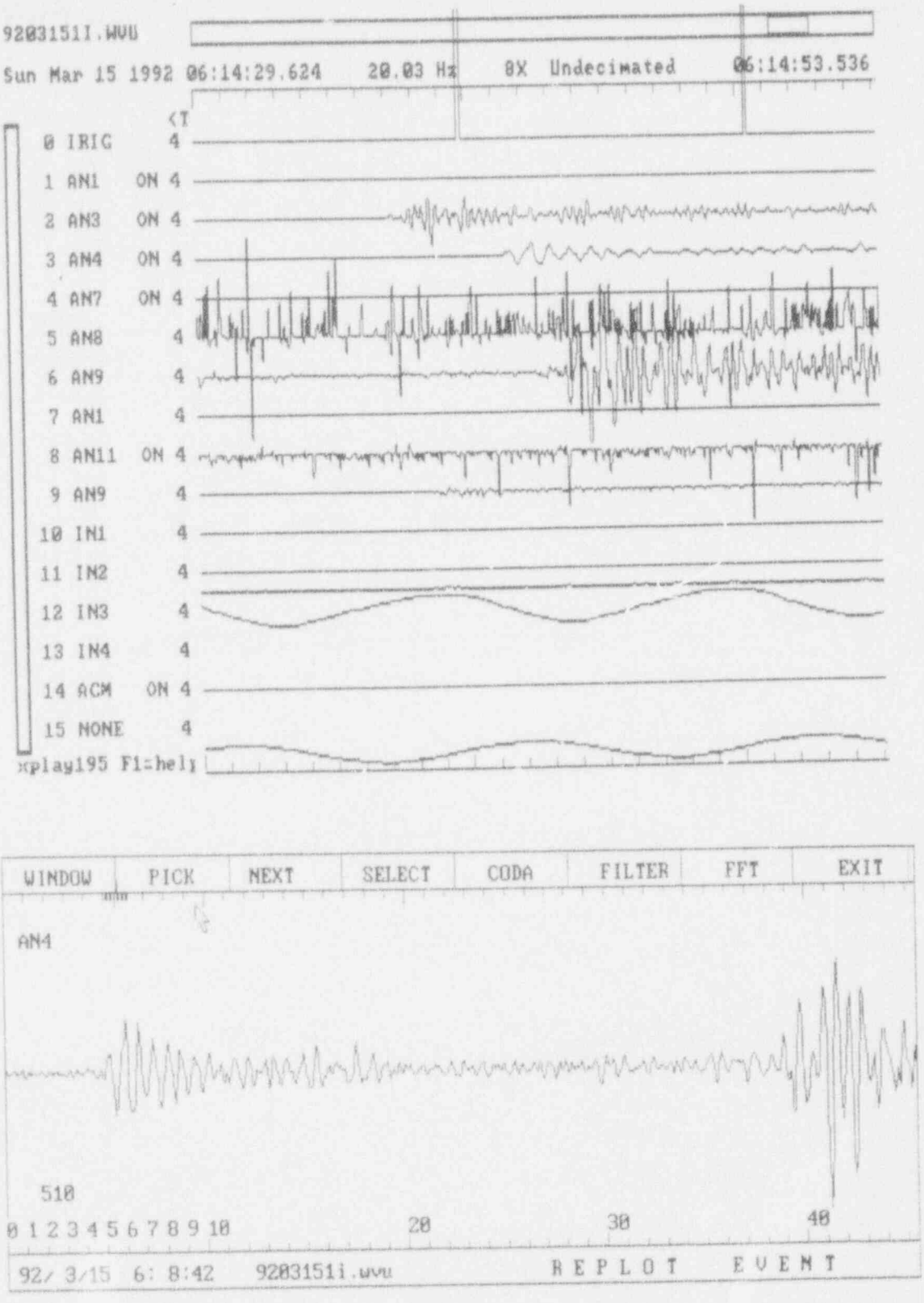

Figure 8b. Example of new-system digital recording of the recent March 15, 1992 earthquake (M=3.3) in Lake Erie near Perry, Ohio. Upper part shows all stations with good P arrivals at AN3, AN4, AN9, and AN12. Lower part shows the full digital trace for AN4 with both P and S arrivals.

2. Crustal Structure

Crustal structure for many parts of the mid-Continent region in Canada and U.S.A. has been determined by refraction and reflection surveys (see compilations of crustal structure studies by Soller et al., 1982, and Braile, 1989). However, there are no regional-scale studies in the Ohio-Indiana-Michigan region. It is important to determine crustal structure for two reasons: to locate earthquake hypocenters and to test whether the Anna seismic zone displays any unusual crustal properties. For the purpose of earthquake location, it is important to define the travel time curves associated with: the direct P and S arrivals (Pg and Sg); the Moho refracted P and S arrival (Pn and Sn); and, if observed as a first arrival, the mid-crustal refracted arrival (P* and S*). These travel time curves will cover the P and S wave first arrivals from zero to several hundred kilometers. P wave travel time curves can be directly obtained by long refraction profiles with artificial sources, while P and S wave travel time curves can be determined from seismic network observations of P and S wave arrival times from earthquakes. As part of Project Early Rise, a long refraction profile runs through the Michigan Basin and continues through central Ohio to the east of the Anna seismic zone (see Iyer et al., 1969). Since southern Michigan and central Ohio are more than 600 km from the sources in Lake Superior, this refraction line can only be used to measure the apparent velocity of the uppermost mantle. A refraction line from artificial sources in Kentucky to the Anna seismic zone was measured in the summer of 1984 as a joint project with the University of Kentucky and Memphis State University. The Anna network served as the terminus of this profile at a distance range from 319 to 400 km. Unfortunately, the P waves were quite weak and the arrival times are quite scattered, but we shall use some information from this profile. As mentioned in the Introduction, reflection surveys in the Anna zone have included proprietary shallow surveys that have delineated faults in the Paleozoic sedimentary section, plus a COCORP profile which has the potential to resolve details of crustal structure down to Moho. Whether or not this potential is realized depends on several factors. One example of a COCORP velocity analysis study is the study of Zhu & Brown (1986) of the COCORP profile across part of the Michigan basin - even their comprehensive effort was not able to resolve crustal velocities beyond mid-crustal depths. Unfortunately, no detailed velocity analysis of the Anna COCORP has been accomplished. It is clear that the travel time curves for the Anna region must be determined from arrival times collected by the Anna network.

As a guide to the crustal structure expected in the pre-Cambrian Central province, we can look at velocity structures determined for the New Madrid zone from earthquake arrivals and for the greater Lake Superior region determined by various refraction studies. The crustal model of Stewart (1968) has a Pg velocity of 6.1 to 6.2 km/s down to a depth of 22 km, then a lower crustal velocity of 6.6 km/s

down to Moho at 40 km, with a Pn velocity of 8.0 km/s. Mitchell & Hashim (1977) used earthquake arrival times in the New Madrid region to find a Pg velocity of 6.19 ± .02 km/s out to a crossover distance of about 100 km, then a velocity of 6.38 ± .06 km/s out to a distance of 175 km, followed by a velocity of 7.17 km/s ± .14 out to a distance of 200 to 250 km; the Pn branch is not found in their study. For the S waves, they found a velocity of 3.62 ± .01 out to 175 km, followed by a S wave velocity of 4.10 ± .09 km/s out to 200 km. Mitchell & Hashim (1977) do not find the Moho velocity nor crustal depth, but their data suggests that Moho is deeper than 40 km. Several crustal models based on refraction profiles are summarized in Braile (1989). The "average mid-continent" model is: velocity of Pg layer is 6.14 km/s with a thickness of 15.9 km, the lower crustal velocity is 6.82 km/s, with a total crustal thickness of 42.5 km, and a Pn velocity of 8.10 km/s.

Travel times at the Ohio-Indiana-Michigan stations from local and regional events have been measured for many years, and preliminary analyses have been performed over the years, e.g. in the report by Christensen et al. (1986). In this study, it was reported that: the first arrivals between 0 and 200 km could be fit with a velocity of 6.36 km/s and an intercept time of 0.63 s, beyond which a Pn velocity of 8.12 km/s is found for first arrivals from 350 to 1500 km, with an intercept time of 7.45 s. Secondary arrivals are occasionally observed in the distance range from 500 to 900 km with an apparent velocity of 6.4 to 6.8 km/s and an intercept time of 3 to 9 s. As for the S wave arrival, the direct Sg phase is observed from 0 to 200 km with a velocity of 3.61 km/s and an intercept time 0.80 s; while observations from 350 to 1500 km give a Sn velocity of 3.58 km/s and an intercept time of 11.3 s.

An examination of earthquake location procedures for the Anna network over the years shows that many different crustal models have been used. In several cases, earthquake locations were tried with different crustal models with the final location based on the model that produced minimum RMS residuals for that particular event. Inhomogeneities in earthquake location procedures, station distributions, and variations in crustal structure will produce unwanted scatter in the resultant travel times. The best illustration of these effects on travel time scatter is simply to plot the data as travel time versus distance using the catalog values of location and origin time. Figure 9 shows detailed plots of a few events located within the Anna seismic zone. It is clear that origin times for each event are offset with respect to each other. Another illustration of this effect is to plot the travel times from far-way regional events. As seen in Figure 10, offsets in travel time baselines introduce unwanted scatter in the travel times, and thus compromise our ability to reliably determine the apparent velocity across the network. Furthermore, if we divide the network into the nine-station Anna sub-network and the four-station Indiana sub-network, there seems to be differences in the apparent velocities. Thus, to eliminate systematic errors and unwanted scatter

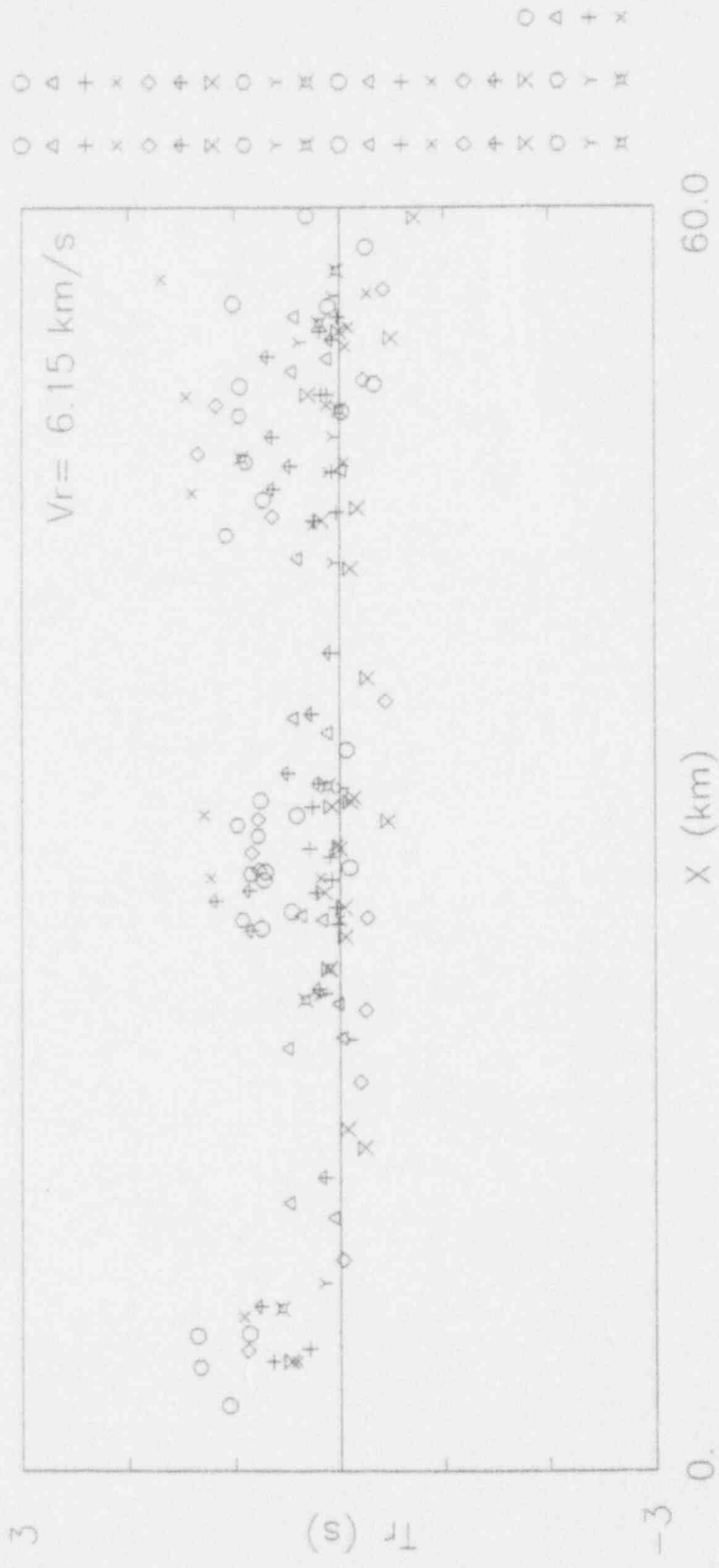

Figure 9. Reduced travel time plot of local P arrivals recorded by the Anna stations. Travel times are with respect to fixed origin times as calculated by various procedures. Different symbols are for different earthquakes. Reduction velocity is shown in the upper-right corner.

Figure 10. Reduced travel times for Anna stations with fixed origin times as given in various catalogs and determined by various investigators. Different symbols are for different earthquakes. Note the large "baseline offsets" in the travel times. The horizontal lines above the plot show the distance ranges of each event.

in our determinations of travel time curves, our analysis must: (1) allow the baselines, i.e the effective origin times, of each event to be free variables that are determined simultaneously with the travel time curves; (2) have the capability of separate tests for the Anna and Indiana sub-networks; and (3) be able to determine the intercept times of the travel time curves. The next section describes in detail the simultaneous linear inversion of arrival time data to find the best travel time curves.

2.1 Simultaneous inversion of arrival times for travel time curves and origin times

We are confronted with a problem where we do not know the precise earthquake location nor the crustal structure. In addition, crustal structure can change across the region of interest. The typical procedure is to assume one, or more, crustal structures that seem reasonable and then find the best possible earthquake locations. As is well-known, the epicentral location is generally much more reliable than the hypocentral depth, which "trades-off" with the origin time. If the event is located within a network of stations, then the epicentral location will typically show only a weak dependence on crustal structure, while depth and origin time can still change in direct correlation with assumed crustal velocity. For events located outside of a network, the major influence of lateral variations in crustal structure is to shift the effective intercept time of the travel time curves. One simple approach to arrival time analysis would be to determine the best-fit slowness across the network for each event, and then to average all determinations of slowness over some distance range. However, it is quite easy to simultaneously invert the arrival times for all events in a certain distance range to find the best overall slowness plus the best origin times.

Epicentral location errors for earthquakes outside of the network tend to shift all epicentral distances to either greater or lesser values and thus will not affect the apparent slowness. Earthquakes within the network that are mislocated can have a more complicated effect on distances that might produce a best-fit slowness different from the "true" slowness. Thus, after determination of the travel time curves, a few earthquakes are relocated to test for any systematic effects. Perhaps the most important events are those for which the epicentral distances span a crossover to a faster velocity. The arrival times from these events determine the intercept times of the higher velocity travel time curve. The stations that are closer than the crossover distance are fixed with respect to the overall best-fitting slowness, and the stations that are further than the crossover distance help fix the intercept time and slowness of the faster travel time branch. The intercept times depend upon the crustal structure beneath the network and beneath the earthquake source. We do not know in advance what are the best choices for crossover distances. Thus, the arrival time data are inverted to find the: (1) best apparent origin

times for each event, (2) best-fit slownesses in specified distance ranges, and (3) the best-fit intercept times for each travel time curve branch. It is necessary to specify the intercept time for the first travel time curve; zero is the most logical choice, although the "true" intercept time might be non-zero due to a low-velocity surficial layer above the earthquake source. Once the best values of slowness and intercept times are obtained, the crustal velocity model derived from these quantities must take into account the shift in intercept times due to source depth. Recall that source depths are not known, nor is the velocity structure far away from the network. Thus, we must use an overall average source depth to produce the final value of crustal thickness.

2.2 Technical details

Let the observed arrival time at the j^{th} station for the i^{th} event be T_{ij}, and the corresponding epicentral distance will be X_{ij}. We must specify in advance the number of travel time curve segments and the distance ranges for each segment. For example, we might try to explain the observations with three travel time segments with the following distance ranges: 10 to 80 km, 80 to 150 km, and 180 to 400 km. In the above example, we are not sure whether the observations in the range from 150 to 180 km belong to the closer or further travel time branch, so we leave these observations out of the inverse problem, though we can still plot these observations. The method allows for each travel time curve to either be a straight line or a quadratic curve. In general, there are a total of N travel time segments with distance ranges $X1_n$ to $X2_n$, with n=1 to N. If the distance range for the i^{th} event falls within $X1_n$ to $X2_n$, then the synthetic arrival times are:

$t_{ij}=O_i + (\tau_n + p_n X_{ij})$,

for a straight line travel time curve where O_i is the origin time of the i^{th} event, τ_n and p_n are the intercept time and slowness of the n^{th} travel time curve. If we use a quadratic curve, then the synthetic arrival times are:

$t_{ij}=O_i + (\tau_n + p1_n X_{ij} + p2_n X_{ij}^2)$,

where $p1_n$ and $p2_n$ are the linear and quadratic coefficients of the travel time curve. For the situation where the distance range for the i^{th} event spans two different travel time segments, the observations will be divided into those with distances less than $X2_n$, and those with distances greater than $X1_{n+1}$. Then, the synthetic arrival times will be, for the example of linear travel time curves:

$t_{ij}= O_i + (\tau_n + p_n X_{ij})$ for $X_{ij} \le X2_n$

$= O_i + (\tau_{n+1} + p_{n+1} X_{ij})$ for $X_{ij} \ge X1_{n+1}$.

As discussed above, the events with epicentral distances that span from $X2_n$ to $X1_{n+1}$ will determine the intercept time for the n+1 segment.

The mismatch between the observed and synthetic arrival times is:

$r_{ij}=T_{ij} - t_{ij}$.
The residuals, r_{ij}, can be rearranged into an error vector $\underline{e}$ by stacking the row vectors of r_{ij}. The observed arrival times, T_{ij}, can likewise be rearranged into data vector, $\underline{d}$. The inverse problem can be stated as follows: given observations for a total of *I* events with unknown origin times O_i, and specification of N travel time segments with unknown parameters τ_n and p_n (possibly $p1_n$, $p2_n$), determine the origin times and travel time curve parameters that minimize the squared length of the error vector. Given the linear dependence between the synthetic arrival times and all the unknown parameters, this inverse problem is a standard linear least squares problem. Place all the unknown parameters, origin times and travel time parameters, into a model vector $\underline{m}$, then the forward problem can be written as:
$A\underline{m}=\underline{d}$,
where $\underline{d}$ is the data vector described above, and the A matrix is mostly zeros but with the epicentral distances and "1"s in the appropriate places. Model estimates are then given by the generalized inverse, A* (Lanczos, 1961):
$\underline{m}=A^*\underline{d}=(A^tA)^{-1}A^t\underline{d}$,
where A^t is the transpose of the A matrix and $(\ )^{-1}$ is the inverse matrix. In contrast to most problems in geophysics, no damping is used to construct the generalized inverse; if the A^tA matrix is singular, we must change the model description. Furthermore, it is important to obtain good estimates of the uncertainties. Thus the model covariance matrix is calculated:
$C=\sigma^2A^*A^{*t}$,
where σ^2 is the *a posteri* uniform estimate of data variance. In other words, σ^2 is the squared RMS value of the residuals:
$\sigma^2=(\underline{e}^t\underline{e}/(K-M))$,
where K is the total number of observations used in the inversion and M is the total number of model parameters. Since it is not practical to list all components of the covariance matrices, uncertainties listed for the travel time curve parameters are the standard deviations, i.e. square roots of the diagonal elements of the covariance matrix. Slowness values are inverted to velocity. In general, the most significant covariance amongst the model parameters is between the intercept time and slowness; these two parameters covary such that the resultant travel time curves cross the best-fit curve in the relevant distance range. This covariance will be considered when estimating crustal thickness.

2.3 Results

The results of the arrival time analysis are presented in the following order, with the section number: (2.3.1) Pg velocity from events within the Anna sub-network; (2.3.2) Pg velocity from events just outside the Anna sub-network; (2.3.3) test for the existence of a P* first arrival; (2.3.4) determination of the Pn crossover distance for the Anna sub-

network; (2.3.5) analysis of Pn velocity; (2.3.6) Pg/P* for the Indiana sub-network; (2.3.7) Pn for the Indiana sub-network; (2.3.8) Sg for the Anna sub-network, and Sg and Sn for the entire network. All of these results will then be synthesized in the following section (2.4).

2.3.1 Pg from events within Anna network

Events that occurred within the network are observed at distances from close to 0 out to 60 km. To avoid the departures from a straight line travel time curve at distances less than the hypocentral depth, a linear travel time curve is fit to the observations from 15 to 60 km. The observations and linear travel time curve are shown in Figure 11a, with the raypaths plotted in Figure 11b. Note that several arrival times at distances around 5 km show a positive residual of about half a second, this is crudely consistent with hypocentral depths of 3 to 6 km. A detailed examination of hypocentral depth will follow in the seismicity section. Travel time lines were also fit to the distance ranges of 10 to 60, 20 to 60, and 35 to 60; the best-fit values for Pg velocity fall in the range from 6.14 to 6.155 km/s, well within the standard deviation of the best-fit velocity for 15 to 60 km as shown in Figure 11. Thus, our first conclusion is that the Pg velocity out to 60 km in the Anna seismic zone is 6.155 ± .055 km/s.

2.3.2 Pg from events outside Anna network

Figure 12a shows the observations at Anna stations from events outside the network but with at least one station closer than 60 km. Event locations and raypaths for these earthquakes, and all others, are shown in Figure 12b. A linear travel time curve fit to the arrival times between 15 and 60 km gives a Pg velocity of 6.27 km/s, but with a range from 6.11 to 6.43 km/s. Hence, this result is not significantly different from the Pg velocity found from the events within the Anna network. One curious visual feature of the observations in Figure 12 is the trend from 60 to 90 km where the apparent velocity seems slower. Beyond 90 km, the arrivals seem to continue with a velocity of around 6.2 km/s. Indeed, a straight line fit to all observations between 15 and 140 km gives a velocity that drops to 6.11 km/s, with a range from 6.06 to 6.16 km/s. Once again, this result is not significantly different from the Pg velocity from the events within the network. However, this result implies that the direct Pg phase is observed as the first arrival out to at least 140 km.

2.3.3 The existence(?) of a P* first arrival

All observations at the Anna stations in the distance range from 0 to 220 km are used to look for a P* arrival. The apparent velocity for all data from 15 to 220 km is 6.20 km/s, but the range is 6.17 to 6.23 km/s. Of course, if two travel time curves occur within this distance range, there would be a systematic scatter in the arrival times. However, Figure 13 does not display an obvious systematic pattern, thus there is no strong visual evidence for a crossover to P* in the 90 to 220 km distance range.

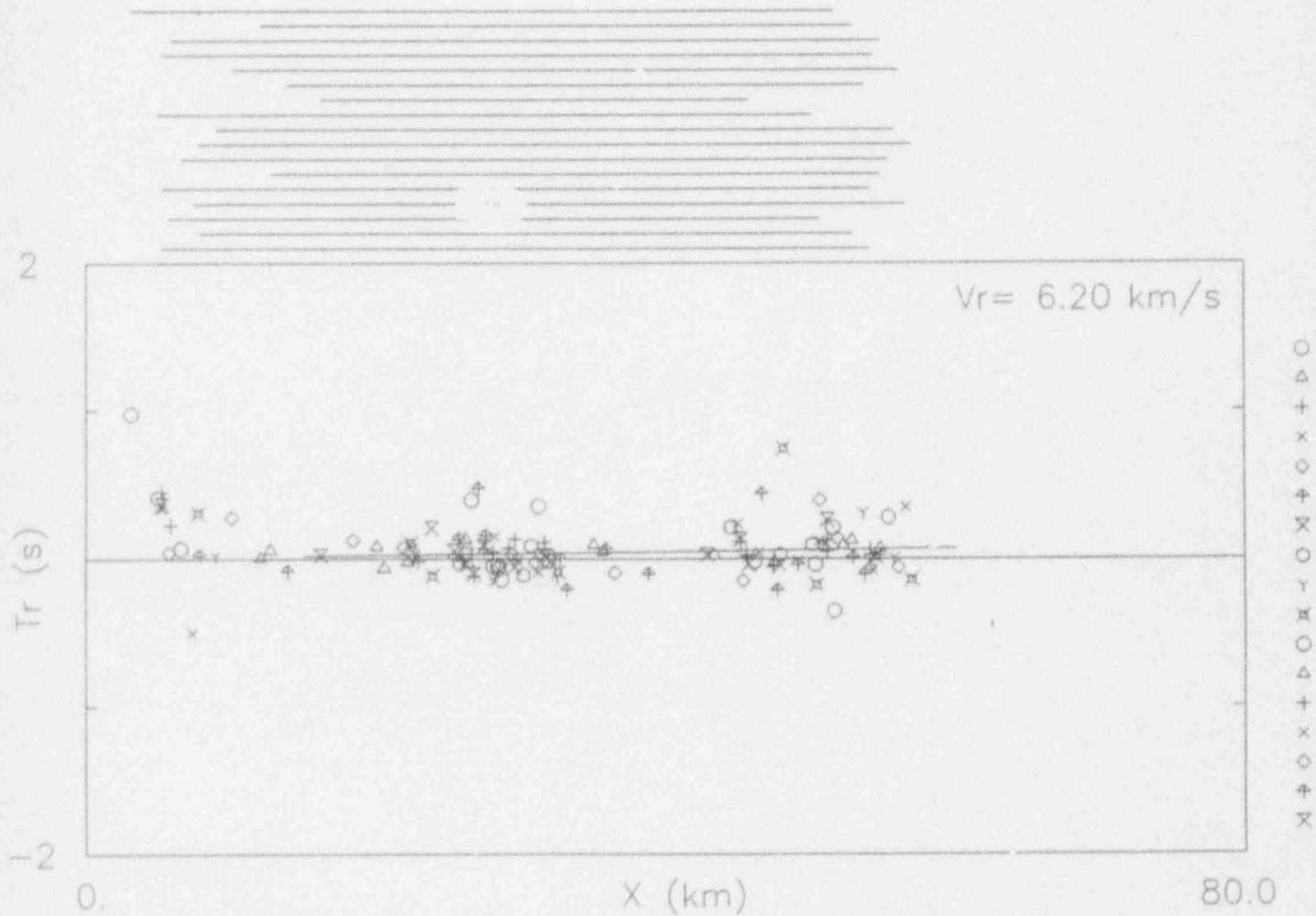

Figure 11a. Reduced travel times for local earthquakes recorded by Anna stations with simultaneous inversion for the best origin times. There are many observations from 0 to 60 km. The positive readings at close to 0 km give information on earthquake depth.

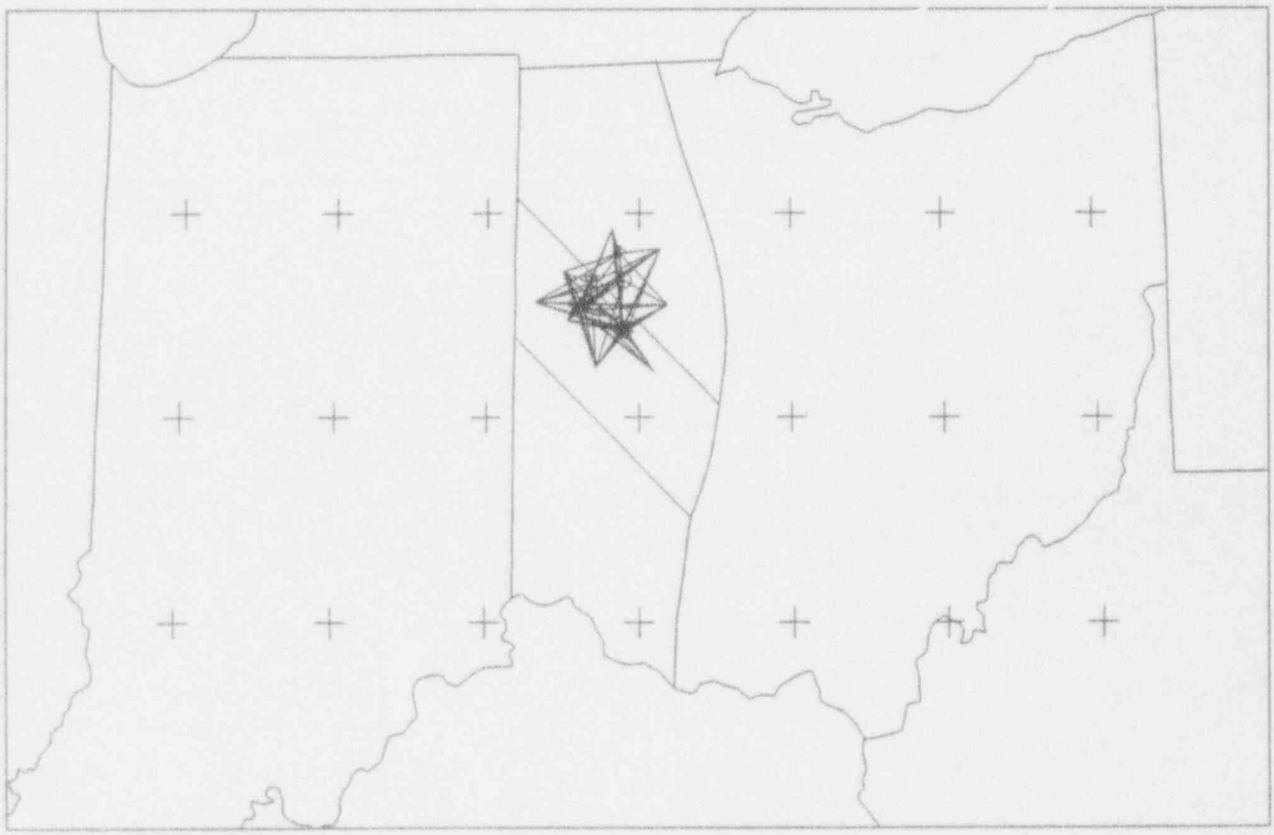

Figure 11b. Raypaths of all the observations in Fig. 11a. Each earthquake epicenter is plotted as the different symbols. Outlines of Ohio and Indiana are plotted; parts of Lake Erie and Lake Michigan are visible. Tic marks are at every degree of latitiude and longitude. In addition, the Grenville front is plotted through Ohio as the north-south curve. The northwest trending lines in the Anna zone are the bounds of the proposed Keewenawan rift.

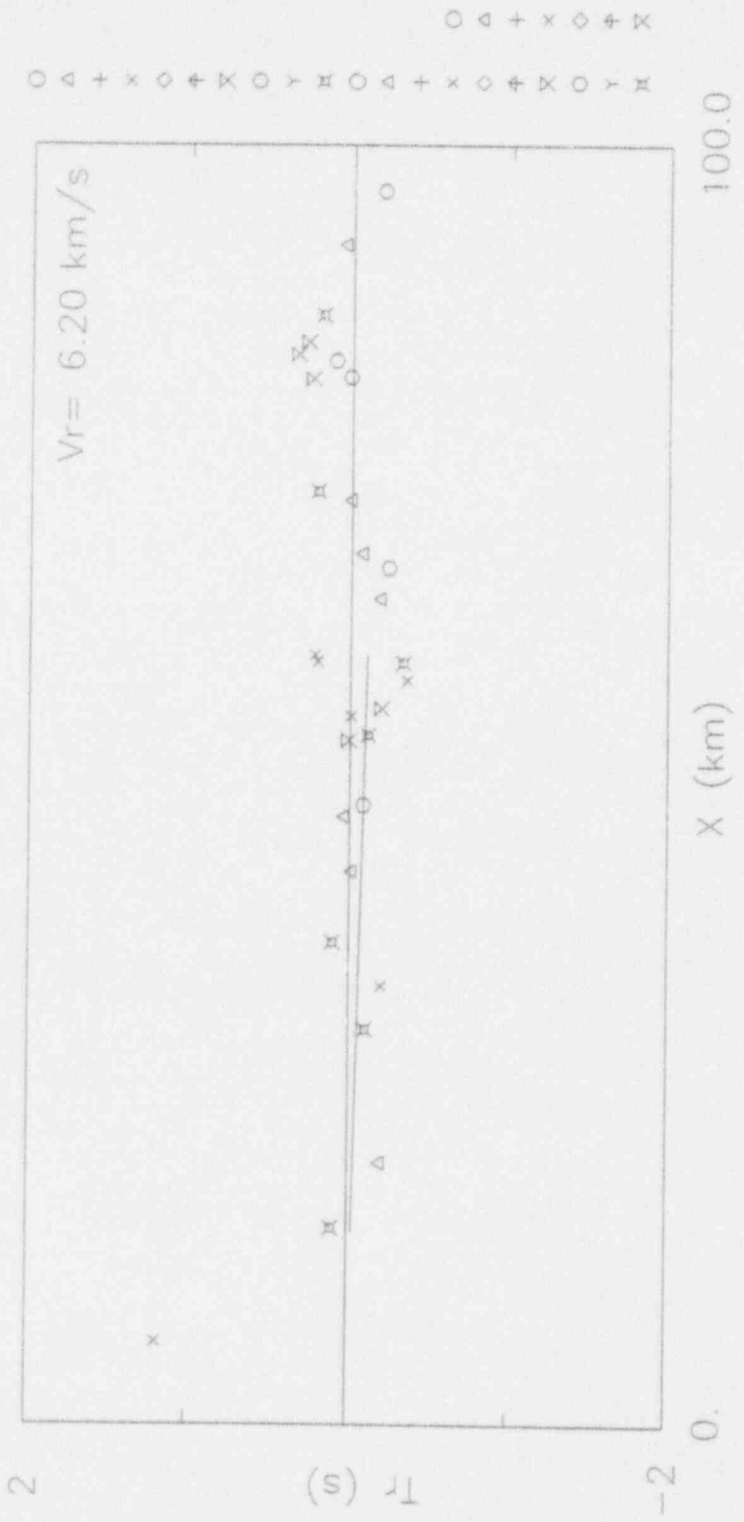

Figure 12a. Reduced travel times for local earthquakes that occurred external to the Anna sub-network, but recorded by the Anna stations.

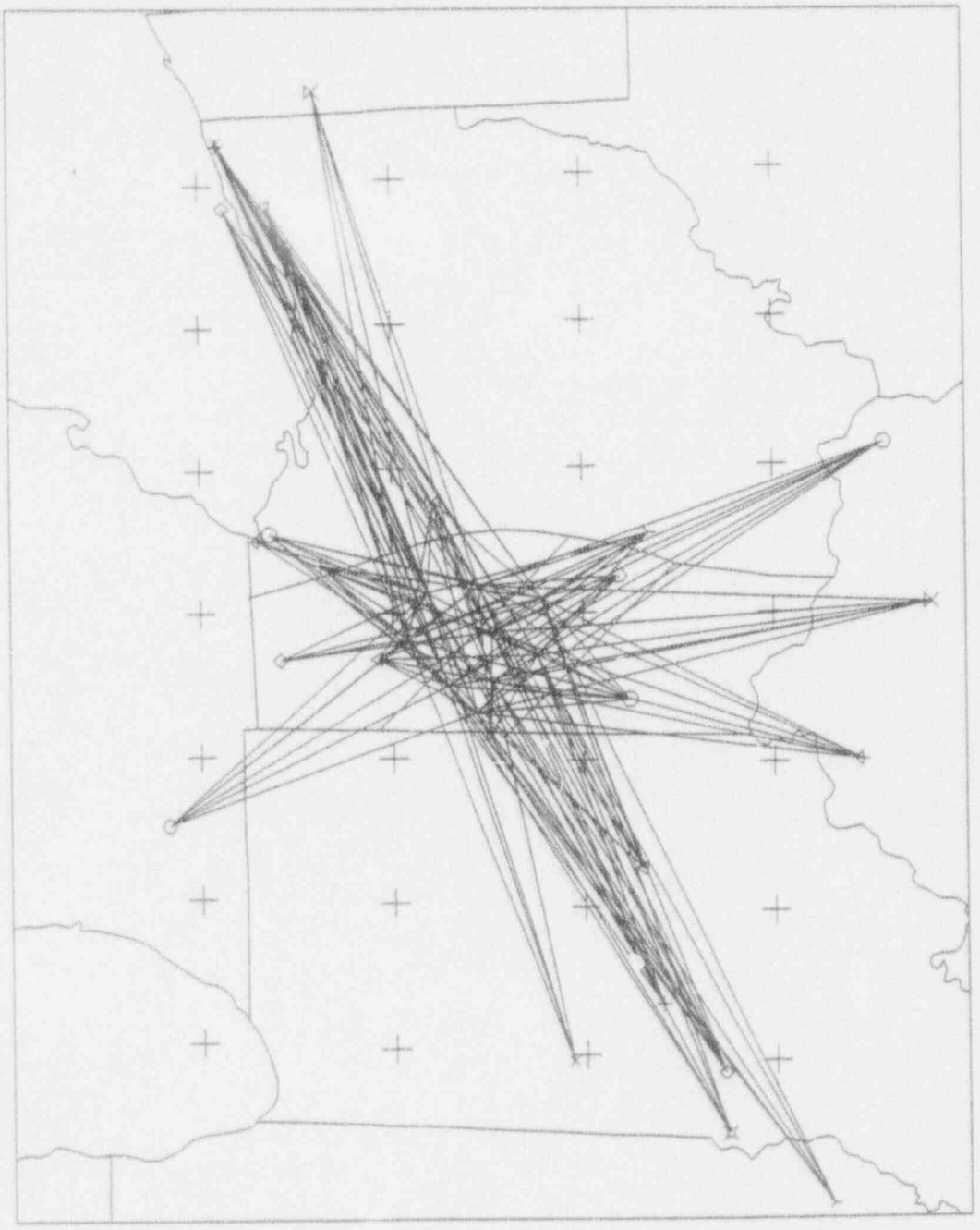

Figure 12b. Raypaths for all the observations of to Anna stations.

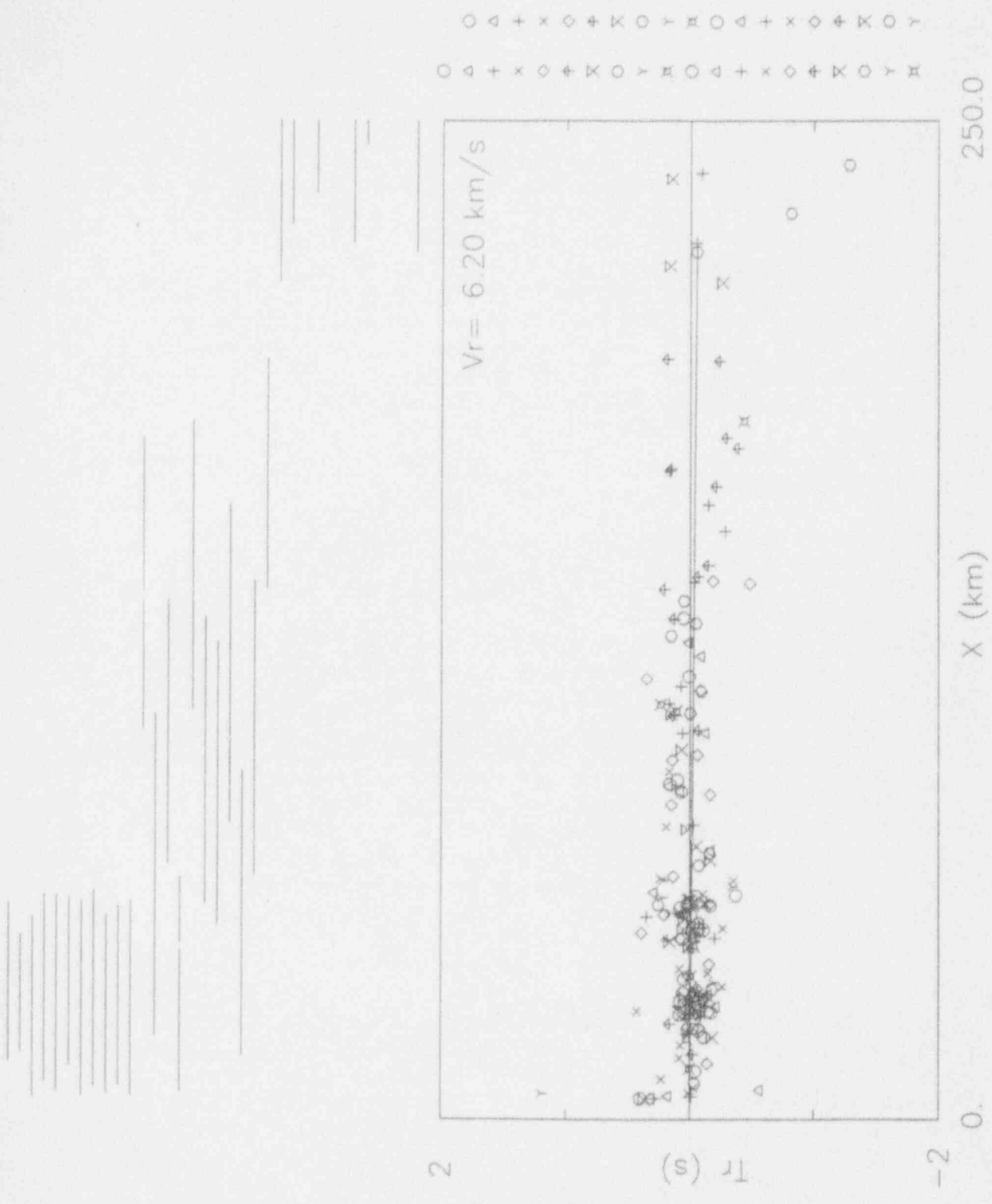

Figure 13. Reduced travel times for all earthquakes to the Anna stations in the distance range of 0 to 220 km.

There are 34 events that contribute observations in the distance range of 0 to 220 km. After we obtain the best-fit origin times and model parameters, we can calculate the RMS travel times residual for event; this allows us to identify "poor" events with more scattered arrival times. Hence, we construct a data sub-set of 29 events where we eliminate the 5 "bad" events with individual RMS values greater than 0.25 s. A travel time curve fit to the observations between 15 and 220 km now gives a velocity of 6.21 ± .03 km/s; thus the "better" data set gives essentially the same result as above.

The best-fit velocity between 15 and 220 km is marginally faster than the best-fit velocity between 15 to 60 km. We can quantitatively test for the existence of P* by allowing two travel time segments. We must test fro different values of the hypothesized crossover distance. Figure 14a shows that the best choice for the crossover distance is 120 km. Figure 14b plots the best-fit velocities and error bars for all cases. Figure 15 shows the case that offers the best fit to all the observations, with a break at 120 km. Note the RMS value is .186, only slightly smaller than the .193 RMS value for one travel time curve between 15 and 220 km. The velocities for the two lines (Pg and P*) are significantly different at one standard deviation, but at two standard deviations, they are not significantly different from the overall best-fit Pg velocity of 6.20 ± .03 km/s found for a single line between 15 and 220 km (see Figure 14b). Thus, while there is no compelling visual evidence for a crossover to a P* travel time branch, a P* branch is marginally preferred from the quantitative analysis. To summarize this analysis, a Pg velocity of 6.20 to 6.21 ± .03 km/s is found for the first arrivals from 15 to 220 km. If this distance range is divided into a Pg and P* branches with the best-fit crossover at 120 km, then the Pg velocity is 6.11 to 6.125 ± .04 km/s and the P* velocity is 6.39 to 6.42 ± .10 km/s. Recall that Christensen et al. (1986) found evidence in secondary arrivals for a P* velocity of 6.63 to 6.68 km/s. These velocities are more typical of lower crustal velocities; in contrast to the velocity of around 6.4 km/s found in the above analysis of first arrival data. We shall return to the difficulties in P* interpretation in section 2.4.

2.3.4 Pn crossover distance to the Anna sub-network

Pn should be observed as the first arrival if we move to larger distances. To fix the crossover distance and the intercept time, we must use some earthquakes with distance ranges that span the crossover. For this purpose, we use earthquakes in western Ohio, Michigan, Indiana, and northern Kentucky. Figure 16 shows the events and raypaths to the Anna sub-network. Two travel time curves are fit to the data between 0 and 340 km, and the distance of the break between the two lines is varied from 180 to 260 km in 10 km increments. The statistical results are shown in Figure 17, the best fit is for a crossover of 220 km. The Kentucky-to-Anna refraction profile offers additional evidence for a Pn crossover at a distance greater than 200 km. Although the travel times at the Anna stations are quite

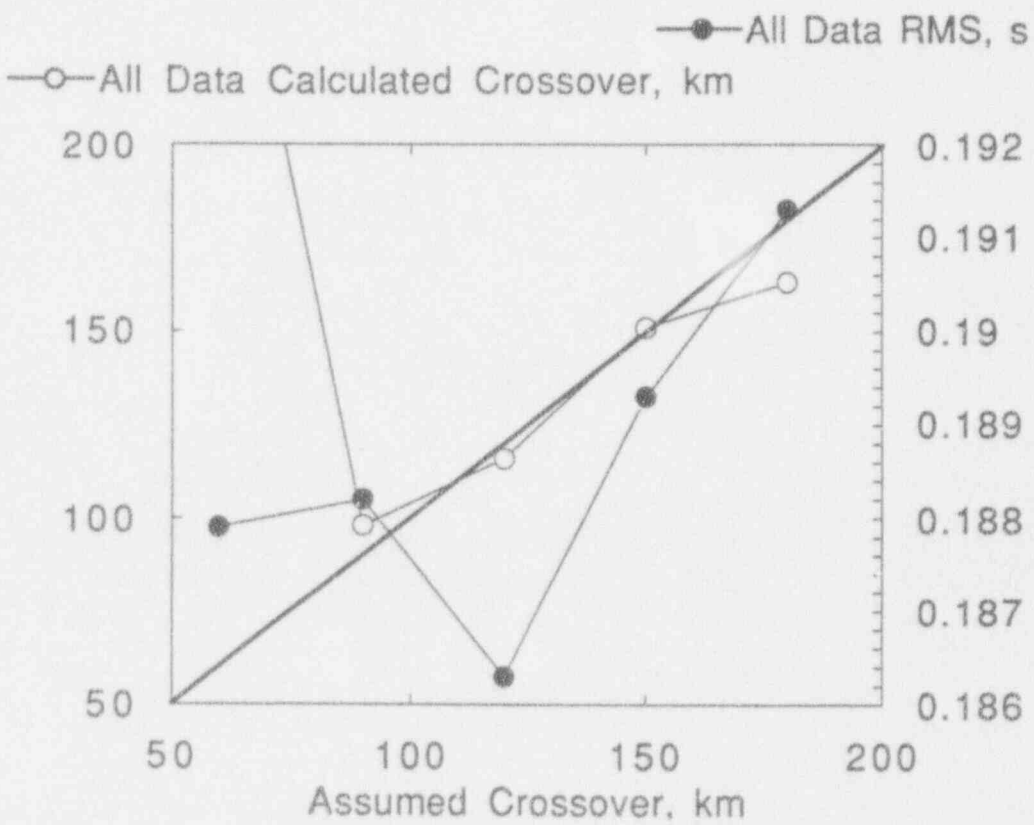

Figure 14a. Determination of the best P* cross-over distance by statistical analysis. Error (RMS, s) as a function of crossover distance (solid symbols). Open symbols show calculated crossover distance as a function of the assumed crossover distance.

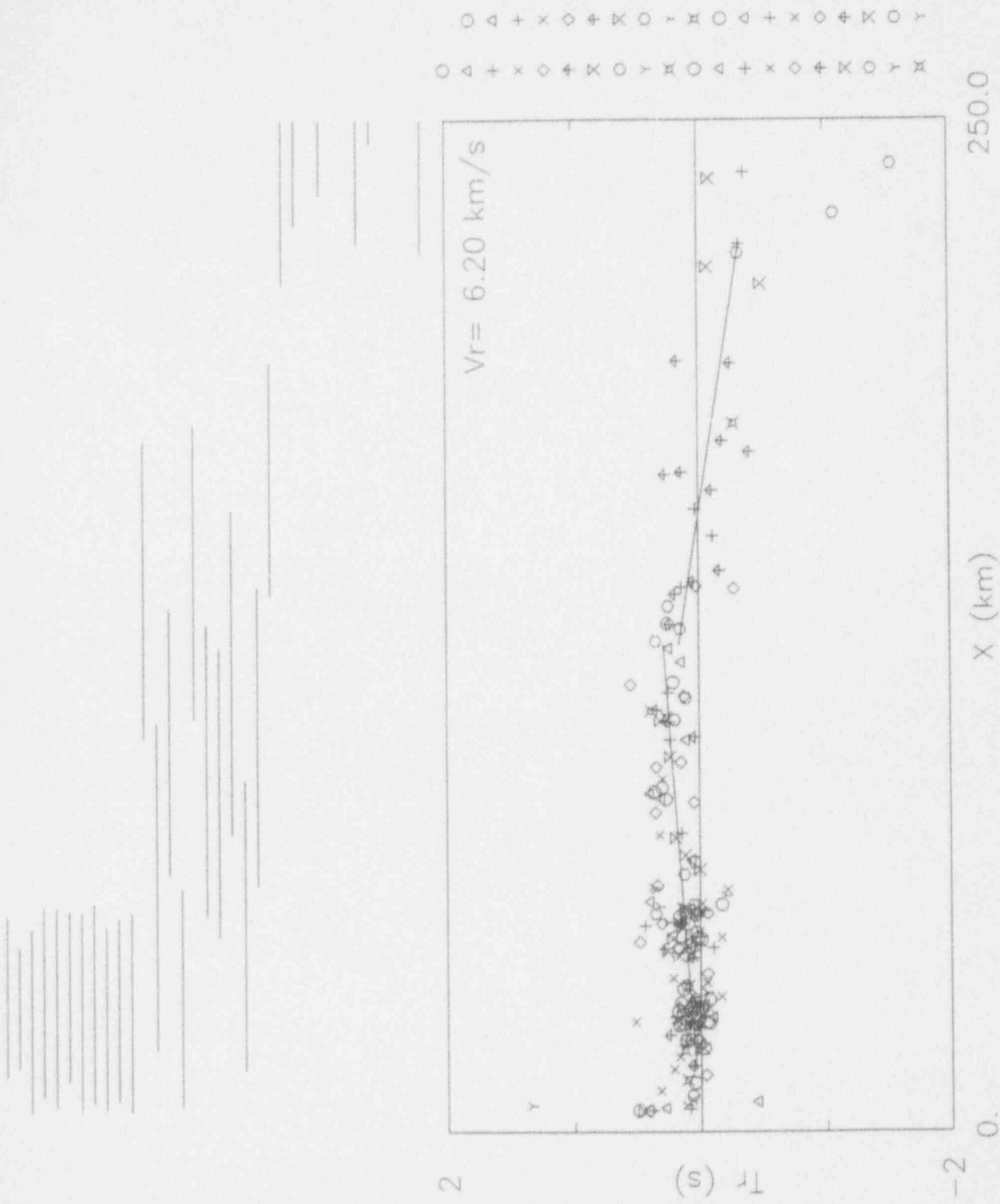

Figure 15. Reduced travel times for Anna stations out to 220 km, with travel times curves from 15 to 120 km and 120 to 220 km. The Pg velocity is 6.11±.04 km/s, P* is 6.39±.10 km/s, and the intercept time is .75±.28 s.

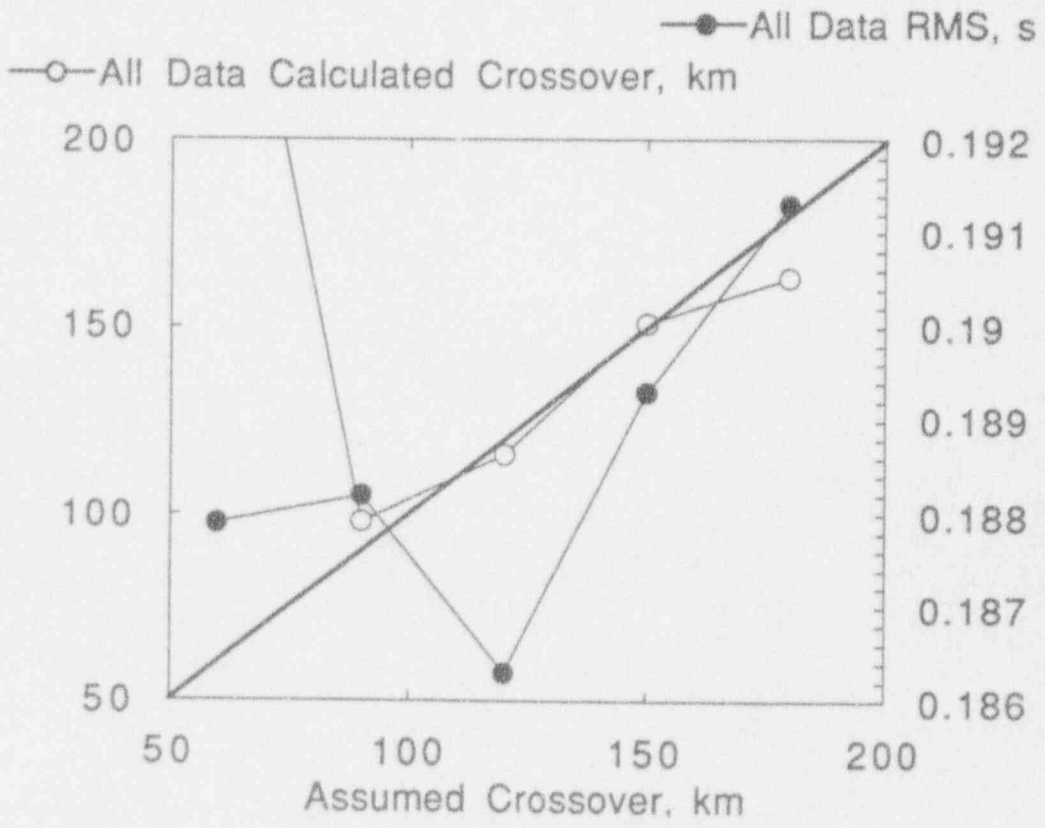

Figure 14a. Determination of the best P* cross-over distance by statistical analysis. Error (RMS, s) as a function of crossover distance (solid symbols). Open symbols show calculated crossover distance as a function of the assumed crossover distance.

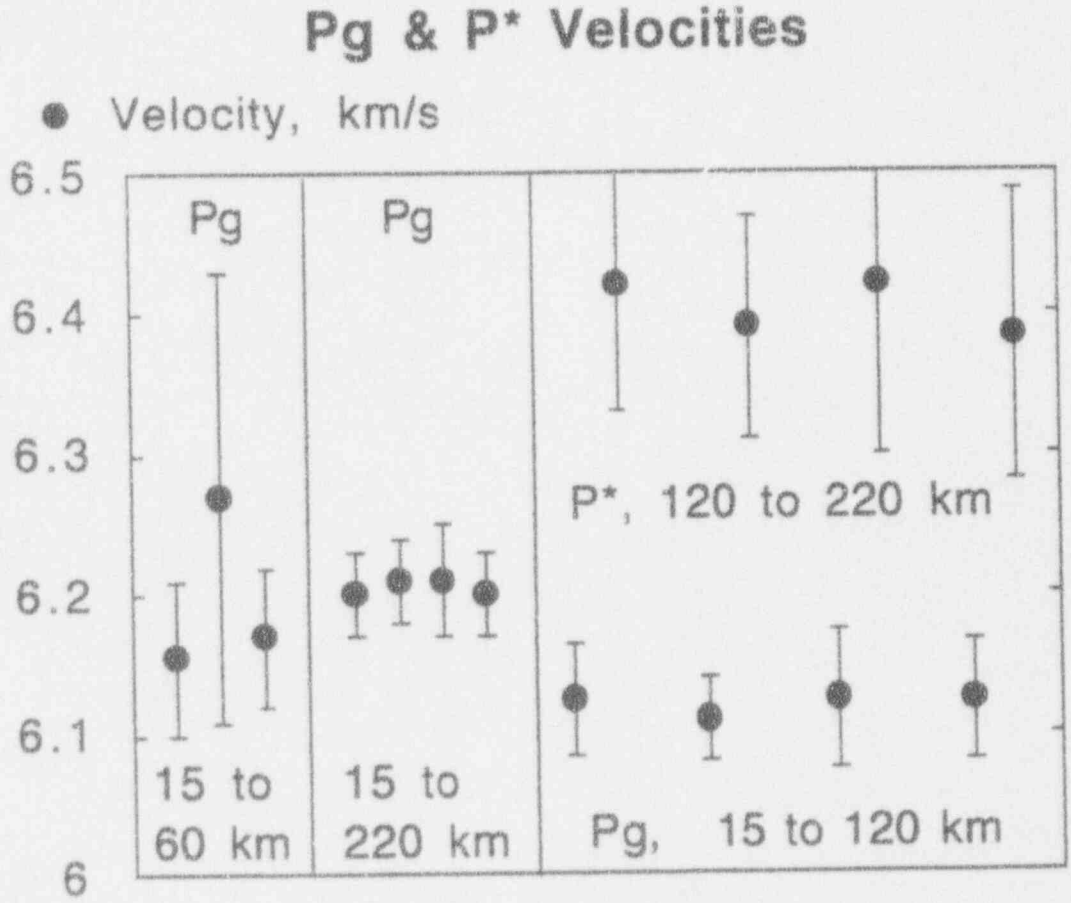

Figure 14b. Pg and P* velocities for the Anna sub-network from various inversion runs.

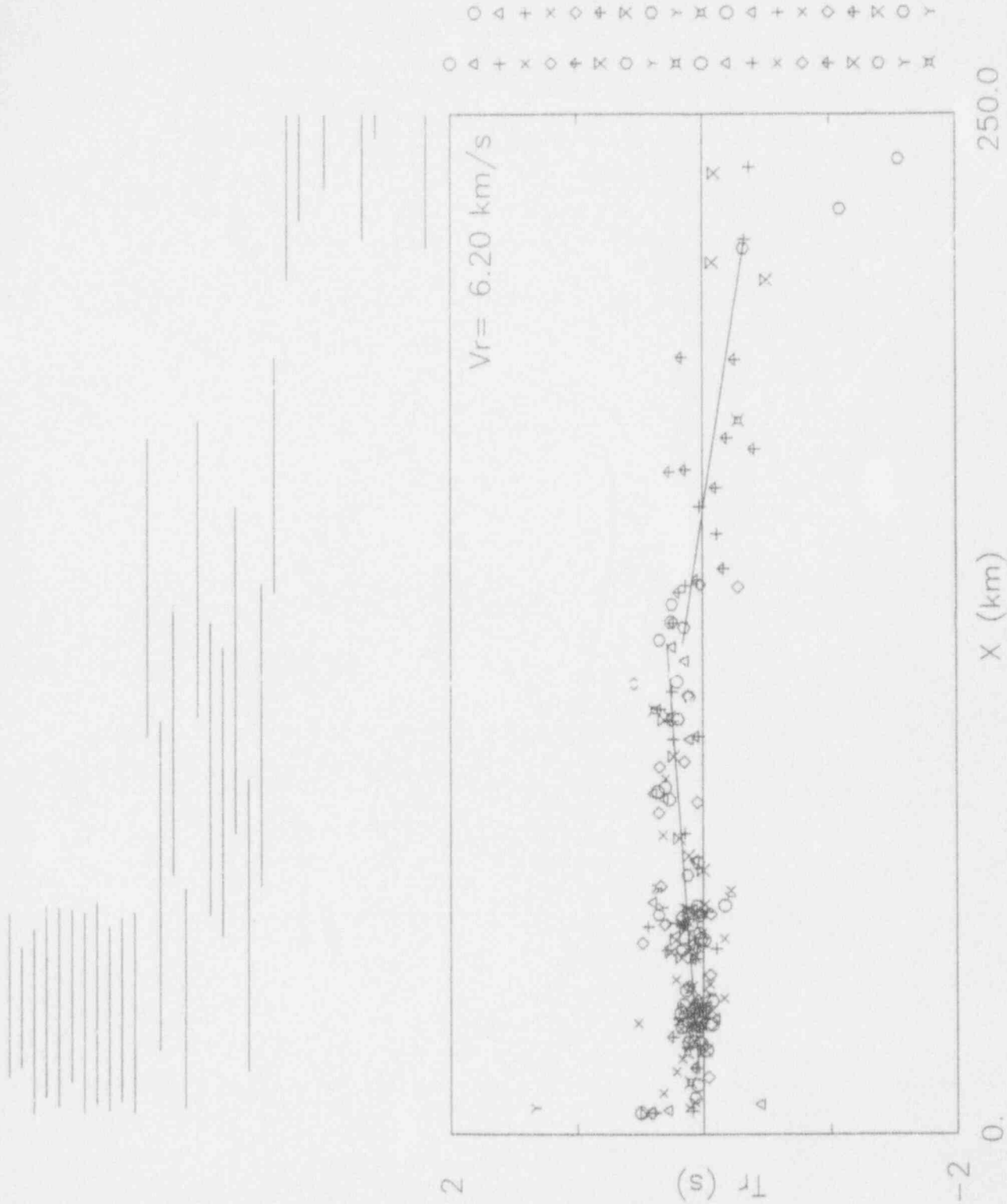

Figure 15. Reduced travel times for Anna stations out to 220 km, with travel times curves from 15 to 120 km and 120 to 220 km. The Pg velocity is 6.11±.04 km/s, P^* is 6.39±.10 km/s, and the intercept time is .75±.28 s.

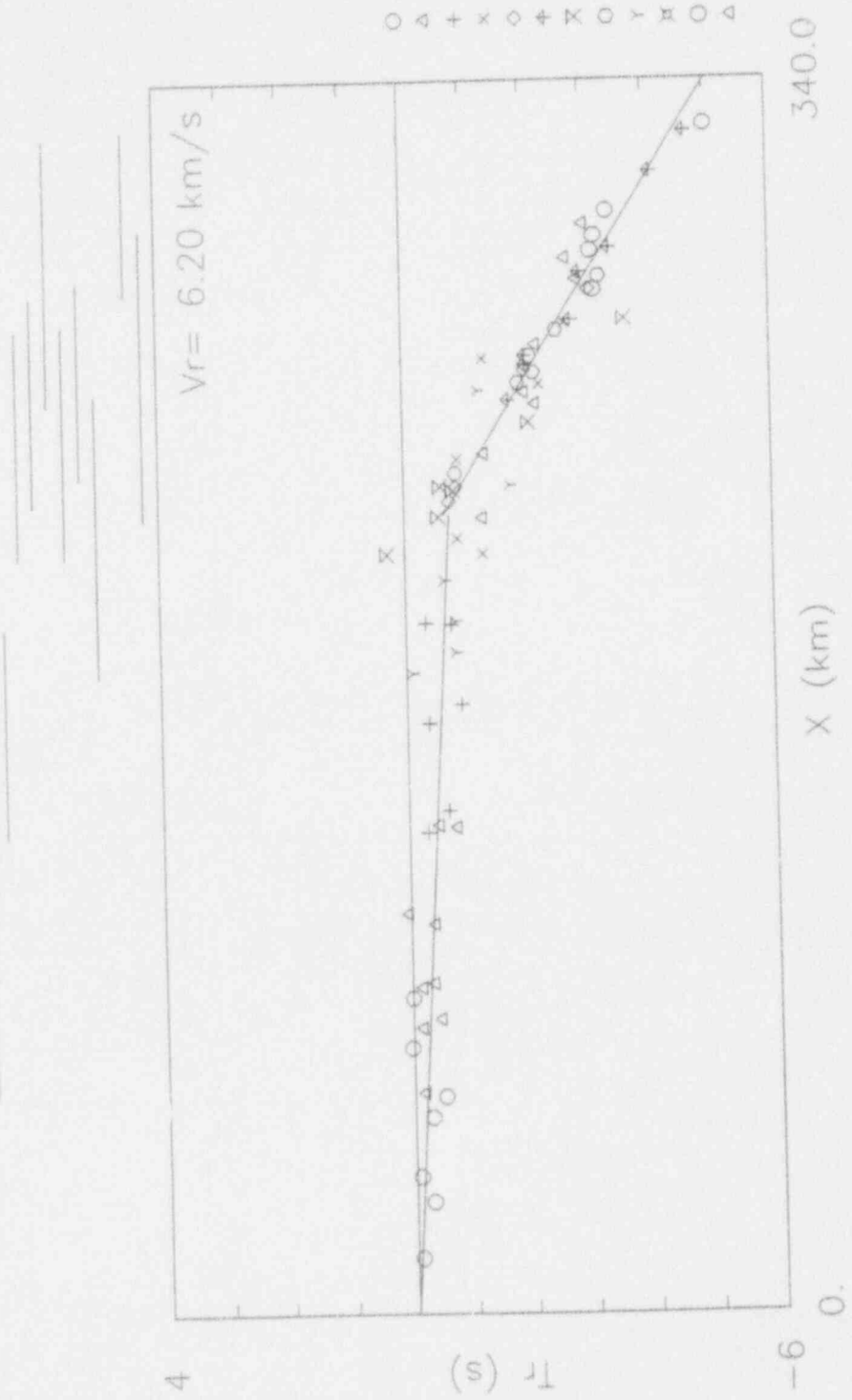

Figure 16a. Reduced travel times to Anna stations from earthquakes at Pn distances to the north, west, and south. The Pg velocity from 15 to 220 km is 6.33±.13 km/s, and the Pn velocity out to 340 km is 8.03±.19 km/s.

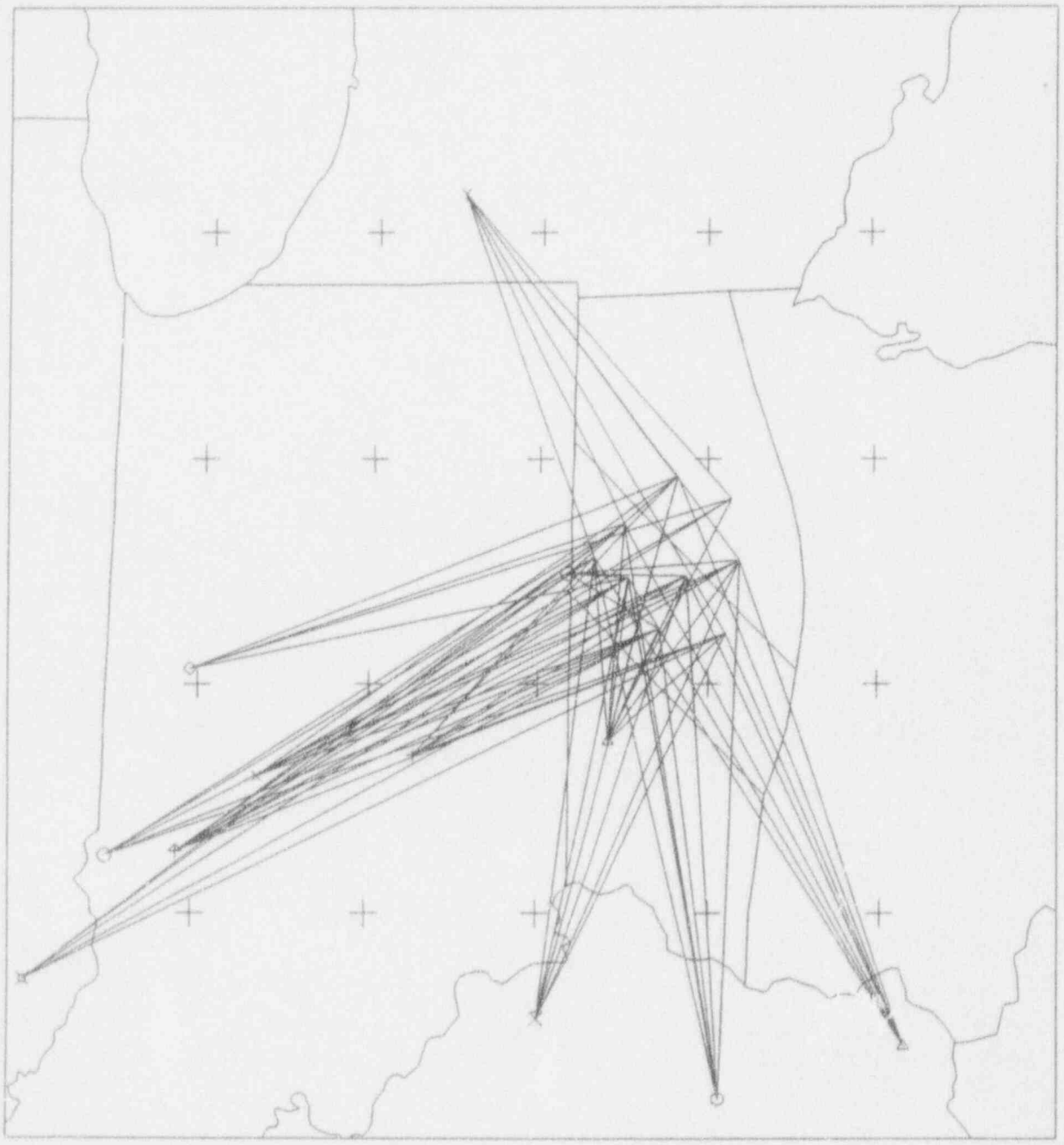

Figure 16b. Raypaths for the observations in Fig. 16a.

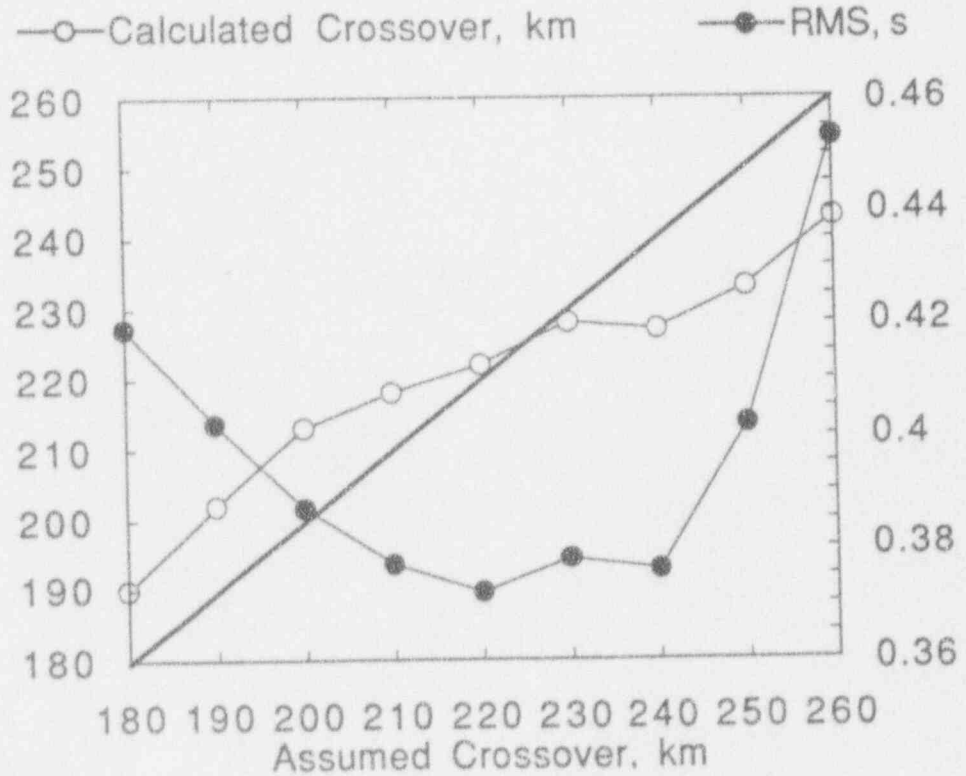

Figure 17. Statistical analysis for Pn velocity to the Anna sub-network.

scattered and there was some ambiguity as to the nature of these arrivals, the apparent velocity is clearly much less than 8 km/s out to a distance of 200 km. The combination of a "slow" crustal velocity and large crossover distance immediately implies a large crustal thickness.

2.3.5 Analysis of Pn velocity

Pn is observed as the first arrival from 220 km out to several hundred kilometers. Large earthquakes have occurred to the northeast, southeast, and south of the Anna network in this distance range. Thus, we can examine whether there is a difference in Pn velocities from different azimuths, which could be interpreted as: (i) dipping Moho, (ii) variable crustal velocity, or (iii) anisotropy. There are several earthquakes in northeastern Ohio, including the 1986 Perry event, that are shown in Figure 18. The Pn velocity at the northeast azimuth is 8.07 ± .15 km/s from six events, or 8.14 ± .14 km/s from just the large 1986 Perry event. Nine events from Figure 16 yield a Pn velocity of 8.29 ± .24 km/s. The Michigan and Kentucky events to the north and south show considerable scatter. If the best three events from Indiana and Illinois are used in the analysis, i.e. from a southeast azimuth, then the Pn velocity is 8.24 ± .08 km/s. Although the Pn velocity from the northeastern Ohio events would appear to be slower than from the other directions, it is not statistically significant. Clearly, the simplest model, i.e. a constant Pn velocity with a flat-lying Moho and a laterally homogeneous crust beneath the Anna sub-network, is an acceptable model.

All the observations for the Anna sub-network from 0 to 400 km are inverted in Figures 19 and 20, where a P* branch is allowed in the latter figure. A total of 44 earthquakes are used in these figures. Examination of individual event RMS values shows that three events have residuals greater than .4 s, The "good" data sub-set of 41 earthquakes produces nearly identical results: for just Pg and Pn, the Pg velocity is 6.20 ± .03 km/s, and τ_n is 8.5 ± .4 s with Pn of 8.07 ± .07 km/s; for Pg, P*, and Pn branches, Pg is 6.12 ± .04 km/s, τ^* is .75 ± .4 s, P* is 6.38 ± .10 km/s, τ_n is 8.2 ± .4 s, and Pn is 8.07 ± .07 km/s. Once again, there is weak quantitative evidence for a P* velocity branch of 6.42 km/s as a first arrival at the Anna sub-network. However, for the purpose of locating local and regional earthquakes with first arrivals, it is quite adequate to use a direct Pg arrival with velocity of 6.2 kms/ out to 220 km, and a linear Pn travel time curve with velocity of 8.07 km/s and intercept time of 8.2 to 8.5 s.

2.3.6 Pg/P* for the Indiana sub-network

Observations for the Indiana sub-network consists data from IN1 through IN4 plus several readings at BLO (Bloomington, Indiana) generously provided by the University of Indiana. This sub-network has only five stations scattered over an aperture of 160 km with only a few earthquakes located within the sub-network. Thus the quantity and quality of results for Indiana falls far behind those for the Anna sub-

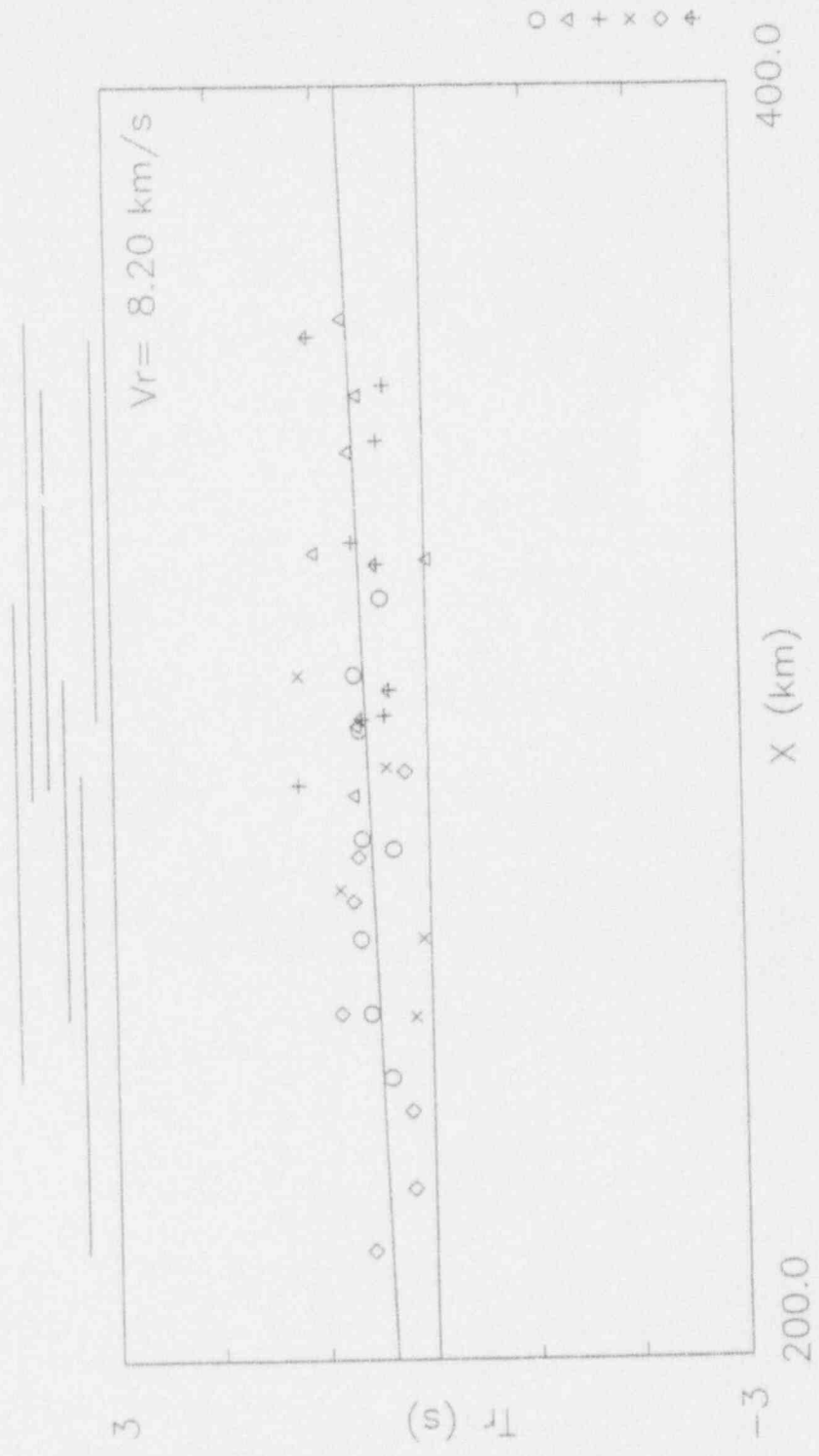

Figure 18. Reduced travel times to Anna stations from earthquakes in eastern Ohio.

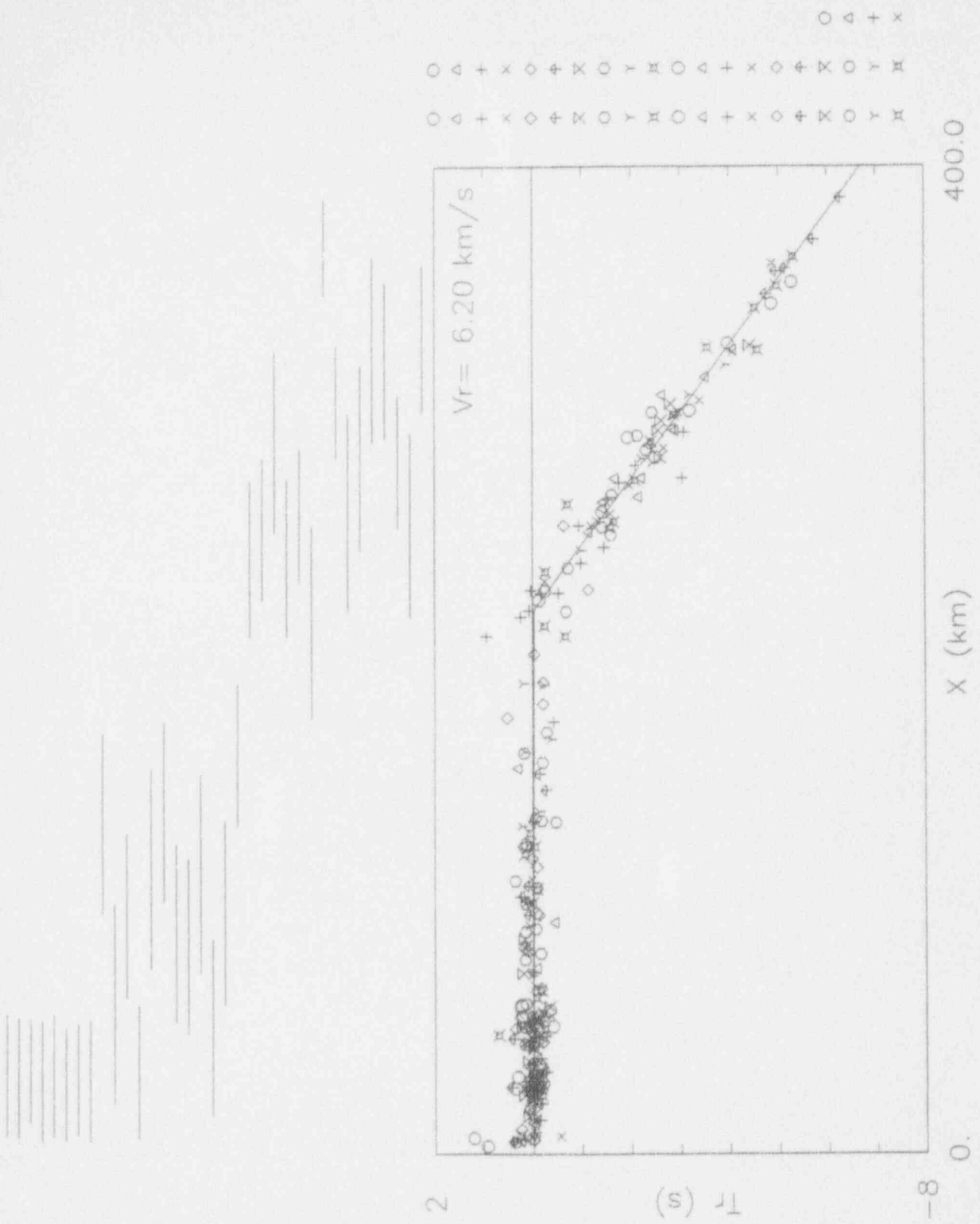

Figure 19. Reduced travel times for all earthquakes to the Anna subnetwork out to a distance of 400 km. Data are inverted with a Pg and Pn travel time branches. Pg velocity is 6.21±.04 km/s, Pn is 8.05±.09 km/s, and Pn intercept time is 8.12±.42 s.

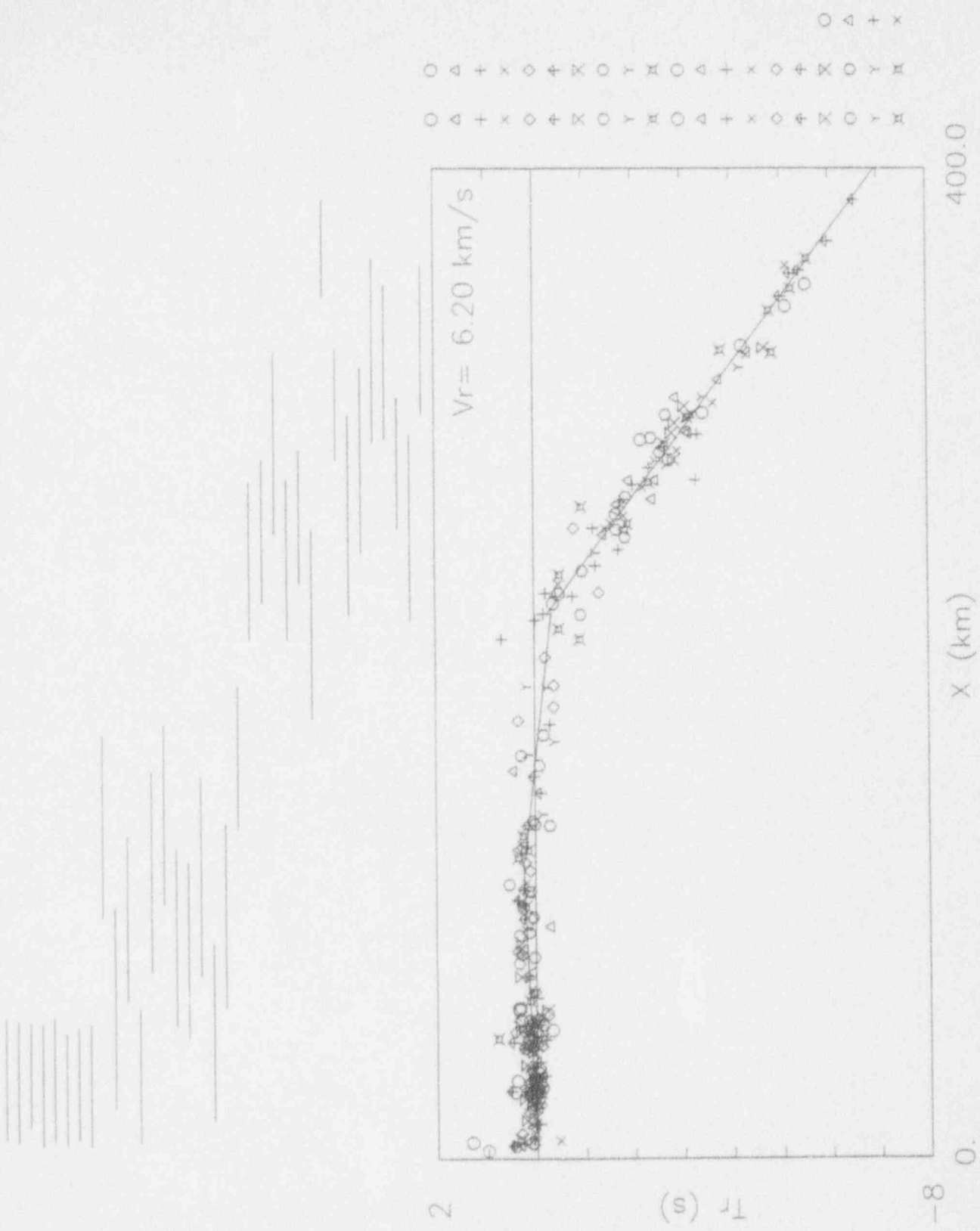

Figure 20. Reduced travel times for all earthquakes to the Anna subnetwork out to a distance of 400 km. Data are inverted with a Pg, P*, and Pn travel time branches. Pg is 6.125±.05 km/s, P* is 6.42±.12 km/s, with τ^* of .86±.42 s, and Pn is 8.05±.08 km/s with τn of 7.89±.43 s.

network. Nonetheless, the results are important. Figure 21 shows the linear travel time curve for all observations in the distance range 0 to 200 km. The immediate and most important conclusion is that the apparent velocity of 6.68 ± .08 km/s is significantly higher than that found for the Anna zone over the same distance range. One additional way to test this conclusion is to plot the travel times to the Indiana stations from events within the Anna zone where the Anna stations fix the origin times. This test is shown in Figure 22, and the apparent velocity for the Indiana stations is again 6.68 km/s, with an apparent intercept time of 1.12 ± .27 s. Since all the raypaths are from one direction in Figure 22, we could interpret the Indiana travel times as a Pg arrival where the velocity increases systematically from northeast to southwest across Indiana. However, the data in Figure 21 includes raypaths from the southwest that still yield a velocity of about 6.68 km/s; this velocity is a typical value for the P* lower crustal travel time branch. The Indiana travel times in Figure 22 imply that a crossover between Pg and P* might occur at a distance less than 100 km, but this can only be proven by analysis of the Indiana sub-network data in Figure 21. Unfortunately, the paucity of observations in the distance range between 0 and 100 km does not allow for a slower Pg travel time branch to be statistically defined. Although it is possible, and perhaps even likely, to have a Pg travel time curve with a 6.2 km/s velocity from 0 out to 100 km, the simplest interpretation for the Indiana sub-network is to use a single travel time curve with a lower crustal velocity of 6.68 km/s out to the crossover distance for Pn.

2.3.7 Pn for the Indiana sub-network

Observations of Pn are infrequent and of poor quality for the Indiana sub-network. Hence, both the crossover distance and the Pn velocity are poorly determined. Figure 21 shows that the Pn crossover occurs around a distance of 200 km; quantitative examination allows the crossover to be anywhere from 180 to 200 km. Figure 23 shows the P* and Pn branches for Indiana data between 0 and 300 km, with an assumed crossover at 200 km. The P*, τ_n, and Pn values all vary systematically as we change the assumed crossover distance. For example, with an assumed crossover distance of 180 km: P* is 6.51 ± .09 km/s, τ_n is 4.76 ± .72 s, and Pn is 7.92 ± .20 km/s (compare these values with those in Fig. 23). Given the covariance between τ_n and Pn, different solutions produce the same Pn travel time at a distance of 200 km. We shall use this constraint later when constructing Indiana crustal models.

There are several observations of Pn in the range from about 200 to 300 km as in Figure 23, and then there is a large data gap with Pn readings from the northeastern Ohio events in the distance range from 390 to 520 km. Dependent upon: (i) the value chosen for Pn crossover distance; and (ii) whether the faraway northeastern Ohio events are used; the value for Pn velocity varies between 7.9 and 8.6 km/s, with even larger formal uncertainties. The northeastern Ohio

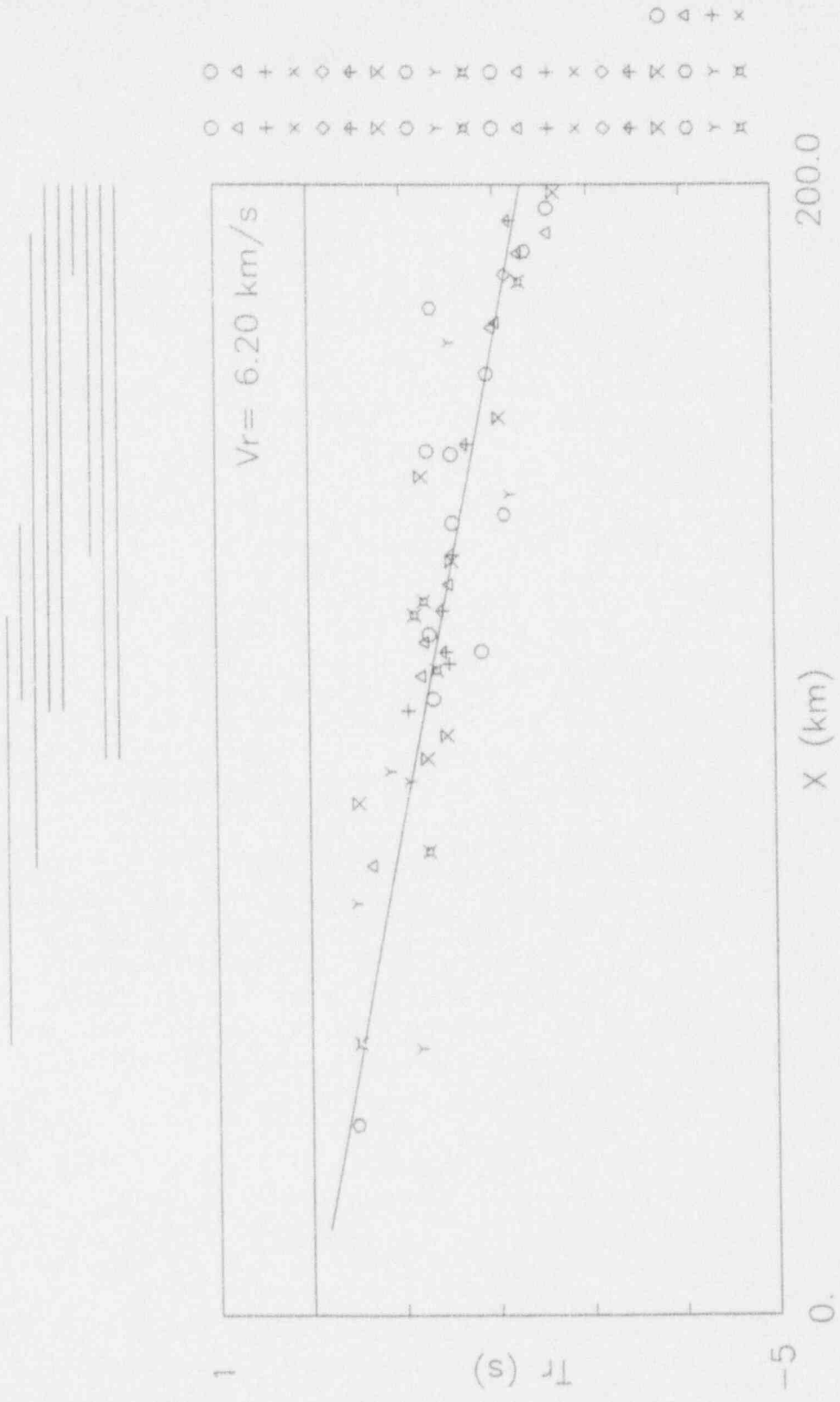

Figure 21. Reduced travel times for the Indiana sub-network.

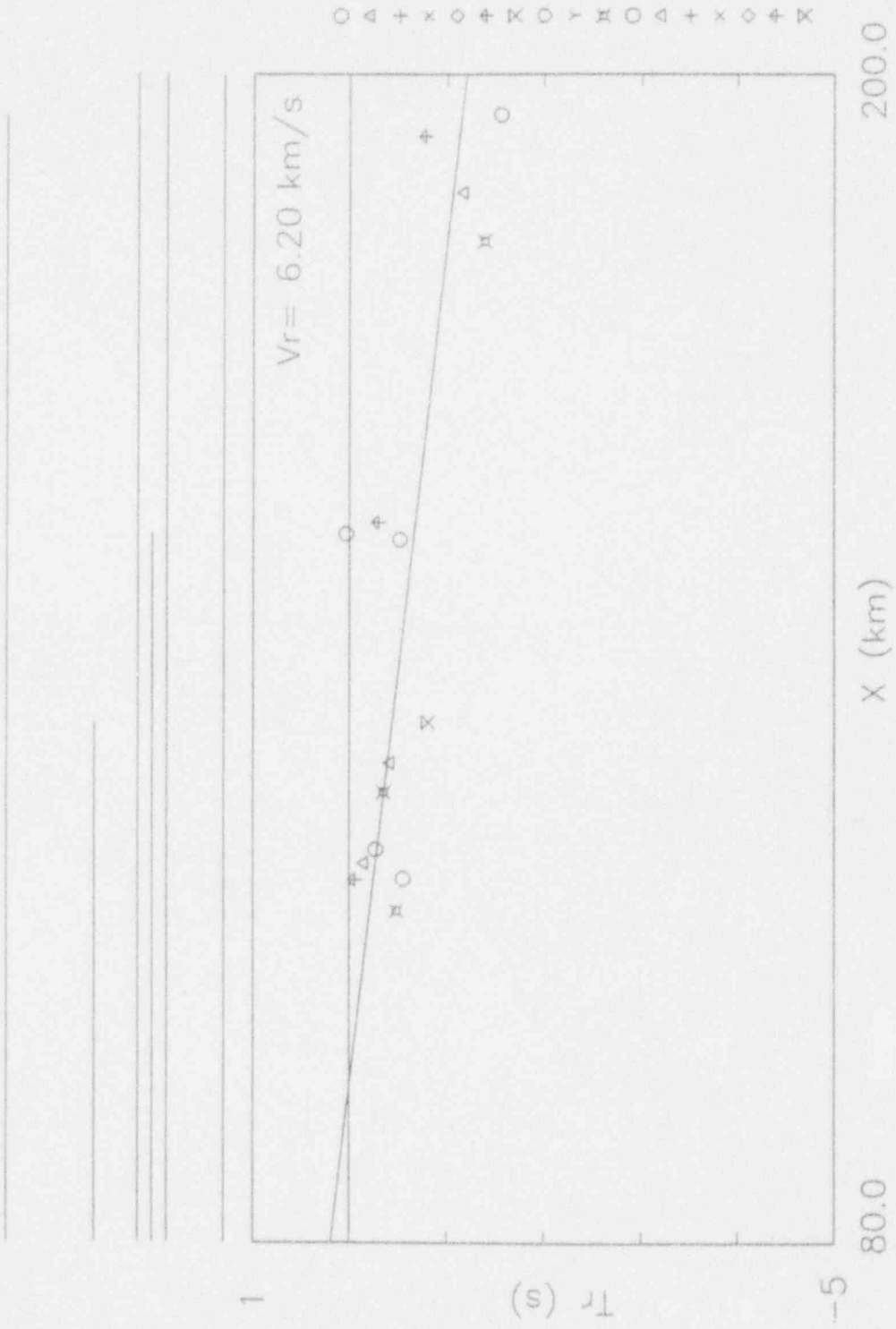

Figure 22. Reduced travel times for the Indiana sub-network with origin times fixed by the Anna sub-network.

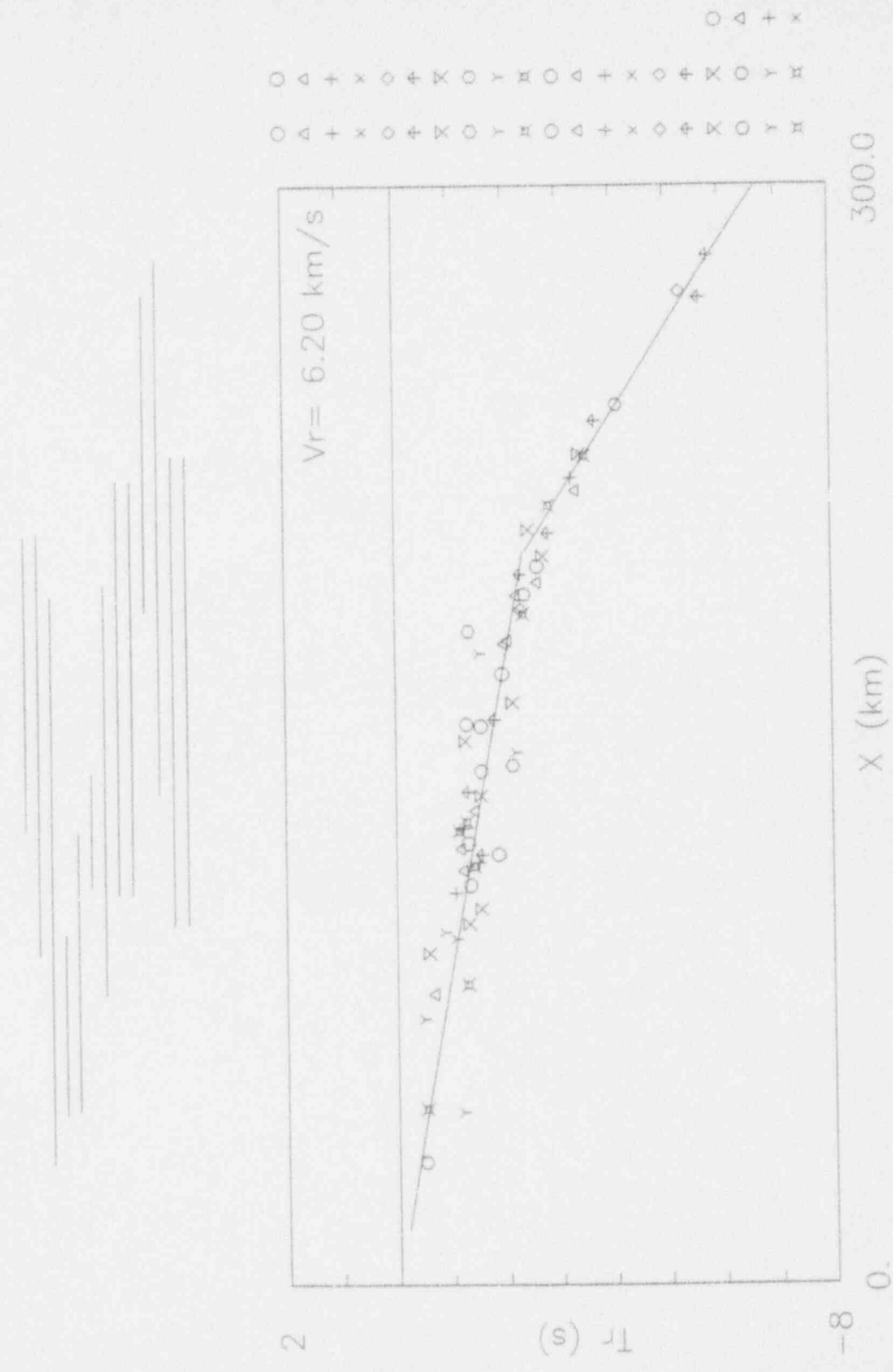

Figure 23. Reduced travel times for the Indiana sub-network with two travel time branches between 15 to 200 km and 200 to 300 km. Pg velocity is 6.67±.07 km/s, τn is 6.20±1.35 s, and Pn is 8.45±.42 km/s.

events tend to force a very high velocity. If we use the three readings from the 1986 Perry event, the velocity is 8.4 km/s. If we use only the Pn arrivals out to 300 km, the Pn velocity is 7.92 ± .20 km/s for a crossover distance of 180 km, or 8.45 ± .42 km/s fro a crossover of 200 km (Fig. 23). These values are not statistically different from each other, nor from the Pn velocity for the Anna sub-network.The safest conclusion is that Pn velocity is not reliably determined, and a "typical" value of 8.1 km/s for Pn in Indiana is consistent with the constraints. If we choose a Pn of 8.1 km/s, then we should a τn (with respect to P*) of 5.35 s to satisfy the travel time constraints.

2.3.8 S waves

While S waves are well observed from earthquake sources, it is difficult to reliably pick S arrival times. The data set of S arrival times is consequently much smaller and of poorer quality than the P wave data set. Figure 24 shows the S wave arrivals recorded by Anna stations out to a distance of 200 km. There is good overlapping coverage out to a distance of 160 km. Beyond that distance, there are only scattered disconnected observations at the Anna sub-network. Visual inspection suggests that the Sn crossover distance is about 180 km. The best-fit velocity over distance range 15 to 90 km is 3.68 ± .07 km/s (see Figure 25), faster than the 3.58 km/s value in Figure 24. If we add the S times from the Indiana stations between 0 and 180 km, the number of observations increases from 86 to 102; but the best-fit velocity is still 3.58 ± .02 km/s between 15 to 180 km. With the combined data set, we find best-fit velocities for the distance ranges: 15 to 60, 15 to 100, 15 to 140, and 15 to 180 km. The best-fit Sg velocity consistently decreases from 3.75 ± .09 km/s for 15 to 60 km to 3.59 ± .03 km/s at 15 to 140 km, then remains about the same for 15 to 180 km. This decrease in apparent Sg velocity beyond 60 km is similar to the behavior observed in the Anna P wave data - but more pronounced. We can not reconcile a change to a slower velocity with distance in the context of a horizontally layered crustal model.

To summarize, Figure 25 shows that if we allow two travel time curves, the S waves prefer a velocity of 3.68 ± .07 km/s up to 90 km and 3.55 ± .05 km/s from 90 to 180 km. A value of 3.75 km/s is found for Sg in the distance range of 15 to 60 km. For the purpose of comparison with the Anna Pg velocity, the best Sg velocity between 0 and 180 km is: 3.58 ± .03 km/s. Although we would like to use just the Indiana sub-network to separately constrain Sg in Indiana, the few observations do not allow for meaningful results.

We can make better use of all the S wave observations if we fix the origin times of each event by use of the P wave inversion origin times. This allows even one S wave arrival time for an event to give some information on the travel time curves. Figure 26 shows all Anna station S times with origin times fixed by the inversion results from Figure 20. The travel time curves plotted in Figure 26 are for a Sg velocity of 3.58, and a Sn velocity of 4.56 km/s with an intercept time of 11.5 s. The safest statement is the S arrival times in the Ohio-Indiana-

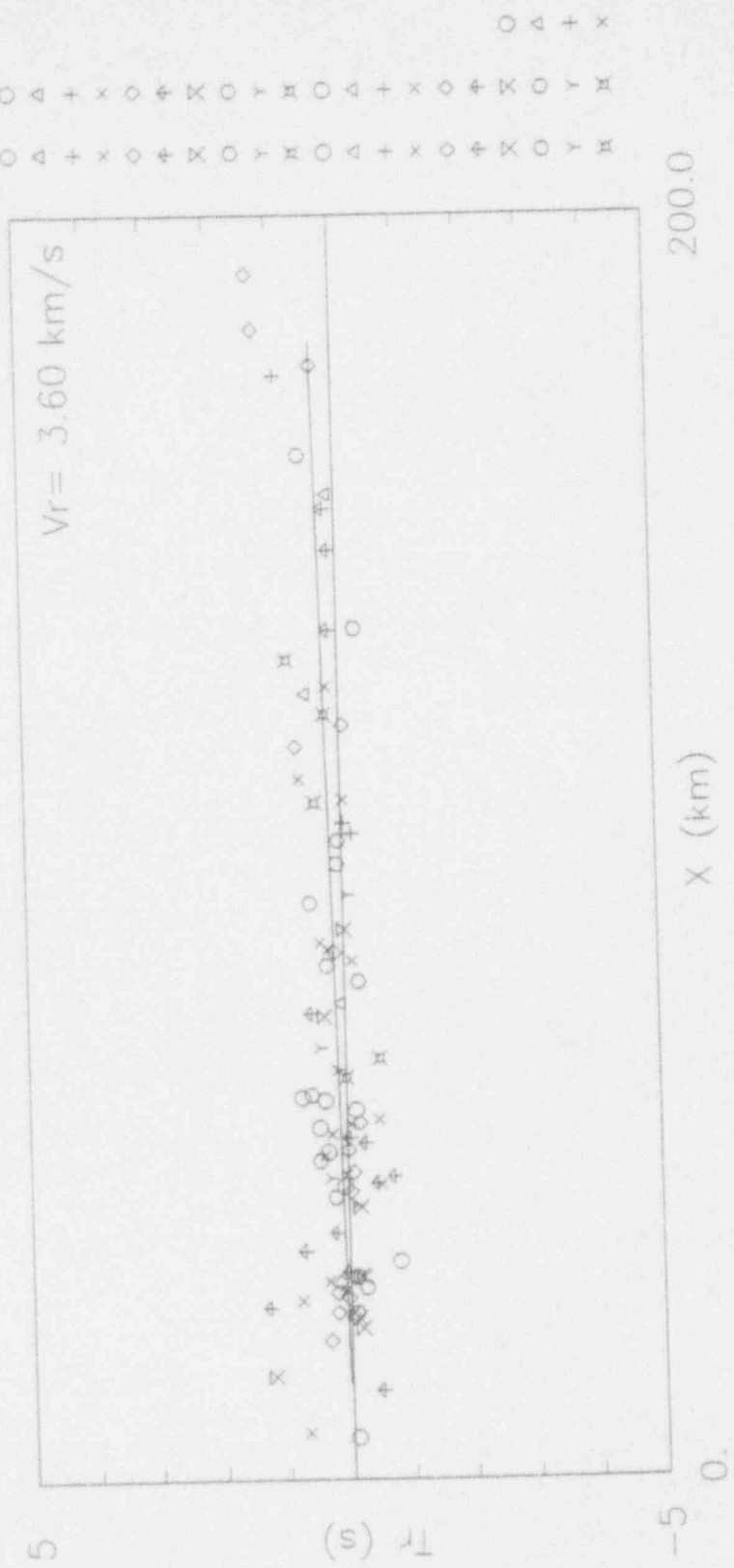

Figure 24. S waves. Reduced S travel times to Anna sub-network. Sg travel time branch is fit between 15 to 180 km, with a velocity of 3.58±.03 km/s.

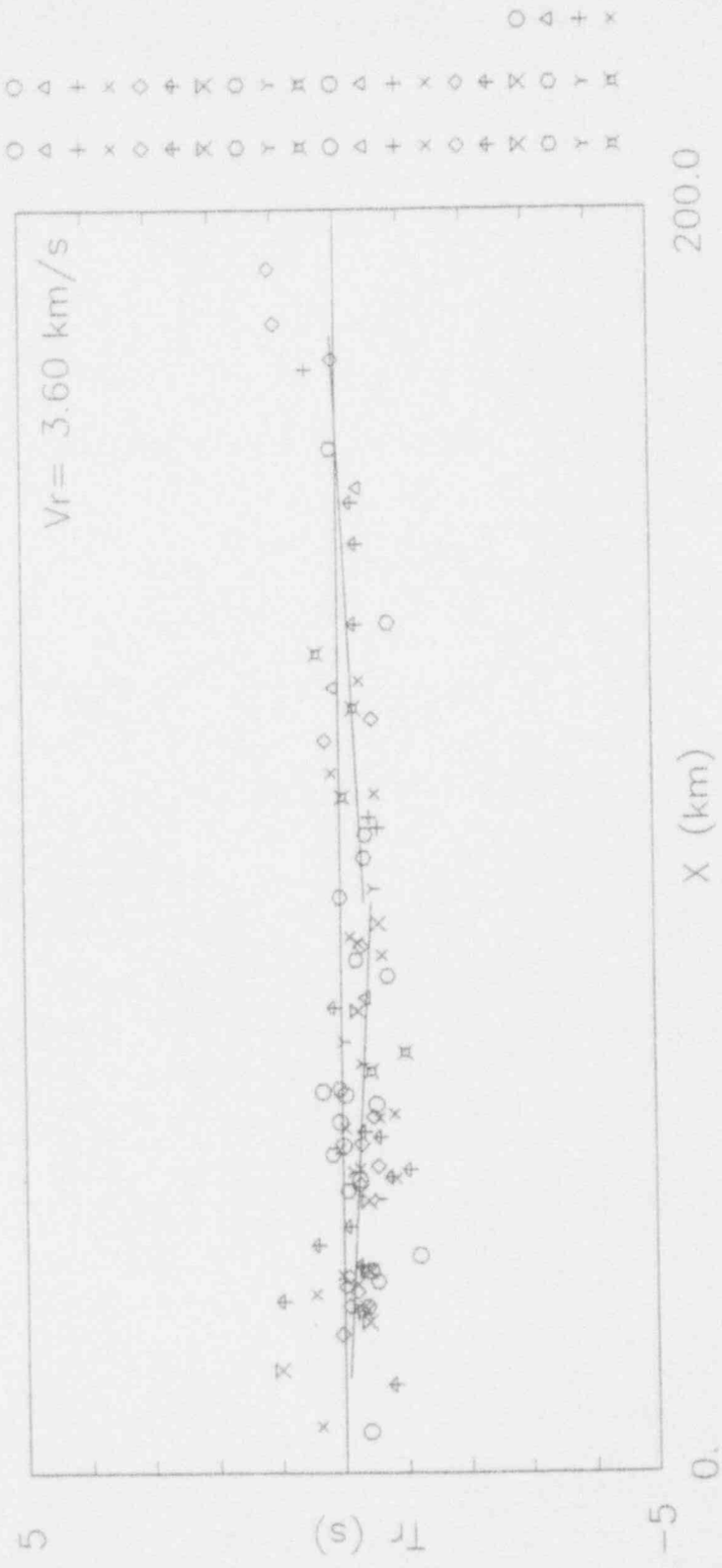

Figure 25. S waves. Two travel time branches are fit to Anna S times. Lines are fit to 15 to 90 and 90 to 180 km distance ranges.

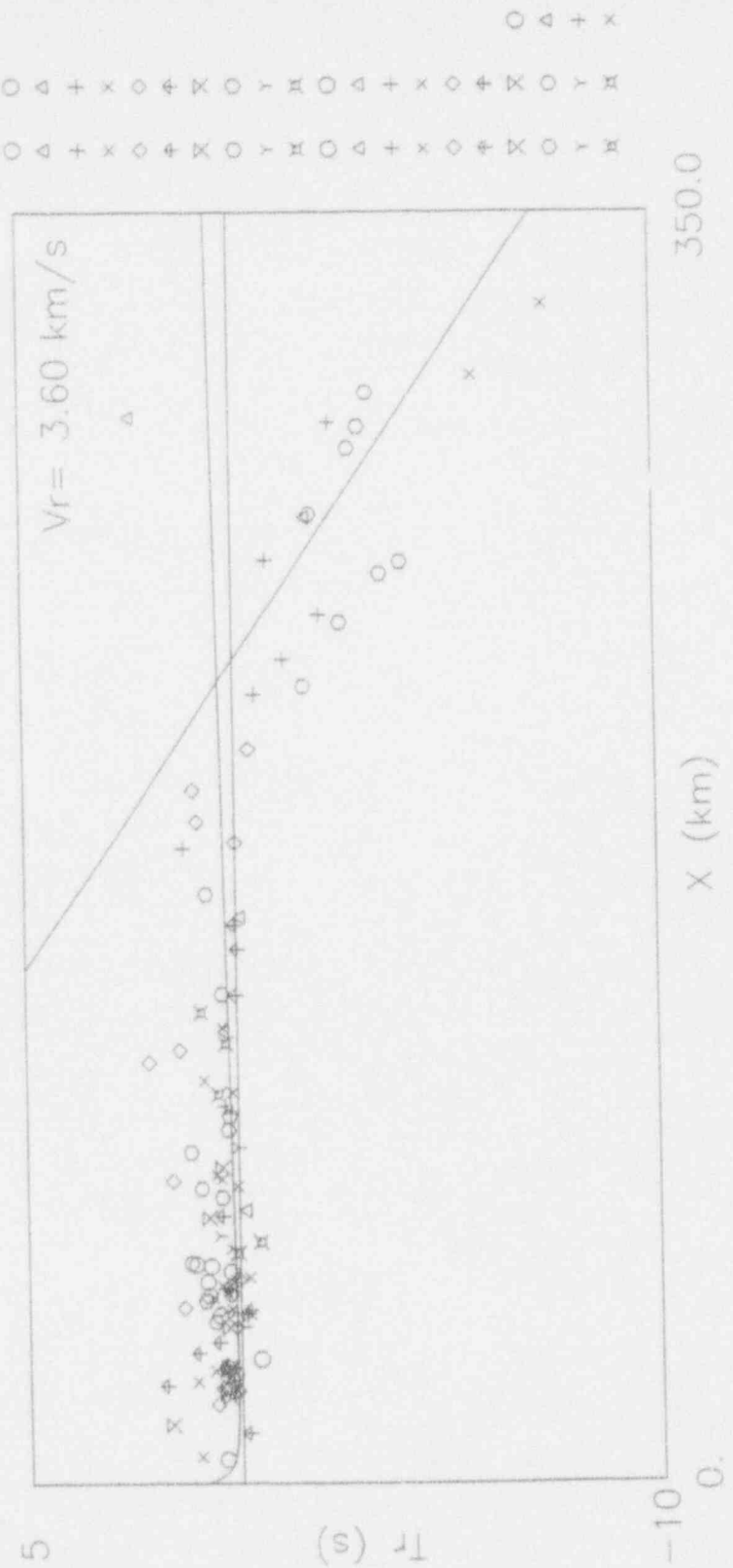

Figure 26. S waves. S waves at Anna sub-network, origin times are fixed by the P wave inversion run shown in Fig. 20.

Michigan region can be reasonably well-explained with a single simple model that uses typical Sg and Sn velocities.

2.4 Crustal structure models

The apparent velocities and intercept times of linear travel time curves can be directly translated into crustal models. A more general statement is that the apparent velocities and intercept times of the first arrival travel time curves place strong constraints on crustal structure. I shall first determine the simplest crustal models for the Anna and Indiana regions, then variations of these models will be considered.

2.4.1 Interpretative framework

The simplest interpretation of the results for the Anna sub-network is a homogeneous crust overlying a flat Moho. The main complication is that the source depth is not at the surface; thus the measured Pn intercept time is less than that for a surface source. The equation for travel time as a function of distance for the direct Pg arrival is:

$T(X)=(X^2+z^2)^{1/2}/Vg=(1+z^2/X^2)^{1/2}\ X/Vg$

where X is epicentral distance, z is source depth, and Vg is the Pg velocity. As X becomes much larger than z, the travel time curve becomes a straight line with T(X)=(X/Vg). If we add a low-velocity surficial layer with velocity V_L and thickness h_L, then the following formulas must be used to calculate X(p) and T(p) as a function of ray parameter, p:

$X(p)=p[z/\eta(Vg,p^{-1}) + h_L/\eta(V_L,p^{-1})]$

$T(p)=[z/(Vg^2\eta(Vg,p^{-1})) + h_L/(V_L^2\eta(V_L,p^{-1}))]$,

where the vertical slowness is $\eta(A,B)=(1/A^2 - 1/B^2)^{1/2}$. As p approaches 1/Vg, it is possible to rearrange the above equations to write travel time as a function of X:

$T(X)= \tau + X/Vg= \eta(V_L,Vg)h_L + X/Vg$

Thus, a thin surficial low velocity zone basically imparts a constant time shift of $\eta(V_L,Vg)h_L$ to the direct Pg travel travel line. In our data analysis, the intercept time of the Pg travel time line is set equal to zero. Therefore, our determination of velocity structure ignores any surficial low-velocity layer above the source depths, and crustal thickness is "approximately" referenced to the top of the layer with Vg velocity. The exact influence of a surficial layer will be considered in a following section on hypocentral depths. For the case of the Ohio-Indiana region, the thickness of the Paleozoic sedimentary layer is less than one kilometer.

We now focus on the downgoing head waves, where we ignore the influence of a thin surficial low-velocity layer. The theoretical travel time for a P* arrival is:

$T(X)=\tau + X/V^* = 2\eta(Vg,V^*)(h_1-z/2) + X/V^*$,
for distances greater than the critical distance,
$X^*_{crit}=[(2h_1-z)/(\eta(Vg,V^*)V^*)]$,
where h_1 is the thickness of the Vg layer and z is the source depth. Given the presumed existence of a lower crustal V* layer, the theoretical travel time for the Pn arrival is:
$T(X)=\tau + X/Vn = 2(\eta(Vg,Vn)(h_1-z/2) + \eta(V^*,Vn)h_2) + X/Vn$,
for distances greater than the critical distance,
$Xn_{crit}=2[(h_1-z/2)/\eta(Vg,Vn) + h_2/\eta(V^*,Vn)]/Vn$,
where h_2 is the thickness of the V* layer. If we choose a crustal model that has only the Vg layer for the entire crust, then:
$\tau=2\eta(Vg,Vn)(h_1-z/2)$,
$Xn_{crit}=(2h_1-z)/(Vn\eta(Vg,Vn))$,
where h_1 is now crustal thickness.

The data analysis provides us with the apparent velocity and τ of a travel time line. While the apparent velocity can be directly equated to the averaged flat-lying layer velocity, the above equations show that intercept time is systematically decreased by the source depth. It is always possible to define an "apparent" Vg layer thickness as:
$h'=h_1-z/2$.
We see that the true layer thickness can be found from $h_1=h'+z/2$ after we determine the earthquake depth. Since the τ for Pn (hereafter τn) is determined from several earthquakes over the Ohio-Indiana-Michigan region, it is quite possible that earthquake depths are different; this scatter in model assumptions will contribute to the statistical uncertainty in τn. The best-fit value for τn is then referenced to the average source depth for those earthquakes that control intercept time.

2.4.2 Models: Anna sub-network

Data analysis for the Anna sub-network indicates a Pg velocity of 6.20 to 6.21 km/s with a Pn velocity and intercept of 8.07 km/s and 8.2 to 8.5 s. These values give an apparent crustal thickness, h', of 39.8 to 41.0 km. If we translate the standard error of τn intercept times (±0.4 s) into crustal thickness error, keeping velocities the same, we find an error of ±2 km. In detail, errors in τn and Pn covary such as to reduce the error in crustal thickness. For example, the covariance from the inversion in Figure 19 translates into a depth error of ±1.4 km rather 2.0 km. However, in the following analysis we will quote the more conservative errors based on τn errors.

Recall that there is evidence of a P* layer, either as: (i) an unusually low velocity as a first arrival; or (ii) a second arrival. We use the inversion results of Figure 20 to find an apparent Pg layer thickness of $h_1'=8.9\pm4.3$ km, and a P* layer thickness of 32.2 km with an error of ±2.3 km from the uncertainty in τn, and an error of -±4.8 km from the

±4.3 km error in h_1'. These results give a crustal thickness of 41.1 ± 2.8 km. To consider the effect of P* as a second arrival, we shall assume a value for P* and then find the maximum thickness of the lower crustal P* layer. For example, choose a value of 6.63 km/s for P*. Then with a τ^* of 2.25 s, the P* travel time curve passes through the Pg-to-Pn crossover at 220 km in Figure 19. Choosing τ^* in this fashion yields the maximum thickness of the P* layer and total crustal thickness. From these parameter values, the layer thicknesses of h_1' and h_2 are 19.7 and 23.6 km, respectively, with a total (apparent) crustal thickness of 43.3 km, which is only 4 km thicker than the estimate from a single layer with Pg velocity. It is possible to derive a general relationship for total apparent crustal thickness for measured values of Vg, Vn, and τ_n, and assumed value of V*:

$$h_{crust}=(\tau_n/2\eta(Vg,Vn))[\eta(Vg,V^*)/\eta(Vg,Vn) + (\eta(Vg,Vn)-\eta(Vg,V^*))/\eta(V^*,Vn)]$$

$$=h' [\eta(Vg,V^*)/\eta(Vg,Vn) + (\eta(Vg,Vn)-\eta(Vg,V^*))/\eta(V^*,Vn)]$$

This formula provides a shortcut to the intermediate results from the above two-layer crust formulas, and shows the effect of an assumed lower crustal layer as a factor multiplying the apparent crustal thickness h'. Figure 27 shows the numerical value of this factor for assumed V* velocities ranging from Vg to Vn. For our measured values of Vg and Vn, the maximum crustal thickness is 45.2 km for V* of 7.4 km/s. Note that the above analysis presumes that V* is greater than Vg; it is possible to reduce the total crustal thickness if we allow the lower crustal velocity to be less than Vg.

Of course, the minimum thickness of the lower crustal layer is 0 km, but the fact that a velocity of about 6.6 to 6.7 km/s is sometimes observed as a second arrival would argue that a faster lower crustal layer of some thickness less than 24 km does exist.

Analysis of Anna sub-network S arrival times gives an Sg velocity of around 3.7 km/s between 0 and 60 km distance, and a velocity of 3.58 km/s for 0 out 180 km. The best estimate of Sn is 4.56 to 4.58 km/s (also see Christensen et al., 1986). The Sg times in Figure 26 seem to be offset by several tenths of a second. This offset with respect to the Pg baseline is consistent with a thin low-velocity surficial layer. If we use an apparent crustal thickness of 40 km from the above simple P model together with the above Sg and Sn velocities, then the intercept time for the Sn branch is 13.94 s. Theoretical travel time curves for this simple S model are plotted in Figure 26; the predicted Sn line fits one group of Sn arrivals. The Sn intercept time of 11.3 s from Christensen et al. (1986) seems to fit the other "branch" of Sn arrivals in Figure 26. Crustal thickness for a τ_n of 11.3 s is only 32 km. This ambiguity in τ_n cannot be resolved at present, more high-quality S times are required. that a lower crustal S velocity is not observed by the Anna sub-network. If one accepts a lower crustal layer for the P waves, then the S model can be modified by assuming a Poisson's ratio.

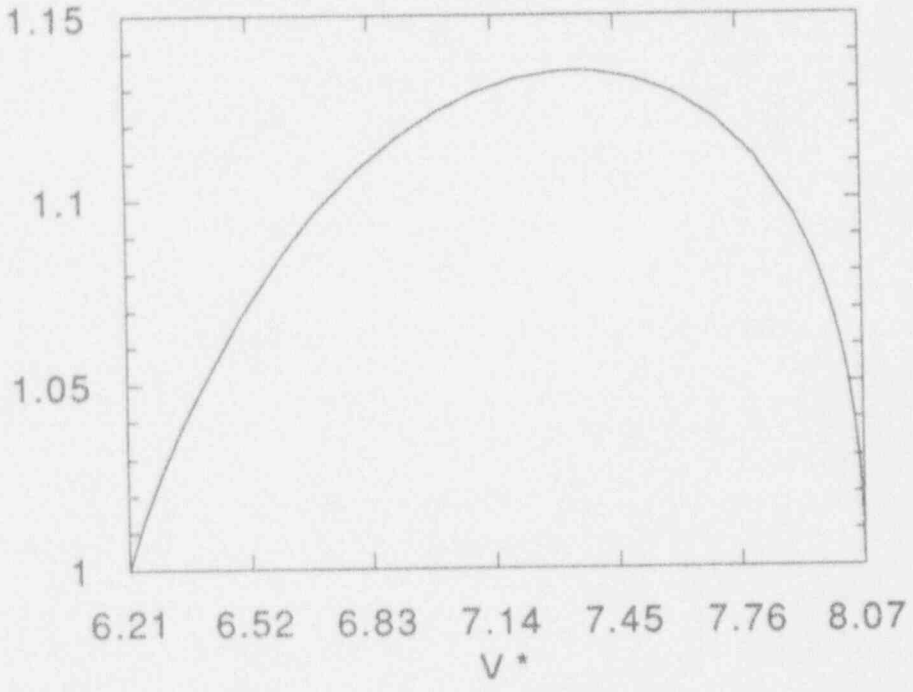

Figure 27. Plot to show h_{crust} factor due to a variable V*.

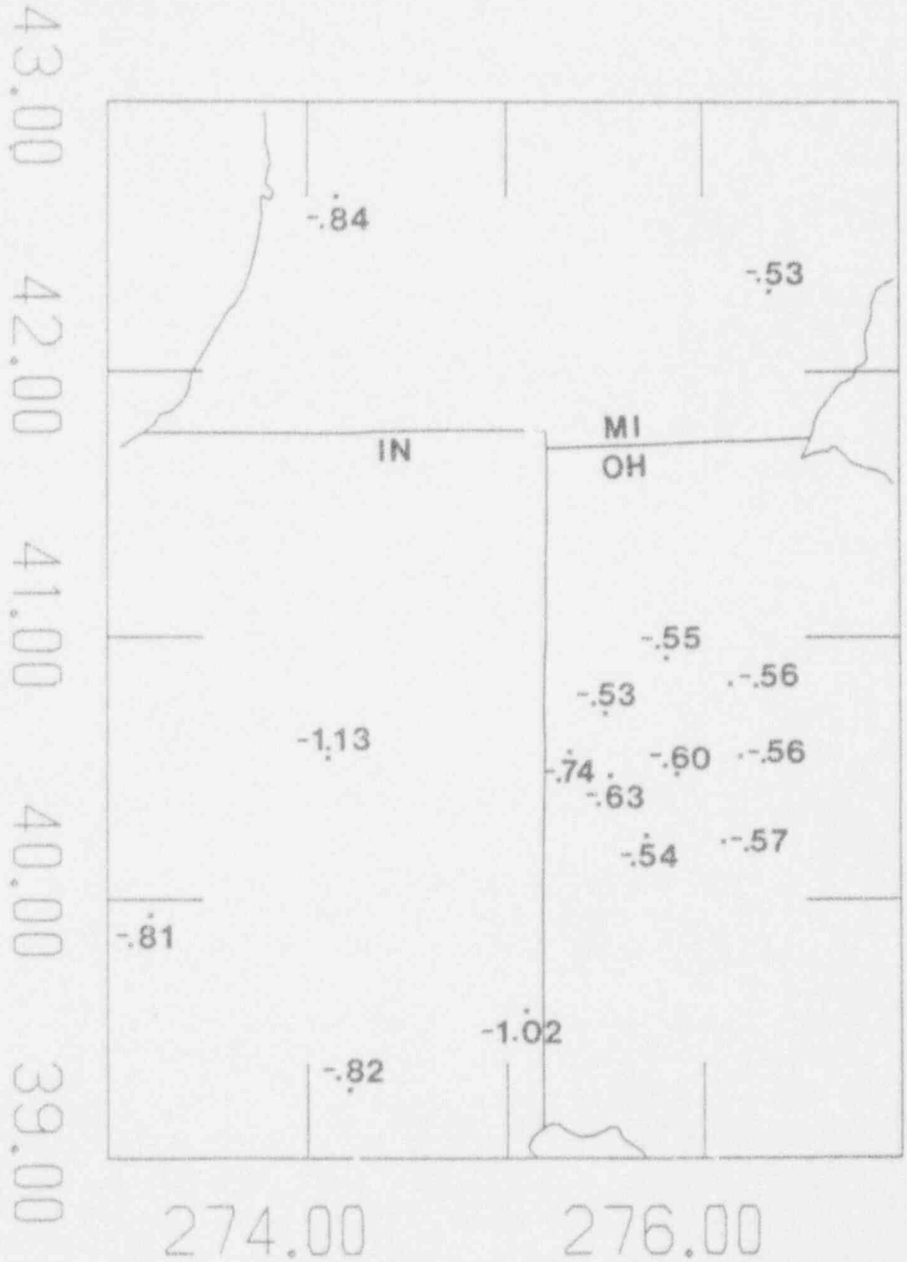

Figure 28. Summary map of average teleseismic P wave residuals at the network stations.

2.4.2 Indiana sub-network

The simplest model is to assume that the apparent velocity of 6.68 km/s is Pg, and assume a Pn and τ_n of 8.1 km/s and 5.35 s. This yields an apparent crustal thickness of 31.5 km. This value is much thinner than found in other parts of the Central Province. We would anticipate that a more typical Pg upper crustal layer should exist. The data analysis would allow a Pg velocity of 6.2 km/s out to a crossover distance of perhaps 100 km, with a τ^* of 1.12 s (see Figure 22). With this assumption, the thickness of the Pg layer would be 9.3 km. The P* layer would be 26.6 km thick and the total crustal thickness is then 35.9 km.

Additional evidence for a "faster" crustal structure beneath Indiana, as compared to Anna, comes from the average teleseismic P wave residuals as compiled by Christensen et al. (1986). Figure 28 shows that the Indiana stations are 0.2 to 0.5 s faster than the Anna stations. In detail, AN11 is faster than the other Anna stations, but strong azimuthal dependence of the travel time residuals complicates any detailed explanation. Nonetheless, the half second difference between Indiana and Anna corroborates the notion of a thinner crust or a faster crust, or both, beneath Indiana as compared to the Anna region. The clear differences in the P travel time data between Anna and Indiana translate into significant differences in crustal structure. Figure 29 shows the various crustal models, referenced to the top of the Pg layer, and vertical travel times. The teleseismic residuals will depend on the one-way vertical times from 50 up to 0 km depth, and the postulated crustal models predict that Indiana teleseismic residuals will be 0.3 s faster than Anna, more or less consistent with the teleseismic observations. The two-way Moho times in Figure 29 are not in violation of the COCORP profiles in Pratt et al. (1989). The paucity of S arrival times for the Indiana sub-network does not allow for any significant distinctions between Anna and Indiana for the S wave structure.

Figure 29 also shows vertically averaged parameters for the average mid-continent model of Braile (1989). While the crustal thickness of any Anna model is the same as the average mid-continent model, average crustal velocity for Anna is anomalously slow. It appears that Indiana, with a well-developed P* layer, is consistent with the "typical" average mid-continent crustal structure. Our estimate of the crustal thickness for Indiana is thinner than the mid-continent average, but this difference is probably not statistically significant. Thus, the safest statement is that the Anna zone would appear to be anomalously slow in its crustal structure compared to the average mid-continent crustal model - an important conclusion given its seismicity.

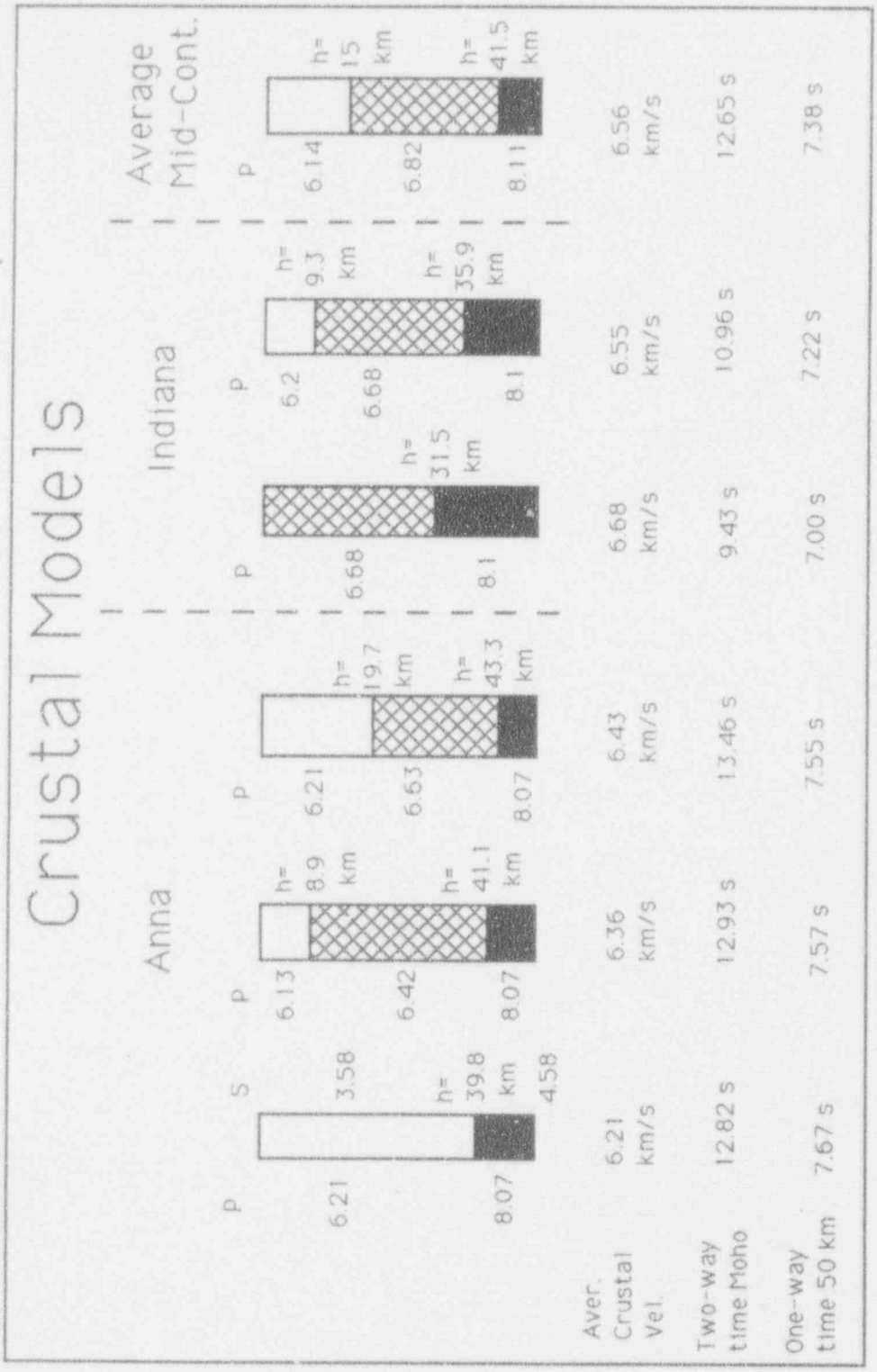

Figure 29. Various crustal sections and properties for the Anna and Indiana regions, with the average Mid-Continent model shown for reference.

TABLE 3

LOCAL AND REGIONAL EVENTS FROM
JUNE 1977 THROUGH SEPTEMBER 1992

No	Date Year	Mo	Da	Origin Time Hr	Mi	Sec (GMT)	Location Lat. #N	Long. #W		Magnitude (duration)	Depth (km)
1	1977	06	17	15:	39:	47.3	40.57	84.67		3.3 m_b	--
				15:	39:	46.9	40.705	84.707	(D&G)	---	--
2	1979	11	09	21:	29:	58.7	38.417	82.869	(NEIS)	3.6 m_{bLg}	--
3	1980	07	10	11:	40:	53.3	40.415	84.111		0.9	--
4	1980	07	27	18:	52:	21.7	38.18	83.94		5.1 m_b	15
5	1980	08	20	09:	34:	54.0	41.97	82.99	(Revised)	3.2 m_{bLg}	--
6	1980	09	26	12:	27:	25.6	40.430	84.085		0.5	--
7	1980	10	04	11:	46:	58.0	39.80	83.75		2.0	--
8	1980	12	10	02:	30:	54.3	40.43	84.11		1.2	--
9	1981	01	04	07:	17:	37.1	40.418	84.087		1.8	5-7
10	1981	02	07	05:	45:	43.0	40.417	84.087		1.8	5-7
11	1981	03	15	03:	46:	30.3	41.10	84.35		1.2	--
12	1981	05	15	23:	15:	14.0	40.88	84.34		0.8	--
13	1981	05	19	05:	56:	11.7	40.407	84.085		1.2	2-8
14	1982	11	26	08:	25:	04.9	42.17	85.48		2.0-2.5	--
15	1983	01	12	02:	49:	41.1	39.28	84.60		1.9	--
16	1983	01	22	07:	46:	59.3	41.86	81.16		2.7 m_{bLg}	--
17	1983	07	05	02:	58:	52.9	40.43	84.10		2.1	5-7
18	1983	07	13	01:	17:	34.8	40.43	84.10		1.4	--
19	1983	09	30	02:	33:	44.8	41.59	84.33		1.3	--
20	1983	11	04	21:	00:	59.8	40.43	84.10		0.4	--
21	1983	11	04	22:	50:	00.5	40.43	84.10		0.9	--
22	1983	11	05	02:	36:	35.8	39.68	85.73		1.1	--
23	1983	12	03	21:	29:	41.0	42.70	88.30		1.4	--
24	1983	12	07	22:	57:	01.6	41.70	83.50		1.1	--
25	1983	12	10	19:	01:	55.2	40.43	84.11		0.7	--
26	1984	01	03	07:	57:	58.6	40.42	84.11		0.4	--
27	1984	01	14	20:	14:	32.5	41.67	83.45	(Revised)	2.6 m_b	--
28	1984	07	28	23:	39:	27.3	39.27	87.09		4.0 m_{bLg}	--
29	1984	08	29	06:	50:	59.0	39.25	87.50		3.2 m_{bLg}	--
30	1984	08	29	18:	56:	27.2	39.09	87.69		2.7 m_{bLg}	--
31	1985	03	10	20:	46:	01.1	40.52	84.39		1.4	--
32	1985	03	10	20:	49:	14.1	40.52	84.40		1.7	--
33	1985	03	17	11:	57:	06.7	39.65	83.46		1.9	--
34	1985	04	14	11:	39:	51.3	41.40	80.37		2.0	--
35	1985	08	25	14:	30:	01.6	38.54	84.98		1.6	--
36	1985	08	25	16:	27:	11.9	40.97	84.22		1.5	--
37	1985	09	09	22:	06:	31.0	41.850	88.006	(NEIS)	3.0 m_{bLg}	--
38	1986	01	12	11:	38:	50.2	40.77	83.27		0.8	--
39	1986	01	13	11:	39:	20.4	40.80	84.13		0.5	--
40	1986	01	31	16:	46:	41.4	41.59	81.21	(NEIS)	5.0 m_b	--
41	1986	03	30	07:	42:	42.1	41.37	83.67		1.4	--
42	1986	07	12	08:	19:	39.5	40.55	84.39	(Revised)	4.5 m_b	5
43	1986	11	17	07:	03:	04.6	40.55	84.37		0.7	--

No	Date Year	Mo	Da	Origin Time Hr	Mi	Sec (GMT)	Location Lat. #N	Long. #W		Magnitude (duration)	Depth (km)
44	1987	02	01	12:01:55.7			39.23	82.43	(UK)		
45	1987	03	27	07:29:30.5			35.57	84.23	(CERI)	4.2 m_{bLg}	19
46	1987	06	10	23:48:54.0			38.80	87.90	(NEIS)	4.9 m_b	5
47	1987	06	11	00:15:50.0			38.87	87.95	(SLU)		--
48	1987	07	11	00:04:29.5			36.10	83.82	(CERI)	3.6	--
49	1987	07	13	05:49:18.9			41.90	80.73	(JCU)	3.8 m_{bLg}	2
50	1987	07	13	07:52:12.2			41.90	80.70	(JCU)	3.0 m_{bLg}	2
51	1987	07	13	13:05:23.1			41.91	80.75	(JCU)	2.9 m_{bLg}	2
52	1987	07	16	04:49:40.3			41.91	80.75	(JCU)	2.7 m_{bLg}	2
53	1987	08	31	17:12:35.2			38.30	89.71	(SLU)	3.1 m_{bLg}	9
54	1987	09	29	00:04:57.5			36.84	89.21	(SLU)		--
55	1987	10	14	15:49:40.3			37.05	88.78	(SLU)	3.8 m_{bLg}	--
56	1987	11	17	15:52:21.4			38.73	87.96		3.2 m_{bLg}	--
57	1988	01	05	14:39:17.9			38.74	87.96		3.3 m_{bLg}	--
58	1988	09	07	02:28:08.6			38.13	83.87	(UK)	4.5 m_b	10
59	1988	10	05	00:38:52.4			38.70	87.90	(NEIS)	3.4 m_b	--
60	1988	10	22	16:46:29.6			40.45	84.11		2.2 m_L	--
61	1988	12	08	02:10:41.2			40.55	84.43		1.1 m_L	--
62	1989	01	04	16:06:34.1			40.64	84.26		0.7 m_L	5
63	1989	04	27	16:47:50.8			36.02	89.77	(SLU)	4.4 m_d	--
64	1989	05	14	00:16:09.6			36.74	89.71	(SLU)	3.9 m_d	--
65	1989	07	15	00:08:01.8			38.70	85.58	(UK)	3.1 m_{bLg}	7
66	1990	01	24	18:20:26.6			38.10	86.47	(UK)	4.0 m_b	--
67	1990	01	30	03:48:00.9			40.65	84.31		1.0 m_L	--
68	1990	03	02	07:01:16.8			38.90	89.10	(NEIS)	3.4 m_{bLg}	10
69	1990	03	09	21:01:54.9			38.11	86.44	(UK)	2.9 m_b	--
70	1990	04	17	10:27:36.5			40.49	84.83		2.2 m_L	--
71	1990	06	04	11:26:48.7			41.08	83.51		2.3 m_L	--
72	1990	09	26	13:18:51.3			37.17	89.58	(NEIS)	4.6 m_bL_g	--
73	1990	10	24	08:20:04.3			38.31	88.99	(NEIS)	3.5 m_bL_g	--
74	1990	12	17	05:24:59.1			40.13	87.14	(UM)	3.2 m_bL_g	--
75	1990	12	20	14:04:17.6			39.60	86.42	(UM)	3.6 m_bL_g	--
76	1991	03	07	10:52:57.6			39.56	86.42	(UM)	0.6 m_d	--
77	1991	05	04	01:18:54.9			36.56	89.82	(SLU)	5.0 m_bL_g	--
78	1991	07	24	21:37:12.3			39.75	84.59	(UM)	1.0 m_d	--
79	1991	11	11	09:20:47.2			38.7	87.9	(NEIS)	3.8 m_bL_g	--

NEIS: National Earthquake Information Service. CERI: Center for Earthquake Research and Information, UK: University of Kentucky, UM: University of Michigan, SLU : St. Louis University, JCU: John Carroll University, D&G: Dewey and Gordon, 1984

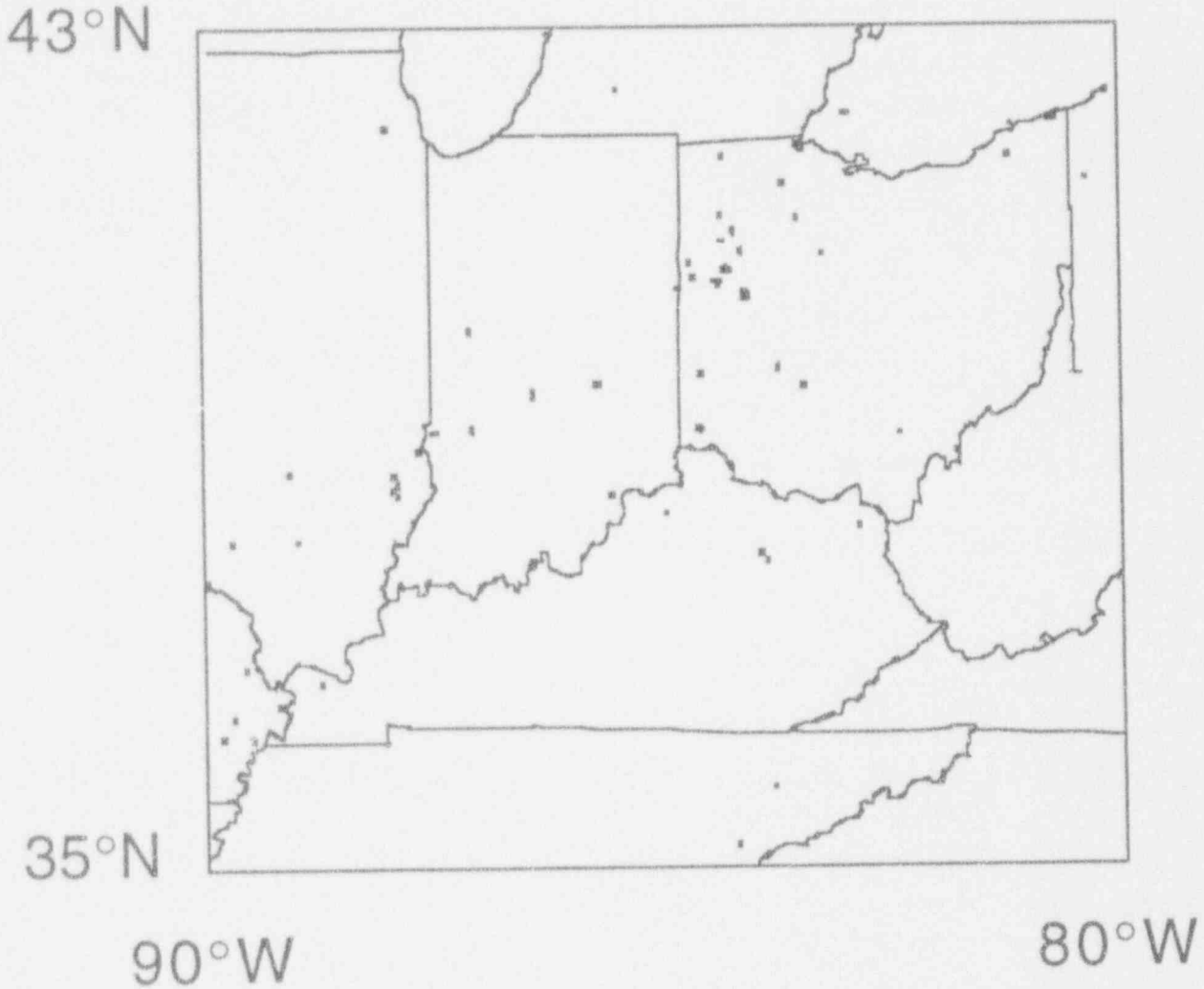

Figure 29A. Map of seismicity in and around the Anna seismic zone, over the entire period of network operation. Epicenters are from Table 3. There were no reliable local epicenters determined in the period from Sept. 1991 to Sept. 1992, although some activity in Indiana was detected.

3. Seismicity

Table 3 lists the earthquakes that have occurred in the Ohio-Indiana-Michigan region since 1977. All listed epicenters are plotted in Figure 29A. Many regional events that occurred in adjacent regions are not listed as they appear in the earthquake catalogs of other regional networks. We shall present detailed discussions of hypocentral depths of Anna zone earthquakes, then offer more speculative results on the association with basement features.

3.1 Earthquake depths

One curious feature of Anna seismicity is the cluster of earthquakes a few kilometers southeast of station AN1. A glance at Figure 11a shows that 6 earthquakes occur close enough to stations such that the travel time deviation from a straight line is detected; 5 of these events are in this Anna cluster. Hypocentral depth is essentially determined by this travel time deviation and the epicentral distance of the closest station. These 5 events not only allow hypocentral depth to be determined, but should also give a clear indication of the expected scatter. The inversion of the arrival times for these 5 events is shown in Figure 30, where we also plot the arrival times grouped by station. Theoretical curves are also shown for hypocentral depths of 4 and 10 km for a velocity of 6.2 km/s, the overall best velocity for Pg recorded by the Anna stations. Figure 30 shows that the scatter in arrival times at AN1 is no greater than the scatter at the other stations. Thus, the scatter at AN1 can be attributed to statistical errors in the readings rather than hypocentral depth variations. In other words, the data are consistent with all five events occurring at the same depth. It seems that a good choice for the depth is around 5 km.

We now consider in detail the influence of a low-velocity surficial layer. A straightforward estimate of hypocentral depth comes from the travel time residual at X=0 with respect to the best-fit straight line travel time curve projected back to the epicenter. Let the travel time at X=0 be $T_0 = z/Vg$, then for a model with just the Pg layer, we would estimate the depth as:

$z=Vg\,T_0$.

Now, let the crustal model have a surficial layer with thickness h_L and velocity V_L. The true travel time at X=0 is:

$T_0=z/Vg + h_L/V_L$,

where z is the depth from the top of the Vg layer. Data analysis of the arrival times finds the travel time curve given by:

$T(X)= \tau + X/Vg$

$T(X)= h_L\eta(V_L,Vg) + X/Vg$.

Thus, the apparent travel time at X=0 will be:

$T_{app}=T_0 - \tau = T_0 - h_L\eta(V_L,Vg) = z/Vg + h_L(1/V_L - \eta(V_L,Vg))$.

But we would still estimate depth as:

$z_{app}= Vg\,T_{app} = z + h_L Vg(1/V_L - \eta(V_L,Vg)) = z + h_L f$

where f is a non-dimensional factor that depends solely on the velocities Vg and V_L. Of course, the true hypocentral depth with respect to the surface is:
$z_{surf} = z + h_L = z_{app} + h_L(1-f)$.
To calculate a particular example relevant to the Anna zone, let Vg=6.2 km/s, V_L=5.0 km/s (see Zhu & Brown, 1986; Braile, 1989; for velocities of Paleozoic sedimentary layer), then f= 0.507 and z_{app} is depth below the top of the Pg layer plus half the thickness of the surficial low-velocity layer. For the example of the Anna zone earthquakes, the Paleozoic section thickness is less than one kilometer, so we can obtain the "best" estimate of hypocentral depth from the top of the V_L layer (i.e. the "surface") by adding half a kilometer to the apparent depths found above. Apparent hypocentral depth will be further tested in the next section.

Two other earthquakes occur within 5 kilometers of a station. The earthquake of 10/22/88 occurs slightly north of the Anna "cluster" and just 3 km to the southeast of AN1. The travel time residual at AN1 is about one second. If we assume that this reading is not in error and that the epicentral distance is correct, then the apparent hypocentral depth of the earthquake is more than 10 km. The earthquake of 8/25/85 is located 6.4 km to the northwest of station AN12, and the residual at AN12 is 1.2 to 1.4 s. Again, this implies an apparent depth of more than 10 km. To minimize the source depth, we can simply place the epicenter at AN12, but the hypocentral depth is still 8 km. There are no other earthquakes in this vicinity, thus we can not decide whether the AN12 reading is in error, or if the 8/25/85 event really is deeper than the events in the Anna cluster.

Hypocentral depth variations can theoretically be determined by the shift in crossover distance. However, reliable results would require that the crossover distance be well resolved, and that crustal structure is known to great precision. I do not believe that either condition is satisfied for the Anna data set.

3.2 Relocations of Anna cluster earthquakes

This cluster is one of the most interesting spatial features in the Anna seismicity over the time period studied. The locations of events in the AN1 cluster are all within 3.5 km of each other. These locations are based on the different procedures and possibly different crustal velocity models over the years. Hence, I have relocated four of the best recorded events in the AN1 seismicity cluster with the same program using a single upper crustal velocity of 6.2 km/s. In addition to the P arrival, S wave arrival times have been used for stations AN8, AN4, AN11,and AN9 for the 1/4/81 event. The hypocentral depth is fixed and the program finds the best epicenter and origin time. The best depth can then be selected by the overall minimum RMS. Except for the 5/19/81 event which has the smallest positive residual at AN1, the best depths are all 5 to 6 km. In addition, the locations are virtually identical to a fraction of a kilometer! We can conclude that these earthquakes define a very small source region that has generated half

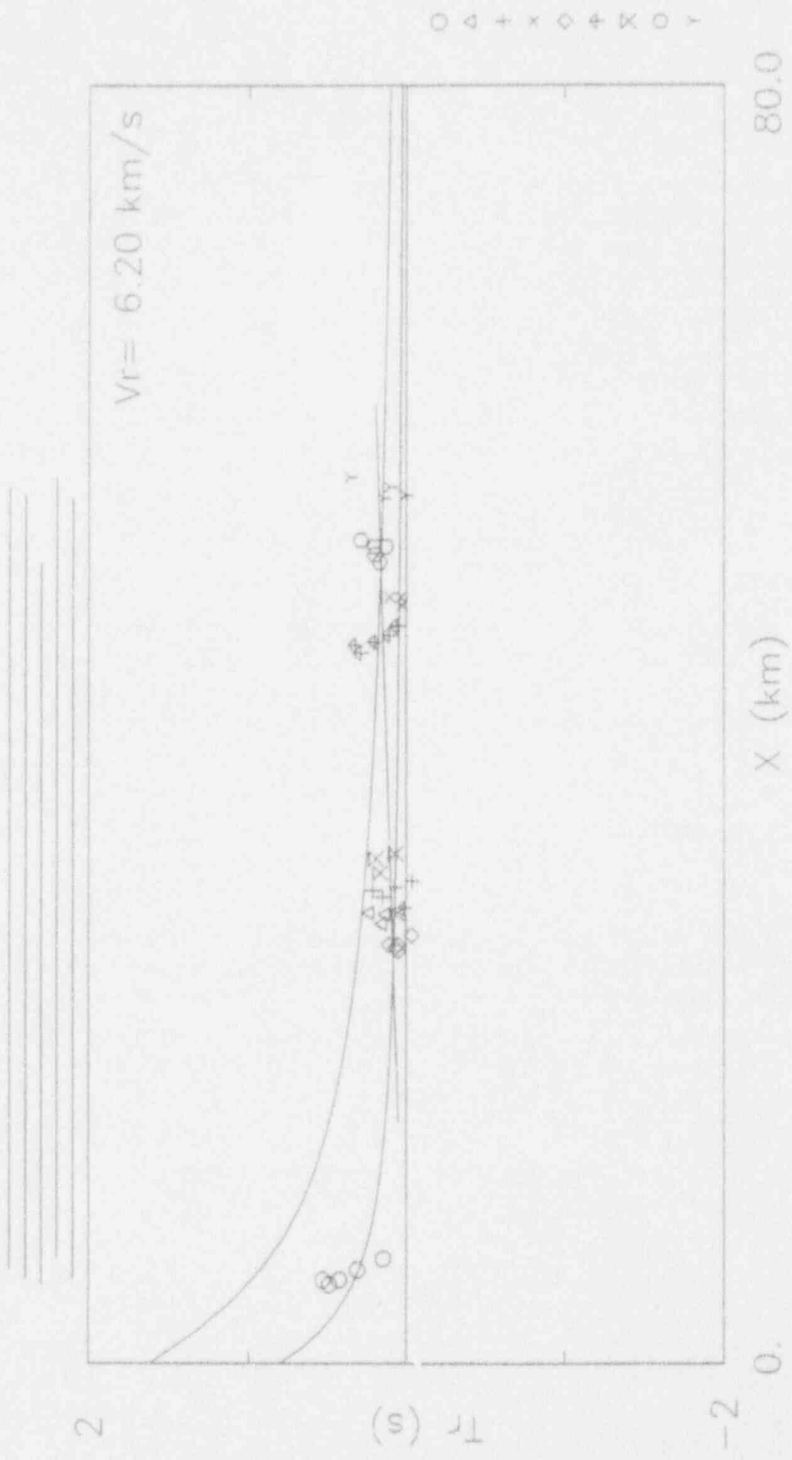

Figure 30. Reduced arrival times from Anna swarm events recorded by Anna stations. For this plot, different symbols represent different stations. The legend is given at the right, with stations listed as follows: AN1, AN3, AN4, AN7, AN8, AN9, AN10, AN11, and AN12. The two theoretical travel time curves are for Pg=6.2 km/s and with two source depths, 5 and 10 km.

of the Anna zone events over a few years. This cluster is located just north of the trace of the Anna-Champaign fault and its intersection with the postulated Auglaize fault. The 8/25/85 event is relocated with a crustal velocity of 6.2 km/s; the location stays at the same place. The largest event in western Ohio in the last two decades, 1986 St. Mary's earthquake, is clearly located about 30 km to the west of the Anna cluster. Given the uncertainties in the locations of the old Anna earthquakes of the 1930's, one could place those old events at various locations along the Anna-Champaign fault from the 1986 St. Marys event to the Anna cluster.

One important conclusion is that several earthquakes in the Anna zone are located within a few kilometers of a station, thus the hypocentral depths can be reliably determined for those events with good recordings. All six earthquakes with reliable hypocentral depths occur within the pre-Cambrian basement.

3.3 Focal Mechanisms

It is quite difficult to obtain reliable focal mechanisms for small local and regional earthquakes. The best focal mechanism available for the Anna zone is for the 1986 St. Marys earthquake. This event was widely recorded by stations at all azimuths in mid-continent region, and Schwartz & Christensen (1987) determined the strike-slip mechanism that is shown in Figure 31a. One nodal plane strike is somewhat similar to the strike of the postulated Anna-Champaign fault. The other large earthquake in Ohio in the past decade was the 1986 Perry earthquake, and it's focal mechanism is remarkably similar to the St. Mary's mechanism (Figure 31b). One obvious interpretation is that both earthquakes are responding to the same crustal stress state. Based on other types of stress measurements, Zoback and Zoback (1980) characterized the stress field in the Ohio region as east-west compression. Indeed, the pressure axes for both the St. Marys and Perry earthquakes are horizontal with a nearly east-west strike. Thus, the simplest explanation is that the focal mechanisms of both the St, Marys and Perry earthquakes reflect the same crustal stress regime across the state of Ohio.

The recent occurrence of several earthquakes in Indiana offers the opportunity to test whether the Ohio stress regime continues into Indiana. The Indiana earthquakes are not as large as the two 1986 events, thus fewer readings are available. Unfortunately, the readings are inconsistent and it is not possible to find a good focal mechanism.

3.4 Association of seismicity with structural features

Recall that the hypocentral depth analysis indicates that the hypocentral depths are about 5 km or so, well into the pre-Cambrian basement throughout western Ohio, Indiana, and southern Michigan. The Grenville front is a major crustal feature, but it does not appear to serve as the major locus of seismicity; the Anna zone is clearly to the west of Grenville front, and the major reflectors within the Grenville

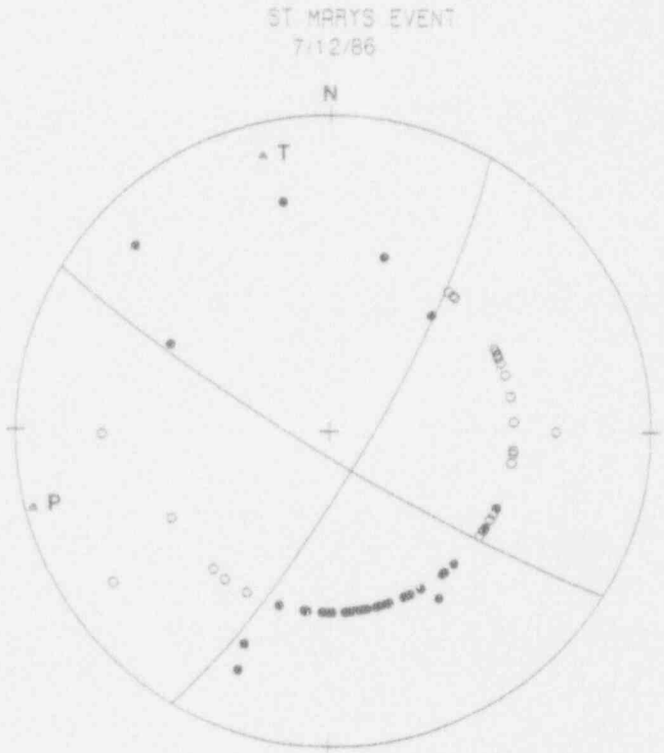

Figure 31a. Focal mechanism of the July 12, 1986 St. Marys earthquake. Compressional arrivals are shown as solid symbols, and dilatational arrivals are shown as open symbols. The P and T axes are also shown.

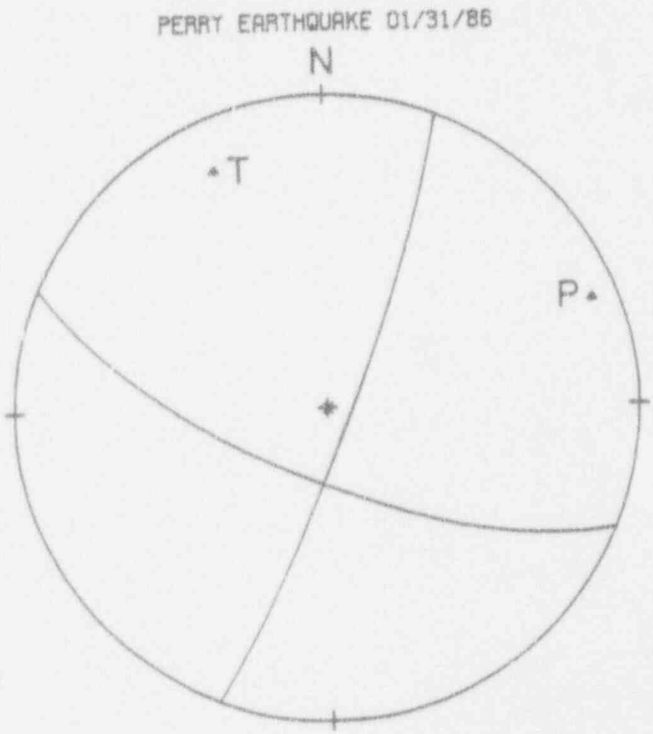

Figure 31b. Focal mechanism of the January 31, 1986 Perry earthquake.

front dip to east away from the Anna zone (Pratt et al., 1989). It does appear that the Anna earthquakes occur near the northern boundary of the inferred Keewenawan rift. In fact, it is possible to speculate that the Anna-Champaign fault which cuts through the Paleozoic section coincides with the northern boundary of the rift. Several earthquakes occur north of the Anna zone and the rift, roughly scattered on both sides of the Grenville front to the crest of the Findlay Arch in Lake Erie.

There are only two confirmed tectonic earthquakes in southern Michigan (Fujita & Sleep, 1990), the 1947 Coldwater earthquake and the small 12/23/82 event that occurred northwest of the Coldwater event. Both earthquakes occurred close to basement lineation that had been identified by magnetic and gravity data (Hinze et al., 1975). Hinze et al. (1975) speculated that this lineation might be a dike. In another interpretation, the basement geology map shows a terrane boundary that crudely coincides with this basement lineation. One speculative suggestion is that the two Michigan earthquakes may have occurred along the same linear crustal feature.

Prior to 1990, only a few isolated events had been located in Indiana after 8 years of monitoring, which seemed to support the notion that there was a relatively aseismic region between the Anna zone the Wabash River seismic zone. However, three felt earthquakes have occurred from December 1990 to July 1991. These earthquakes are scattered about central Indiana and they now indicate that a long-term view of the seismicity might have a continuous zone from New Madrid all the way to the Anna zone, albeit not with the same intensity. The recording of these events in the last years of operation of the Anna network is a reminder that 14 years of microseismicity monitoring may not give us a completely representative view of mid-continent seismicity.

4. Discussion and Conclusions

4.1 Crustal structure

P wave arrival times clearly show that crustal structure is different beneath the Anna and Indiana sub-networks. It appears that a "typical" mid-continent crustal model is allowed by the Indiana sub-network data. In this context, the Anna zone has anomalous crustal structure. However, if we allow the maximum thickness of a P* layer (velocity of 6.63 km/s) beneath the Anna zone; then the Anna Pg layer is 20 km thick versus 15 km for "typical" mid-continent, and the P* layer is 24 km thick versus 26.5 km for "typical" mid-continent, and the total Anna crustal thickness is 43.3 km versus 41.5 km for "typical" mid-continent. The Anna crustal thickness is still less than values found in

the Lake Superior region. We can compare the vertical travel times through the Anna zone to other crustal structures in Figure 29. The difference between Anna and Indiana vertical travel times is roughly consistent with the teleseismic observations. A receiver function study in the Anna zone would provide additional constraints on the crustal travel time.

Recall that a Keewenawan rift has been proposed to pass through the Anna seismic zone. Our results for the Anna zone crustal velocities argue against the existence of a Keewenawan rift similar to the one in Lake Superior. Mafic igneous rocks such as basalts and gabbros usually have seismic velocities of 6.5 km/s or higher. Indeed, seismic refraction studies across the Lake Superior rift in Minnesota and Wisconsin show that a P velocity of at least 6.5 km/s is encountered at a depth of 3 to 5 km (Cohen & Meyer, 1966; Braile, 1989). Refraction profiles across Lake Superior show that velocities of 6.8 km/s are encountered at depths less than 10 km (Smith et al., 1966), despite the thick accumulation of rift-related sediments. The mid-Michigan geophysical anomaly is also a Keewenawan rift, and basaltic rocks are encountered beneath the thick Paleozoic sediments of the Michigan Basin. Therefore, the crustal velocity of 6.2 km/s in the Anna zone is not consistent with a Keewenawan rift underlain with mafic igneous rocks.

It seems that the current interpretation of a basaltic Keewenawan rift in the Anna zone is based largely on the presence of positive gravity anomalies and the occurrence of mafic igneous rocks in parts of western Ohio. A critical view of the geophysical evidence shows that the positive gravity anomaly in the Anna zone compared to the Central Province is about 30 mgals (see Lucius & Von Frese, 1988), while the gravity anomaly over the Lake Superior rift system is about 90 mgals in Lake Superior and 30 to 40 mgals in Minnesota-Wisconsin. To provide more examples, the gravity anomaly over the: mid-Michigan rift system is about 40 to 50 mgals; the postulated rift in Kentucky-Tennessee (Keller et al., 1982) is 60 to 80 mgals; and for the New Madrid rift system, the anomaly is 30 to 40 mgals. Thus, the gravity anomaly over the Anna zone is indeed consistent with a Keewenawan-type rift. However, another characteristic of the Keewenawan rifts in Lake Superior, mid-Michigan, and Kentucky-Tennessee are strong positive magnetic anomalies: more than 500 gammas across Lake Superior; about 500 gammas across the mid-Michigan anomaly; and several hundred gammas across the Kentucky-Tennessee anomaly. Localized positive anomalies of several hundred gammas are also found across the edges of the New Madrid rift complex. In contrast, there is no significant magnetic anomaly correlated with the gravity high in the Anna zone. The largest short-wavelength magnetic anomalies in Ohio are associated with the Grenville front and the Seneca Anomaly just to the east of the Grenville front. In comparison, magnetic anomalies throughout the Central province in western Ohio are smooth anomalies with low amplitude. Indeed, Lucius & Von Frese (1988) comment on the extension of the Keewenawan rift from Indiana into

western Ohio: "The southeastward-trending Fort Wayne limb is characterized by a series of strong, mostly positive gravity anomalies in association with a correlative trend of weakly defined magnetic minima." These magnetic characteristics are different from the other mid-continent rifts. Furthermore, basement lithologies for deep wells in Ohio (Lucius & Von Frese, 1988) show some mafic igneous rocks along the intersection of the Keewenawan rift and the Grenville front and further to the south, and for one site in the northwestern corner of Ohio, but the igneous rocks found in the Anna zone are characterized as "felsic" or "intermediate". This limited direct sampling of the pre-Cambrian basement in the Anna zone suggests a more typical "felsic" upper-crustal rock type. Indeed, examination of the early basement lithology map of Bayley & Muehlberger (1968) shows their interpretation that the igneous rocks in the Anna zone are "acidic", as opposed to "basic" in the Indiana segment of the rift. Thus, a Keewenawan rift may indeed extend from northeastern Indiana through the Anna zone southward to Kentucky-Tennessee, and it may be characterized by shallow mafic igneous rocks over most of its length, but the extrusive igneous rocks appear to be "felsic" in the Anna zone. Furthermore, the crustal structure determined for the Anna zone implies that the "felsic" rocks are anomalously thick compared to the "typical" mid-continent velocity model.

4.2 Seismicity

The two largest earthquakes in Ohio over the last two decades are the July 12, 1986 St. Marys earthquake in the Anna zone and the January 31, 1986 Perry event in the Cleveland area. Focal mechanisms for these two events are essentially identical strike-slip mechanisms with an east-northeast striking compressional axis. There is weak evidence that focal mechanisms of Indiana earthquakes might be different. Fourteen years of seismic monitoring at Anna has found: 34 events in western and central Ohio; 5 events in northeastern Ohio; 1 event in Michigan; and 7 events in Indiana. Of the 34 events in western and central Ohio, 21 are within the Anna sub-network. The most notable spatial clustering of events is the cluster of 12 events just five kilometers southeast of station AN1. Hypocentral depth analysis of these earthquakes shows that they could all be at the same depth of 5 km below the top of the Pg layer, or 6 km below the surface (top of the Paleozoic rocks). Since the Paleozoic sedimentary section is less than 1 km thick in the Anna zone, these earthquakes are clearly within the pre-Cambrian basement. Hypocentral depths of two other earthquakes are somewhat deeper than the depth of the Anna cluster. No additional events have been located in the Anna cluster since January 3, 1984. Other temporal features in the seismicity is the activity of 1986 and the occurrence of 3 events in Indiana from December 1990 to July 1991. While seismicity is widely scattered through western Ohio, there is a concentration of activity in the Anna zone where damaging historic earthquakes have occurred. This seismicity can be associated with a proposed Keewenawan-type rift

that trends NW-SE through the southern half of the Anna seismic network. In detail, one can further associate the Anna cluster, the 1986 St. Marys event, and possibly the damaging earthquakes of the 1930's with NW-SE trending Anna-Champaign fault which has been identified in the Paleozoic sediments. The pre-glacial Teays River Valley also trends NW-SE through the Anna zone, but there is no evidence for active faulting in the Anna zone. While the fundamental cause of mid-continent seismicity remains unknown, the Anna seismic zone offers another example of intra-plate seismicity associated with an old rift. The interesting twist is that the Anna seismicity occurs in a segment of the rift that is characterized by an unusually thick upper-crustal zone of "felsic" rocks rather than the "mafic" rocks that underlie other rifts including the New Madrid rift zone.

References

Bayley, R.W., and W.R. Muehlberger, Basement rock map of the United States, U.S.G.S., Washington D.C., 1968.

Braile, L.W., Crustal structure of the continental interior, Chapt. 15 in: Pakiser, L.C., W.D. Mooney, eds., Geophysical framework of the continental United States, Geol. Soc. Am., Memoir 172, 1989.

Braile, L.W., G.R. Keller, W.J. Hinze, and E.G. Lidiak, An ancient rift complex and its relation to contemporary seismicity in the New Madrid seismic zone, Tectonics, 1, 225-237, 1982.

Bradley, E.A., and T.J. Bennett, Earthquake history of Ohio, Bull. Seism. Soc. Am., 55, 745-752, 1965.

Christensen, D.H., H.N. Pollack, T. Lay, and S.Y. Schwartz, Geophysical investigations of the western Ohio-Indiana region, Final report 1981-1986, NUREG/CR-3145, 1986.

Cohen, T.J., and R.P. Meyer, The midcontinent gravity high: gross crustal structure, in: Steinhart, J.S. and T.J. Smith, eds., The earth beneath the continents, Am. Geophys. Union Geophys. Monograph 10, 141-165, 1966.

Fujita, K. and N.H. Sleep, A re-examination of the seismicity of Michigan, Tectonophysics, 186, 75-106, 1991.

Hinze, W.J., R.L. Kellogg, and N. W. O'Hara, Geophysical studies of basement geology of southern peninsula of Michigan, Am. Assoc. Pet. Geol. Bull., 59, 1562-1584, 1975.

Iyer, H.M., L.C. Pakiser, D.J. Stuart, and D.H. Warren, Project Early Rise: Seismic probing of the upper mantle, J. Geophys. Res., 74, 4409-4441, 1969.

Jackson, P.L., D.H. Christensen, F.J. Mauk, Geophysical investigations of the western Ohio-Indiana region, Final report 1975-1981, NUREG/CR-2484, 1981.

Keller, G.R., A.E. Bland, and J.K. Greenberg, Evidence for a major late precambrian tectonic event (rifting?) in the eastern midcontinent region, United States, Tectonics, 1, 213-224, 1982.

Kiefer, M.L., and J.S. Trapp, Interpretation of mechanisms for the Anna, Ohio earthquakes for the Marble Hill generating station, report from Dames & Moore to Public Service Indiana, 1975.

Lanczos, C., Linear Differential Operators, Van Nostrand, London, 1961.

Lucius, J.E., and R.R.B. Von Frese, 1988, Aeromagnetic and gravity anomaly constraints on the crustal geology of Ohio, Geol. Soc. Am. Bull., 100, 104-116, 1988.

McGuire, D., Geophysical survey of the Anna, Ohio area, M.S. thesis, Bowling Green State Univ., 79 pp, 1975.

Mitchell, B.J., and B.M. Hashim, Seismic velocity determinations in the New Madrid seismic zone: A new method using local earthquakes, Bull. Seism. Soc. Am., 67, 413-424, 1977.

Nuttli, O.W., and K.G. Brill, Earthquake source zones in the central United States determined from historical seismicity, in: Barstow, N.L., K.G. Brill, O.W. Nuttli, and P.W. Pomeroy, eds, An approach to seismic zonation for siting nuclear electric power generating facilities in the eastern United States, NUREG/CR-1577, 97-143, 1981.

Nuttli, O.W., and R.B. Herrmann, Credible earthquakes for the central United States, state-of-the-art for assessing earthquake hazards in the United States, Report 12, Misc. paper S-73-I, U.S. Army Corps of Engineers, Washington, D.C., 98 pp, 1978.

Pratt, T., R. Culotta, E. Hauser, D. Nelson, L. Brown, S. Kaufman, J. Oliver, and W. Hinze, Major proterozoic basement features of the eastern midcontinent of North America revealed by recent COCORP profiling, Geology, 17, 505-509, 1989.

Schwartz, S.Y., and D.H. Christensen, Geophysical investigations of the western Ohio-Indiana region, annual report Oct 1986 to Sept 1987, NUREG/CR-3145, 1987.

Smith, T.J., J.S. Steinhart, and L.T. Aldrich, Lake Superior crustal structure, J. Geophys. Res., 71, 1141-1172, 1966.

Soller, D.R., R.D. Ray, and R.D. Brown, A new crustal thickness map, Tectonics, 1, 125-150, 1982.

Stead, F.L., Basement faulting in Logan and Champaign counties of western Ohio, report to Dames & Moore, 1975.

Stewart, S.W., Crustal structure in Missouri by seismic-refraction methods, Bull. Seism. Soc. Am., 58, 291-323, 1968.

Sykes, L.R., Intraplate seismicity, reactivation of pre-existing zones of weakness, alkaline magmatism, and other tectonism postdating continental fragmentation, Rev. Geophys. Space Phys., 16, 621-688, 1978.

Thompson, S.N., J.H. Peck, A.R. Patterson, and D.E. Willis, Faulting and seismicity in the Anna, Ohio region, (abstract) Geol. Soc. Am. annual meeting, 1976.

Zhu, T., and L.D. Brown, COCORP Michigan surveys: reprocessing and results, J. Geophys. Res., 91, 11,477-11,495, 1986.

Zoback, M.L., and M. Zoback, State of stress in the conterminous United States, J. Geophys. Res., 85, 6113-6156, 1980.

Appendix A.

Local and Near-regional Arrival Time Data

***** 17 JUNE 1977 - OHIO *****

O.T.=15:39:47.3 LAT=40.57#N LONG=84.67#W MAG=3.3m_b

O.T.=15:39:46.9 LAT=40.705#N LONG=84.707#W (Dewey and Gordon, 1984)

STA	PHASE	ARRIVAL TIME	PHASE	ARRIVAL TIME
AN1a	iP	15:39:55.80	eS	15:40:01.70
AN3	iP	15:40:00.00	eS	15:40:08.60
AAM	eP	15:40:19.20	eS	15:40:46.00
BGO	eP	15:40:08.70	eS	15:40:23.50

(The coordinates for station AN1a are 40.4310#N, 84.1240#W)

***** 9 NOVEMBER 1979 - KENTUCKY *****

O.T.=21:29:58.7 LAT=38.417#N LONG=82.869#W MAG=3.6m_{bLg}

(Location and magnitude from NEIS)

STA	PHASE	ARRIVAL TIME	PHASE	ARRIVAL TIME
AN1	eP	21:30:37.00	eS	21:31:04.20
AN3	eP	21:30:36.30	eS	21:31:03.80
AN4	iP	21:30:32.20	eS	21:30:57.00
AN8	iP	21:30:35.00	eS	21:31:01.00
AN9	eP	21:30:42.28	eS	21:31:15.50
AN10	iP	21:30:38.93	eS	21:31:10.00
AN11	iP	21:30:41.15	eS	21:31:14.10
AN12	iP	21:30:43.50	eS	21:31:17.90
ACM	eP	21:31:10.50	eS	21:31:05.40
AAM	eP	21:31:02.40		

(Additional arrival times can be found in Mauk et al., 1980)

***** 10 JULY 1980 - OHIO *****

O.T.=11:40:53.3 LAT=40.415#N LONG=84.111#W MAG=0.9

STA	PHASE	ARRIVAL TIME	PHASE	ARRIVAL TIME
AN1	iP	11:40:55.40	eS	11:40:57.70
AN4	iP	11:40:59.10	eS	11:41:03.55
AN9	iP	11:41:02.25	eS	11:41:07.35
AN10	iP	11:40:59.65	eS	11:41:03.95
AN11	iP	11:41:03.05	eS	11:41:09.50
AN12	eP	11:41:04.20	eS	11:41:10.20

***** 27 JULY 1980 - KENTUCKY *****

O.T.=18:52:21.7 LAT=38.18#N LONG=83.94#W MAG=5.1m_b

DEP=15km

STA	PHASE	ARRIVAL TIME	PHASE	ARRIVAL TIME
AN1	iP	18:52:59.30		
AN3	iP	18:53:00.30		
AN8	iP	18:52:56.40		
AN9	iP	18:53:02.70		
AN10	iP	18:52:59.50		
AN11	iP	18:53:01.00		
AAM	iP	18:53:24.30		

(Additional arrival times can be found in Mauk et al., 1982)

***** 20 AUGUST 1980 - CANADA *****

O.T.=09:34:54.0 LAT=41.97#N LONG=82.99#W MAG=3.2m_{bLg}

STA	PHASE	ARRIVAL TIME	PHASE	ARRIVAL TIME
UTO	iP	09:35:03.30	eS	09:35:10.90
AAM	iP	09:35:03.50	iS	09:35:09.70
ACM	iP	09:35:32.60	eS	09:36:02.00
CLE	iP	09:35:15.00	eS	09:35:31.20
BLA	eP	09:36:10.5		

***** 26 SEPTEMBER 1980 - OHIO *****

O.T.=12:27:25.6 LAT=40.430#N LONG=84.085#W MAG=?.5

STA	PHASE	ARRIVAL TIME	PHASE	ARRIVAL TIME
AN1	iP	12:27:28.10		
AN3	iP	12:27:31.20	iS	12:27:35.10
AN4	iP	12:27:31.60	iS	12:27:35.30
AN8	iP	12:27:31.20	eS	12:27:34.00
AN9	iP	12:27:34.40	iS	12:27:40.10
AN10	iP	12:27:31.50	eS	12:27:37.20

***** 4 OCTOBER 1980 - OHIO *****

O.T.=11:46:58.0 LAT=39.80#N LONG=83.75#W MAG=2.0

STA	PHASE	ARRIVAL TIME	PHASE	ARRIVAL TIME
AN1	iP	11:47:12.70		
AN3	iP	11:47:13.05	eS	11:47:24.00
AN4	iP	11:47:07.30	eS	11:47:14.00
AN8	iP	11:47:10.05		
AN9	iP	11:47:18.65	eS	11:47:33.70
AN10	iP	11:47:14.85		
AN11	iP	11:47:18.00	eS	11:47:33.50

***** 10 DECEMBER 1980 - OHIO *****

O.T.=02:30:54.3 LAT=40.43#N LONG=84.11#W MAG=1.2

STA	PHASE	ARRIVAL TIME	PHASE	ARRIVAL TIME
AN1	iP	02:30:56.10		
AN3	iP	02:30:59.70	eS	02:31:03.20
AN4	iP	02:30:59.90	eS	02:31:03.60
AN8			eS	02:31:02.30
AN9	iP	02:31:02.30	eS	02:31:07.80
AN10	iP	02:31:00.10	eS	02:31:04.00
AN11	iP	02:31:03.70		

***** 4 JANUARY 1981 - OHIO *****

O.T.=07:17:37.1 LAT=40.418#N LONG=84.087#W MAG=1.8

DEP=5-7km

STA	PHASE	ARRIVAL TIME	PHASE	ARRIVAL TIME
AN1	iP	07:17:38.61		
AN3	iP	07:17:41.95		
AN4	iP	07:17:42.15		
AN7	iP	07:17:45.18		
AN8	iP	07:17:41.67	eS	07:17:44.93
AN9	iP	07:17:44.81	eS	07:17:50.34
AN10	iP	07:17:42.45		
AN11	iP	07:17:45.84	eS	07:17:52.14

***** 7 FEBRUARY 1981 - OHIO *****

O.T.=05:45:43.0 LAT=40.417#N LONG=84.087#W MAG=1.8

DEP=5-7km

STA	PHASE	ARRIVAL TIME	PHASE	ARRIVAL TIME
AN1	iP	05:45:45.02		
AN3	iP	05:45:48.33		
AN4	iP	05:45:48.57	eS	05:45:53.00
AN7	iP	05:45:51.62		
AN8	iP	05:45:48.00		
AN9	iP	05:45:51.22	eS	05:45:56.73
AN10	iP	05:45:48.87		
AN11	iP	05:45:52.28	eS	05:45:58.63
IN1	eP	05:46:08.40		
IN2	eP	05:46:19.70		
IN3	eP	05:46:14.32		
IN4	eP	05:46:02.70	eS	05:46:17.65

***** 15 MARCH 1981 - OHIO *****

O.T.=03:46:30.3 LAT=41.10#N LONG=84.35#W MAG=1.2

STA	PHASE	ARRIVAL TIME	PHASE	ARRIVAL TIME
AN3	iP	03:46:43.20		
AN4	iP	03:46:47.97		
AN7	iP	03:46:39.23	eS	03:46:45.10
AN8	iP	03:46:46.47		
AN9	iP	03:46:38.49	eS	03:46:43.80
AN10	iP	03:46:42.45	eS	03:46:50.85
AN11	iP	03:46:41.53	eS	03:46:49.59
AN12	iP	03:46:34.64		
IN1	iP	03:46:53.97		

***** 15 MAY 1981 - OHIO *****

O.T.=23:15:14.0 LAT=40.88#N LONG=84.34#W MAG=0.8

STA	PHASE	ARRIVAL TIME	PHASE	ARRIVAL TIME
AN1	iP	23:15:22.90		
AN3	iP	23:15:24.30	eS	23:15:31.30
AN4	eP	23:15:29.00		
AN7	iP	23:15:21.60		
AN8	iP	23:15:26.60		
AN9	iP	23:15:18.60	eS	23:15:20.80
AN10	iP	23:15:22.40	eS	23:15:28.60
AN11	iP	23:15:22.10		
AN12	iP	23:15:16.90		
IN4	iP	23:15:39.00		

***** 19 MAY 1981 - OHIO *****

O.T.=05:56:11.7 LAT=40.407#N LONG=84.085#W MAG=1.2

DEP=2-8km

STA	PHASE	ARRIVAL TIME	PHASE	ARRIVAL TIME
AN1	iP	05:56:13.32	eS	05:56:14.22
AN3	iP	05:56:16.62		
AN4	iP	05:56:16.80		
AN8	iP	05:56:16.32		
AN9	iP	05:56:19.46	eS	05:56:25.35
AN10	iP	05:56:17.26	eS	05:56:21.22
AN11	iP	05:56:20.77	eS	05:56:27.10
AN12	eP	05:56:21.46		
IN4	eP	05:56:30.40		

***** 26 NOVEMBER 1982 - MICHIGAN *****

O.T.=08:25:04.9 LAT=42.17#N LONG=85.48#W MAG=2.0-2.5

STA	PHASE	ARRIVAL TIME	PHASE	ARRIVAL TIME
AN3	iP	08:25:40.70		
AN4	eP	08:25:45.40		
AN7	iP	08:25:37.60	eS	08:26:01.00
AN9	iP	08:25:34.20	eS	08:25:56.70
AN11	iP	08:25:35.60	eS	08:25:59.20
AN12	eP	08:25:34.00	eS	08:25:54.20
IN1	iP	08:25:34.90	eS	08:25:58.20
IN2	iP	08:25:45.90		
ACM	iP	08:25:14.70	eS	08:25:22.00

***** 12 JANUARY 1983 - OHIO *****

O.T.=02:49:41.1 LAT=39.28#N LONG=84.60#W MAG=1.9

STA	PHASE	ARRIVAL TIME	PHASE	ARRIVAL TIME
AN1	eP	02:50:01.20		
AN4	iP	02:50:00.90		
AN7	iP	02:50:10.00	eS	02:50:31.70
AN8	iP	02:49:59.10		
AN11	iP	02:50:03.70	eS	02:50:21.50
AN12	iP	02:50:10.80		
IN2	iP	02:50:12.40		
IN3	iP	02:49:57.90		
IN4	iP	02:49:48.20	eS	02:49:53.00
L6KY	iP	02:50:07.05	eS	02:50:26.80
SBKY	iP	02:50:02.20	eS	02:50:18.30

***** 22 JANUARY 1983 - OHIO *****

O.T.=07:46:59.3 LAT=41.86#N LONG=81.16#W MAG=2.7m_{bLg}

STA	PHASE	ARRIVAL TIME	PHASE	ARRIVAL TIME
AN1	iP	07:47:41.30		
AN3	iP	07:47:38.70	eS	07:48:09.50
AN7	iP	07:47:36.30		
AN9	iP	07:47:43.90		
AN12	iP	07:47:39.40		
ELF	iP	07:47:23.04		
LDN	iP	07:47:20.75		
DLA	iP	07:47:17.67		
DHN	iP	07:47:38.79		
WVLY	iP	07:47:33.08		

***** 5 JULY 1983 - OHIO *****

O.T.=02:58:52.9 LAT=40.43#N LONG=84.10#W MAG=2.1

DEP=5-7km

STA	PHASE	ARRIVAL TIME	PHASE	ARRIVAL TIME
AN1	iP	02:58:54.35		
AN3	iP	02:58:57.62		
AN4	iP	02:58:57.90		
AN7	iP	02:59:00.90		
AN8	iP	02:58:57.37		
AN9	iP	02:59:00.55		
AN10	iP	02:58:58.30		
AN11	iP	02:59:01.35		
AN12	iP	02:59:01.97		
IN2	eP	02:59:27.80		
IN3	eP	02:59:22.75		
ACM	eP	02:59:34.40		

***** 13 JULY 1983 - OHIO *****

O.T.=01:17:34.8 LAT=40.43#N LONG=84.10#W MAG=1.4

STA	PHASE	ARRIVAL TIME	PHASE	ARRIVAL TIME
AN1	iP	01:17:36.10		
AN3	iP	01:17:39.40		
AN4	iP	01:17:39.60		
AN8	iP	01:17:39.10		
AN9	iP	01:17:42.30		
AN10	iP	01:17:40.00		
AN11	iP	01:17:43.40		
AN12	iP	01:17:43.60		

***** 30 SEPTEMBER 1983 - OHIO *****

O.T.=02:33:44.8 LAT=41.59#N LONG=84.33#W MAG=1.3

STA	PHASE	ARRIVAL TIME	PHASE	ARRIVAL TIME
AN1	iP	02.34:05.20	eS	02:34:19.60
AN4	iP	02:34:10.40	eS	02:34:28.00
AN7	iP	02:33:59.60		
AN12	eP	02:33:57.00	eS	02:34:05.50
IN1	iP	02:34:13.20		
ACM	iP	02:34:12.90		

***** 4 NOVEMBER 1983 - OHIO *****

O.T.=21:00:59.8 LAT=40.43#N LONG=84.10#W MAG=0.4

STA	PHASE	ARRIVAL TIME	PHASE	ARRIVAL TIME
AN1	iP	21:01:01.00		
AN3	iP	21:01:04.40		
AN4	iP	21:01:04.70	eS	21:01:08.30
AN8	iP	21:01:04.00		
AN9	iP	21:01:07.10		
AN11	iP	21:01:08.30		

***** 4 NOVEMBER 1983 - OHIO *****

O.T.=22:50:00.50 LAT=40.43#N LONG=84.10#W MAG=0.9

STA	PHASE	ARRIVAL TIME	PHASE	ARRIVAL TIME
AN1	iP	22:50:01.70		
AN3	iP	22:50:05.10		
AN4	iP	22:50:05.30		
AN8	iP	22:50:04.70		
AN9	iP	22:50:07.90		
AN11	iP	22:50:08.90		
AN12	iP	22:50:09.40		

***** 5 NOVEMBER 1983 - INDIANA *****

O.T.=02:36:35.8 LAT=39.68#N LONG=85.73#W MAG=1.1

STA	PHASE	ARRIVAL TIME	PHASE	ARRIVAL TIME
AN1	iP	02:37:02.20		
AN3	iP	02:37:06.20		
AN4	iP	02:37:02.50		
AN8	iP	02:36:58.00		
AN11	iP	02:36:57.40		
AN12	iP	02:37:06.70		
IN1	iP	02:36:51.50		
IN2	iP	02:36:51.00		
IN3	iP	02:36:43.30	eS	02:36:49.00
IN4	iP	02:36:48.10		

***** 3 DECEMBER 1983 - WISCONSIN *****

O.T.=21:29:41.0 LAT=42.70#N LONG=88.30#W MAG=1.4

STA	PHASE	ARRIVAL TIME	PHASE	ARRIVAL TIME
IN1	iP	21:30:29.50		
IN2	iP	21:30:28.10		
ACM	iP	21:30:13.30	iS	21:30:36.50

***** 7 DECEMBER 1983 - OHIO *****

O.T.=22:57:01.6 LAT=41.70#N LONG=83.50#W MAG=1.1

STA	PHASE	ARRIVAL TIME	PHASE	ARRIVAL TIME
AN7	iP	22:57:18.20	iS	22:57:30.00
AN8	iP	22:57:29.40	eS	22:57:51.30
AN12	iP	22:57:18.60	iS	22:57:30.60

***** 10 DECEMBER 1983 - OHIO *****

O.T.=19:01:[illegible] LAT=40.43#N LONG=84.11#W MAG=0.7

STA	PHASE	ARRIVAL TIME	PHASE	ARRIVAL TIME
AN1	iP	19:01:56.50		
AN3	iP	19:02:00.00		
AN4	iP	19:02:00.10	eS	19:02:03.80
AN7	iP	19:02:03.00	eS	19:02:08.80
AN8	iP	19:01:59.50	eS	19:02:02.70
AN9	iP	19:02:02.80		
AN11	iP	19:02:03.60		
AN12	iP	19:02:04.00	eS	19:02:10.80

***** 3 JANUARY 1984 - OHIO *****

O.T.=07:57:58.60 LAT=40.42#N LONG=84.11#W MAG=0.4

STA	PHASE	ARRIVAL TIME	PHASE	ARRIVAL TIME
AN1	iP	07:57:59.70		
AN4	iP	07:58:03.20	eS	07:58:07.00
AN7	eP	07:58:06.40		
AN8	iP	07:58:02.70		
AN9	eP	07:58:06.00	eS	07:58:11.40

AN11	iP	07:58:07.10
AN12	iP	07:58:08.20

***** 14 JANUARY 1984 - OHIO *****

O.T.=20:14:32.5 LAT=41.67#N LONG=83.45#W MAG=2.6m_b

STA	PHASE	ARRIVAL TIME	PHASE	ARRIVAL TIME
AN3	iP	20:14:52.70		
AN4	iP	20:14:58.70	eS	20:15:18.00
AN7	iP	20:14:48.00	eS	20:14:59.50
AN8	iP	20:14:59.60		
AN9	iP	20:14:54.20		
AN11	iP	20:14:57.70		
AN12	iP	20:14:48.80	eS	20:15:00.50
ACM	eP	20:15:07.60	eS	20:15:35.10
AAM	eP	20:14:43.20		
DLA	iP	20:15:04.80	eS	20:15:30.00
LDN	iP	20:15:08.45	eS	20:15:37.75
ELF	iP	20:15:09.00	eS	20:15:38.25

***** 28 JULY 1984 - INDIANA *****

O.T.=23:39:27.3 LAT=39.27#N LONG=87.09#W MAG=4.0m_{bLg}

STA	PHASE	ARRIVAL TIME	PHASE	ARRIVAL TIME
AN1	iP	23:40:09.20		
AN3	iP	23:40:12.50		
AN4	iP	23:40:09.80		
AN7	iP	23:40:13.70		
AN8	eP	23:40:06.40		
AN9	eP	23:40:07.20		
AN10	iP	23:40:06.00		
AN11	iP	23:40:04.70		
IN1	iP	23:39:55.20		
IN2	iP	23:39:41.10		
IN3	iP	23:39:46.00		
IN4	iP	23:39:57.30		
BBG	iP	23:40:43.90		
ETT	iP	23:40:35.20		
BHT	eP	23:40:25.80		
GBTN	eP	23:40:32.50		
TKL	eP	23:40:35.62		
ELC	eP	23:40:09.15		
WCK	eP	23:40:10.85		
TYS	eP	23:40:12.30		
FVM	eP	23:40:14.00		
WSIL	iP	23:39:46.40		

***** 29 AUGUST 1984 - INDIANA *****

O.T.=06:50:59.0 LAT=39.25#N LONG=87.50#W MAG=3.2m_{bLg}

STA	PHASE	ARRIVAL TIME	PHASE	ARRIVAL TIME
AN4	eP	06:51:45.20		
AN8	eP	06:51:42.10		
AN9	eP	06:51:43.00		
AN10	iP	06:51:41.50		
AN11	iP	06:51:39.70		
IN1	iP	06:51:29.80	eS	06:51:54.20
IN2	iP	06:51:15.00		
IN3	iP	06:51:23.10	eS	06:51:40.90
IN4	iP	06:51:33.60	eS	06:52:01.10
BLO	iP	06:51:13.60	eS	06:51:22.60
WSIL	iP	06:51:13.80	eS	06:51:24.10
GOIL	iP	06:51:34.88	eS	06:52:03.04
FVM	iP	06:51:42.13	eS	06:52:15.60

***** 29 AUGUST 1984 - ILLINOIS *****

O.T.=18:56:27.2 LAT=39.09#N LONG=87.69#W MAG=2.7m_{bLg}

STA	PHASE	ARRIVAL TIME	PHASE	ARRIVAL TIME
IN1	iP	18:57:01.10		
IN3	iP	18:56:54.10		
IN4	iP	18:57:04.00		
FVM			eS	18:57:35.82
WCK			eS	18:57:34.89
TYS			eS	18:57:33.42
ELC			eS	18:57:29.84
GOIL			eS	18:57:23.22

***** 10 MARCH 1985 - OHIO *****

O.T.=20:46:01.10 LAT=40.52#N LONG=84.39#W MAG=1.4

STA	PHASE	ARRIVAL TIME	PHASE	ARRIVAL TIME
AN1	iP	20:46:04.97		
AN3	iP	20:46:09.20		
AN4	iP	20:46:10.25		
AN7	iP	20:46:10.30		
AN8	iP	20:46:06.40		
AN9	iP	20:46:05.00		
AN10	iP	20:46:02.75		
IN1	eP	20:46:21.20	eS	02:46:37.00
IN4	eP	20:46:19.30	eS	02:46:33.50

***** 10 MARCH 1985 - OHIO *****

O.T.=20:49:14.1 LAT=40.52#N LONG=84.40#W MAG=1.7

STA	PHASE	ARRIVAL TIME	PHASE	ARRIVAL TIME
AN1	iP	20:49:18.07		
AN3	iP	20:49:22.30		
AN4	iP	20:49:23.15		
AN7	iP	20:49:23.40		
AN8	iP	20:49:19.50		
AN9	iP	20:49:18.05		
AN10	iP	20:49:15.90		
AN12	eP	20:49:22.85		
IN1	ip	20:49:34.25		
IN2	eP	20:49:46.65		
IN3	eP	20:49:42.35		
IN4	eP	20:49:32.15		

***** 17 MARCH 1985 - OHIO *****

O.T.=11:57:06.7 LAT=39.65#N LONG=83.46#W MAG=1.9

STA	PHASE	ARRIVAL TIME	PHASE	ARRIVAL TIME
AN1	iP	11:57:24.5		
AN3	iP	11:57:23.9		
AN4	iP	11:57:18.8	eS	11:57:27.6
AN7	iP	11:57:28.6	eS	11:57:44.1
AN8	iP	11:57:22.6		
AN9	iP	11:57:30.4	eS	11:57:47.6
AN12	iP	11:57:31.6	eS	11:57:49.5
IN1	eP	11:57:41.3		
IN2	eP	11:57:49.4		
IN3	iP	11:57:38.4	eS	11:58:03.5
IN4	iP	11:57:27.0		

***** 14 APRIL 1985 - PENNSYLVANIA *****

O.T.=11:39:51.3 LAT=41.40#N LONG=80.37#W MAG=2.0

STA	PHASE	ARRIVAL TIME	PHASE	ARRIVAL TIME
AN3	iP	11:40:35.30	eS	11:41:08.70
AN7	iP	11:40:35.00		
AN10	eP	11:40:42.80		
AN12	iP	11:40:37.80	eS	11:41:12.50
IN1	iP	11:40:56.20		
SCP	iP	11:40:26.50	eS	11:40:52.10
BV1	eP	11:40:42.50		
WVLY	iP	11:40:21.59	eS	11:40:44.18
PTN	eP	11:41:10.67	eS	11:42:04.64
WNY	iP	11:41:15.52	eS	11:42:18.36
PRIN	eP	11:40:57.18	eS	11:41:49.03
GPD	eP	11:40:59.83	eS	11:41:49.54
WEO	iP	11:40:38.30		
CKO	iP	11:41:05.80		
WBO	iP	11:41:08.10		
EEO	iP	11:41:09.85		
GAC	iP	11:41:14.70		

VDQ iP 11:41:32.10

***** 25 AUGUST 1985 - KENTUCKY *****

O.T.=14:30:01.6 LAT=38.54#N LONG=84.98#W MAG=1.6

STA	PHASE	ARRIVAL TIME	PHASE	ARRIVAL TIME
AN1	eP	14:30:37.1		
AN3	eP	14:30:38.4		
AN4	eP	14:30:35.0		
AN10	iP	14:30:35.8		
AN11	iP	14:30:36.7		
AN12	eP	14:30:41.4		
IN2	eP	14:30:35.2		
IN3	iP	14:30:19.1	eS	14:30:31.8
IN4	iP	14:30:20.0	eS	14:30:34.7

***** 25 AUGUST 1985 - OHIO *****

O.T.=16:27:11.9 LAT=40.97#N LONG=84.22#W MAG=1.5

STA	PHASE	ARRIVAL TIME	PHASE	ARRIVAL TIME
AN1	iP	16:27:21.0	eS	16:27:28.1
AN3	iP	16:27:21.1	eS	16:27:28.3
AN7	iP	16:27:17.4	eS	16:27:21.0
AN10	iP	16:27:21.9	eS	16:27:29.2
AN11	iP	16:27:22.0	eS	16:27:29.7
AN12	iP	16:27:14.3		
IN4	iP	16:27:37.6		

***** 9 SEPTEMBER 1985 - ILLINOIS *****

O.T.=22:06:31.0 LAT=41.85#N LONG=88.01#W MAG=3.0m_{bLg}

(NEIS)

STA	PHASE	ARRIVAL TIME	PHASE	ARRIVAL TIME
ACM	iP	22:07:02.2		
IN1	iP	22:07:06.4	eS	22:07:32.5
IN2	iP	22:07:08.1	eS	22:07:34.9

***** 12 JANUARY 1986 - OHIO *****

O.T.=11:38:50.2 LAT=40.77#N LONG=83.27#W MAG=0.8

STA	PHASE	ARRIVAL TIME	PHASE	ARRIVAL TIME
AN1	eP	11:39:03.6	eS	11:39:13.4
AN3	iP	11:38:58.6	eS	11:39:05.4
AN4	eP	11:39:03.7	eS	11:39:13.8
AN7	eP	11:38:58.4		
AN9			eS	11:39:19.7
AN10	iP	11:39:07.8	eS	11:39:21.3
AN11	eP	11:39:10.2	eS	11:39:24.9
AN12	eP	11:39:03.2	eS	11:39:12.5

***** 13 JANUARY 1986 - OHIO *****

O.T.=11:39:20.4 LAT=40.80#N LONG=84.13#W MAG=0.5

STA	PHASE	ARRIVAL TIME	PHASE	ARRIVAL TIME
AN1	eP	11:39:26.5	eS	11:39:31.6
AN3	iP	11:39:26.8	eS	11:39:31.9
AN7	eP	11:39:24.3		
AN9	iP	11:39:25.9	eS	11:39:30.0
AN10	eP	11:39:28.6	eS	11:39:33.4
AN11	iP	11:39:29.2	eS	11:39:35.8
AN12	iP	11:39:22.8	eS	11:39:24.3
IN1			eS	11:40:02.1
IN4			eS	11:40:03.4

***** 31 JANUARY 1986 - OHIO *****

O.T.=16:46:43.3 LAT=41.65#N LONG=81.16#W MAG=5.0m_b (NEIS)

DEP=10km (Location from NEIS)

STA	PHASE	ARRIVAL TIME	PHASE	ARRIVAL TIME
AN1	ePd	16:47:26.1		
AN3	iPd	16:47:22.7		
AN4	iPd	16:47:25.6		
AN7	iPd	16:47:21.3		
AN9	ePd	16:47:28.2		
AN10	iPd	16:47:29.3		
AN11	ePd	16:47:30.5		
AN12	iPd	16:47:24.2		
IN1	iPd	16:47:41.4		
IN2	ePd	16:47:52.7		
IN4	iPd	16:47:38.5		

***** 30 MARCH 1986 - OHIO *****

O.T.=07:42:42.1 LAT=41.37#N LONG=83.67#W MAG=1.4

STA	PHASE	ARRIVAL TIME	PHASE	ARRIVAL TIME
AN1	iP	07:42:59.4	eS	07:43:12.2
AN4	iP	07:43:03.2	eS	07:43:18.9
AN7	iP	07:42:52.4	eS	07:42:59.7
AN9	iP	07:42:58.6		
AN10	iP	07:43:01.9	eS	07:43:15.9
AN11	iP	07:43:02.2		
AN12	eP	07:42:52.8	eS	07:43:00.0
IN4	iP	07:43:16.8	eS	07:43:45.1
UTO	iP	07:42:47.5	eS	07:42:50.8

***** 12 JULY 1986 - OHIO *****

O.T.=08:19:39.5 LAT=40.55#N LONG=84.39#W MAG=4.5m_b (NEIS)

DEP=5-10km

STA	PHASE	ARRIVAL TIME	PHASE	ARRIVAL TIME
AN4	iPc	08:19:48.3		
AN7	iPd	08:19:47.9		
AN8	iPc	08:19:45.2		
AN9	iP	08:19:42.7		
AN10	iPc	08:19:41.5		
AN11	iPd	08:19:43.6		
AN12	iPc	08:19:46.4		
IN1	iPd	08:19:59.8		
IN2	eP	08:20:12.0		
IN3	iPd	08:20:08.5		
IN4	iPc	08:19:58.4		
AA1	iPc	08:20:11.7		
U10	ePd	08:20:01.6		

***** 17 OCTOBER 1986 - OHIO *****

O.T.=07:03:4.6 LAT=40.55#N LONG=84.37#W MAG=0.7

STA	PHASE	ARRIVAL TIME	PHASE	ARRIVAL TIME
AN1	iPc	07:03:08.2	eS	07:03:11.0
AN3	iPc	07:03:12.3	eS	07:03:17.8
AN7	iPc	07:03:13.3	eS	07:03:20.0
AN8	iPc	07:03:10.4	eS	07:03:14.9
AN9	eP	07:03:07.9		
AN10	eP	07:03:06.6		
AN11	eP	07:03:09.0	eS	07:03:12.0
AN12			eS	07:03:16.9
IN1	eP	07:03:25.2	eS	07:03:41.2
IN3	eP	07:03:33.9		

***** 1 FEBRUARY 1987 - OHIO *****

O.T. =12:01:55.7 LAT=39.323#N LONG=82.428#W

DEP=4km (Location from Univ. of Kentucky)

STA	PHASE	ARRIVAL TIME	PHASE	ARRIVAL TIME
AN3	eP	12:02:24.8		
AN7	iP	12:02:28.7		
AN8	eP	12:02:25.9		

***** 27 MARCH 1987 - TENNESSEE*****

O.T. =07:29:30.45 LAT=35.568#N LONG=84.230#W MAG=4.2m_{bLg}

DEP=19km (Location from CERI)

STA	PHASE	ARRIVAL TIME	PHASE	ARRIVAL TIME
AN1	eP	07:30:44.6		
AN3	eP	07:30:45.9		
AN4	eP	07:30:41.0		
AN9	eP	07:30:49.0		
AN10	eP	07:30:45.0		
AN11	eP	07:30:46.5		
IN1	eP	07:30:46.5		
IN2	eP	07:30:43.8		
IN3	ePc	07:30:30.5		
IN4	eP	07:30:35.3		

***** 10 JUNE 1987 - ILLINOIS*****

O.T. =23:48:54.8 LAT=38.713#N LONG=87.954#W MAG=4.9m_{bLg}

DEP=5km (Location from SLM)

STA	PHASE	ARRIVAL TIME	PHASE	ARRIVAL TIME
AN3	iPd	23:49:44.1		
AN4	iPd	23:49:47.3		
AN7	iPd	23:49:47.9		
AN8	iPd	23:49:43.8		
AN9	iPd	23:49:45.1		
AN10	iPd	23:49:43.8		
AN11	iPd	23:49:42.5		
AN12	iPd	23:49:44.0		
IN1	iPd	23:49:33.2		
IN4	iPd	23:49:34.9		
ACM	iPc	23:49:57.7		

***** 11 JUNE 1987 - ILLINOIS*****

O.T. =00:15:50.0 LAT=38.67#N LONG=87.95#W MAG=2.6

(Location from SLM)

STA	PHASE	ARRIVAL TIME	PHASE	ARRIVAL TIME
IN1	eP	00:16:29.5		

***** 11 JULY 1987 - TENNESSEE*****

O.T. =00:04:29.46 LAT=36.102#N LONG=83.817#W MAG=3.6m_{bLg}

DEP=25km (Location from CERI)

STA	PHASE	ARRIVAL TIME	PHASE	ARRIVAL TIME
AN3	eP	00:05:36.2		
AN4	eP	00:05:32.0		
AN8	eP	00:05:32.2		
AN12	eP	00:05:41.4		
IN1	eP	00:05:39.6		
IN4	eP	00:05:24.7		

***** 13 JULY 1987 - OHIO*****

O.T. =05:49:18.94 LAT=41.90#N LONG=80.726#W MAG=3.8m_{bLg}

DEP=2km (Location from John Carrol Univ.)

STA	PHASE	ARRIVAL TIME	PHASE	ARRIVAL TIME
AN1	eP	05:50:08.2		
AN3	eP	05:50:04.5		
AN4	eP	05:50:07.0		
AN7	eP	05:50:03.2		
AN8	eP	05:50:10.8		
AN9	eP	05:50:09.8		
AN11	eP	05:50:12.4		
IN1	eP	05:50:23.8		
IN3	eP	05:50:29.7		

***** 13 JULY 1987 - OHIO*****

O.T. =07:52:12.22 LAT=41.90#N LONG=80.703#W MAG=3.0m_{bLg}

DEP=2km (Location from John Carrol Univ.)

STA	PHASE	ARRIVAL TIME	PHASE	ARRIVAL TIME
AN1	eP	07:53:01.5		
AN3	eP	07:52:57.9		
AN7	eP	07:52:57.4		
AN8	eP	07:53:04.2		
AN9	eP	07:53:03.2		
IN1	eP	07:53:17.9		

***** 13 JULY 1987 - OHIO*****

O.T. =13:05:23.1 LAT=41.908#N LONG=80.75#W MAG=2.9m_{bLg}

DEP=2km (Location from John Carrol Univ.)

STA	PHASE	ARRIVAL TIME	PHASE	ARRIVAL TIME
AN7	eP	13:06:07.9		
AN8	eP	13:06:14.6		

***** 16 JULY 1987 - OHIO*****

O.T. =04:49:40.27 LAT=41.905#N LONG=80.75#W MAG=2.7m_{bLg}

DEP=2km (Location from John Carrol Univ.)

STA	PHASE	ARRIVAL TIME	PHASE	ARRIVAL TIME
AN7	eP	04:50:25.3		
AN8	eP	04:50:32.0		
AN11	eP	04:50:32.1		

***** 31 AUGUST 1987 - ILLINOIS*****

O.T. =17:12:35.2 LAT=38.30#N LONG=89.71#W MAG=3.1m_{bLg}

DEP=9km (Location from SLM)

STA	PHASE	ARRIVAL TIME	PHASE	ARRIVAL TIME
IN 3	eP	17:13:24.8		

***** 29 SEPTEMBER 1987 - MISSOURI*****

O.T. =00:04:57.5 LAT=36.84#N LONG=89.21#W MAG=3.6m_{bLg}

DEP=1km (Location from SLM)

STA	PHASE	ARRIVAL TIME	PHASE	ARRIVAL TIME
AN1	eP	00:06:18.3		
AN3	eP	00:06:22.0		
AN8	eP	00:06:14.4		
AN9	eP	00:06:17.8		
AN10	eP	00:06:16.1		
AN11	eP	00:06:16.3		
IN1	iPc	00:05:55.2		
IN2	iPc	00:05:55.4		

***** 14 OCTOBER 1987 - KENTUCKY*****

O.T. =15:49:40.3 LAT=37.05#N LONG=88.78#W MAG=3.8m_{bLg}

(Location from SLM)

STA	PHASE	ARRIVAL TIME	PHASE	ARRIVAL TIME
AN3	eP	15:50:51.5		
IN1	iP	15:50:43.9		
IN2	iP	15:50:41.6		

***** 17 NOVEMBER 1987 - ILLINOIS*****

O.T. =15:52:21.4 LAT=38.73#N LONG=87.96#W MAG=3.2m_{bLg}

STA	PHASE	ARRIVAL TIME	PHASE	ARRIVAL TIME
AN4	P	15:53:19.0		
AN7	P	15:53:06.4		
IN1	P	15:53:01.1		
IN2	P	15:52:48.2		
IN3	P	15:52:52.6		
IN4	P	15:53:02.8		
WSIL	P	15:52:25.9		
SPIN	P	15:52:27.5		
BPIL	P	15:52:34.3		
NHIL	P	15:52:35.9		
GOIL	P	15:52:47.9		
ELC		15:52:51.8		

***** 5 JANUARY 1988 - ILLINOIS*****

O.T. =14:39:17.9 LAT=38.74#N LONG=87.96#W MAG=3.3m_{bLg}

DEP=5km (Location from SLM)

STA	PHASE	ARRIVAL TIME	PHASE	ARRIVAL TIME
IN1	iPd	14:39:57.7		
IN2	iPd	14:39:45.1		
IN3	P	14:39:49.8		
IN4	iPd	14:39:59.1		
ACM	P	14:40:22.7		

***** 7 SEPTEMBER 1988 - KENTUCKY*****

O.T. =02:28:08.6 LAT=38.13#N LONG=83.87#W MAG=4.5m_b

DEP=10km (Location from Kentucky Univ.)

STA	PHASE	ARRIVAL TIME	PHASE	ARRIVAL TIME
AN1	iPc	02:28:49.6		
AN3	iPc	02:28:50.5		
AN4	iPd	02:28:45.7		
AN7	iPd	02:28:53.9		
AN9	iPd	02:28:52.8		
AN10	iPd	02:28:49.5		
AN11	eP	02:28:51.2		
AN12	iPd	02:28:55.3		
IN1	eP	02:28:55.9		
IN2	eP	02:28:57.2		
IN3	iPc	02:28:42.3		
IN4	iPc	02:28:38.0		
CLE	eP	02:29:09.2		

***** 5 OCTOBER 1988 - ILLINOIS*****

O.T. =00:38:52.4 LAT=38.70#N LONG=87.90#W MAG=3.4 m_b

(Location from NEIS)

STA	PHASE	ARRIVAL TIME	PHASE	ARRIVAL TIME
AN1	eP	00:39:46.5		
AN9	eP	00:39:44.8		
AN10	eP	00:39:43.3		
AN11	eP	00:39:44.0		
IN1	eP	00:39:32.7		
IN2	eP	00:39:20.0		
IN3	iPc	00:39:24.7		
IN4	eP	00:39:34.3		

***** 22 OCTOBER 1988 - OHIO*****

O.T. =16:46:29.6 LAT=40.45#N LONG=84.11#W MAG=2.2 m_L

STA	PHASE	ARRIVAL TIME	PHASE	ARRIVAL TIME
AN1	iP	16:46:30.9		
AN3	iP	16:46:34.1		
AN8	iP	16:46:33.9		
AN10	iPd	16:46:34.8		
AN11	iP	16:46:37.5		
AN12	iP	16:46:37.4		
IN1	iPd	16:46:53.4		
IN3	iPd	16:46:59.4		
IN4	iPd	16:46:48.5		

***** 8 DECEMBER 1988 - OHIO*****

O.T. =02:10:41.2 LAT=40.55#N LONG=84.43#W MAG=1.1 m_L

STA	PHASE	ARRIVAL TIME	PHASE	ARRIVAL TIME
AN1	P	02:10:45.3	S	02:10:48.7
AN3	P	02:10:49.5	S	02:10:55.6
AN7	P	02:10:50.0	S	02:10:56.6
AN8	Pc	02:10:46.8		
AN9	Pc	02:10:44.1		
AN10	P	02:10:42.9		
AN11	P	02:10:44.6	S	02:10:47.6
IN1	P	02:11:02.0	S	02:11:15.9
IN4	P	02:10:59.7	S	02:11:14.3

***** 04 JANUARY 1989 - OHIO*****

O.T. =16:06:34.1 LAT=40.64#N LONG=84.26#W MAG=0.7 m_L

STA	PHASE	ARRIVAL TIME	PHASE	ARRIVAL TIME
AN1	eP	16:06:39.6		
AN7	eP	16:06:45.3		
AN8	eP	16:06:40.7		
AN9	eP	16:06:37.6		
AN10	eP	16:06:40.8		
AN12	eP	16:06:39.3		

***** 27 APRIL 1989 - MISSOURI *****

O.T. =16:47:50.8 LAT=36.02#N LONG=89.77#W MAG=4.4 m_d

(Location from St. Louis U.)

STA	PHASE	ARRIVAL TIME	PHASE	ARRIVAL TIME
AN1	eP	16:49:26		
AN3	eP	16:49:27.8		
AN7	eP	16:49:28		
AN8	eP	16:49:18.0		
AN9	eP	16:49:23.5		
AN12	eP	16:49:29		
IN1	eP	16:49:10.5		
IN2	eP	16:49:00		
IN3	eP	16:49:00		
IN4	eP	16:49:07.8		

***** 14 MAY 1989 - MISSOURI *****

O.T. =00:16:09.6 LAT=36.74#N LONG=89.71#W MAG=3.9 m_d

(Location from St. Louis U.)

STA	PHASE	ARRIVAL TIME	PHASE	ARRIVAL TIME
AN1	eP	00:17:50		
AN7	eP	00:17:42.3		
AN9	eP	00:17:50.5		
IN2	eP	00:17:11.5		
IN3	eP	00:17:13.5		

IN4 eP 00:17:21.5

***** 15 JULY 1989 - KENTUCKY*****

O.T. =08:01.78 LAT=38.70#N LONG=83.58#W MAG=3.1 m_{bLg}

DEP=7km (Location from U. of Kentucky)

STA	PHASE	ARRIVAL TIME	PHASE	ARRIVAL TIME
AN1	iP	00:08:34.3		
AN3	eP	00:08:34.6		
AN7	iP	00:08:39.2		
AN8	eP	00:08:34.2		
AN9	iP	00:08:38.8		
AN10	eP	00:08:35.2		
AN11	iP	00:08:37.8		
AN12	iP	00:08:40.8		
IN1	iP	00:08:43.7		
IN2	eP	00:08:47.0		
IN3	iP	00:08:33.2		
IN4	iP	00:08:25.2		

***** 24 JANUARY 1990- KENTUCKY *****

O.T. =18:20:26.6 LAT=38.10 N LONG=86.47 W MAG=4.0 m_b

Location from University of Kentucky

STA	PHASE	ARRIVAL TIME	PHASE	ARRIVAL TIME
AN1	eP	18:21:14.3	S	18:21:50
AN3			S	18:21:55
AN4	eP	18:21:13	S	18:21:52
AN7	eP	18:21:20	S	18:22:00
AN8	eP	18:21:10		
AN9			S	18:21:50
AN10	iP	18:21:10.5	S	18:21:45
AN11	eP	18:21:10	S	18:21:45
IN2	iP	18:20:57.8		
ACM	eP	18:21:33		

***** 30 JANUARY 1990- OHIO *****

O.T. =03:56:48 LAT=40.65 N LONG=84.31 W MAG=1.0 m_b

STA	PHASE	ARRIVAL TIME	PHASE	ARRIVAL TIME
AN1	iP	03:56:52.0	S	03:56:55.2
AN7	eP	03:56:54.8	S	03:57:00.0
AN8	iP	03:56:55.2		
AN9	iP	03:56:50.5	S	03:56:54.0
AN10	iP	03:56:51.9	S	03:56:54.7
AN11	iP	03:56:53.0	S	03:56:57.0
AN12	iP	03:56:53.0	S	03:56:56.9
IN1	iP	03:57:08.5	S	03:57:25.0
IN2	eP	03:57:22.2	S	03:57:50.5

***** 02 MARCH 1990 CLINTON, ILLINOIS *****
O.T. =07:01:16.8 LAT=38.90 N LONG=89.10 W MAG=3.4 $m_b L_g$
DEPTH=10 km (Location from NEIS)

STA	PHASE	ARRIVAL TIME	PHASE	ARRIVAL TIME
AN1	eP	07:02:53.3		
AN3	eP	07:02:57.5		
AN4	eP	07:03:02.6		
AN7	eP	07:02:58.3		
AN8	eP	07:02:50.7		
AN9	eP	07:02:47.2		
AN11	eP	07:02:47.9		
IN1	iP	07:02:36.6		
IN2	iP	07:02:25.4		
IN3	iP	07:02:32.6		
IN4	iP	07:02:41.5		

***** 09 MARCH 1990 KENTUCKY *****
O.T. =21:01:54.9 LAT=38.11 N LONG=86.44 W MAG=2.9 m_b
(Location from University of Kentucky)

STA	PHASE	ARRIVAL TIME	PHASE	ARRIVAL TIME
IN1	eP	21:02:38.1	S	21:03:11
IN3	eP	21:02:20.9	S	21:02:38.3
IN4	eP	21:02:30.8	S	21:02:56.8

***** 17 APRIL 1990 CELINA, OHIO *****
O.T.= 10:27:36.5 LAT=40.49 N LONG=84.83 W MAG=2.2 m_L

STA	PHASE	ARRIVAL TIME	PHASE	ARRIVAL TIME
AN1	iP	10:27:45.4		
AN3	eP	10:27:50.3	S	10:28:00.5
AN8	eP	10:27:44.7		
AN9	eP	10:27:42.3		
AN10	iP	10:27:41.0		
AN11	eP	10:27:38.7		
AN12	eP	10:27:48.1	S	10:27:57.6
IN1	eP	10:27:51.0		
IN3	eP	10:28:00.4	S	10:28:20.5
IN4	eP	10:27:52.0	S	10:28:04.8
ACM	eP	10:28:14.5		
BLO	iP	10:28:07.8	S	10:28:32.8

***** 04 JUNE 1990 FOSTORIA, OHIO *****
O.T.= 11:26:48.7 LAT=41.08 N LONG=83.51 W MAG= 2.3 m_L

STA	PHASE	ARRIVAL TIME	PHASE	ARRIVAL TIME
AN1	eP	11:27:00.0		
AN3	eP	11:26:58.7		
AN9	eP	11:27:02.0		
AN10	eP	11:27:11.0		
AN11	eP	11:27:09.0		
ACM	eP	11:27:29.0		
UTO	iP	11:26:58.3	S	11:27:05.1
FLKY	P	11:27:33.5	S	11:28:08.1
ROKY	P	11:27:41.8		
PKKY	P	11:27:34.4	S	11:28:11.3

***** 26 SEPTEMBER 1990 MISSOURI *****
O.T.= 13:18:51.3 LAT:37.17 N LONG=89.58 W MAG= 4.6 $m_b L_g$
(Location from NEIS)

STA	PHASE	ARRIVAL TIME	PHASE	ARRIVAL TIME
AN1	eP	13:20:11.0		
AN3	iP	13:20:14.0		
AN7	eP	13:20:15.3		
AN8	eP	13:20:07.1		
AN11	eP	13:20:07.6		
AN12	eP	13:20:14.1		
IN1	iP	13:19:46.5		
IN2	iP	13:19:46.9		
IN3	eP	13:19:47.3		

***** 4 OCTOBER 1990 ILLINOIS *****
O.T.= 08:20:04.3 LAT:38.31 N LONG=88.99 W MAG= 3.5 $m_b L_g$
(Location from NEIS)

STA	PHASE	ARRIVAL TIME	PHASE	ARRIVAL TIME
AN3	eP	08:21:14.5	S	08:22:25.0
IN1	iP	08:20:43.5	S	08:22:10.0
IN3	eP	08:20:57.5	S	08:21:21.9

***** 4 MAY 1991 MISSOURI *****
O.T.= 01:18:54.9 LAT:35.56 N LONG=89.82 W MAG= 5.0 $m_b L_g$
(Location from NEIS)

STA	PHASE	ARRIVAL TIME	PHASE	ARRIVAL TIME
AN1	eP	01:20:36.0	S	01:21:56.5
AN3	eP	01:20:30.0	S	01:22:00.0
AN4	eP	01:20:26.0	S	01:22:00.0

AN7	eP	01:20:27.0	S	01:22:10.0
AN8	eP	01:20:23.0		
AN10	e(p)	01:20:?0.0	S	01:21:55.0
AN11	iP	01:20:20.0	S	01:21:50.0
AN12	iP	01:20:27.5	S	01:22:08.5
IN1	iP	01:20:09.5	S	01:21:20.0
IN3	eP	01:20:01.0		

***** 17 DECEMBER 1990 INDIANA *****

O.T.= 05:24:59.12 LAT:40.125 N LONG=87.139 W MAG= 3.2 m_b

STA	PHASE	ARRIVAL TIME	PHASE	ARRIVAL TIME
AN1	iP	05:25:39.5		
AN3	iP	05:25:44.0		
AN7	iP	05:25:40.0		
AN9	iP	05:25:33.5		
AN10	iP	05:25:33.0		
AN12	iP	05:25:37.5		
IN1	iP	05:25:18.2		
IN3	iP	05:25:23.0	S	05:25:40.0
BLO	iP	05:25:18.2	S	05:25:31.3
WSIL	iP	05:25:36.9		
BPIL	iP	05:25:38.0		
NHIL	iP	05:25:01.0		
CSIL	iP	05:25:44.5		

***** 20 DECEMBER 1990 INDIANA *****

O.T.= 14:04:17.62 LAT:39.595 N LONG=86.642 W MAG= 3.6 $m_b L_g$

STA	PHASE	ARRIVAL TIME	PHASE	ARRIVAL TIME
AN1	iP	14:04:54.2		
AN3	iP	14:04:58.2		
AN7	iP	14:04:58.4		
AN8	iP	14:04:50.7		
AN10	iP	14:04:49.6		
AN12	iP	14:04:56.1		
IN1	iP	14:04:37.0		
IN3	iP	14:04:30.1		
BLO	iP	14:04:25.4	S	14:04:3[illegible].2
BPIL	iP	14:04:52.5		
NHIL	iP	14:04:52.5		
CSIL	iP	14:04:59.8		

***** 7 MARCH 1991 INDIANA*****

O.T.= 10:52:57.63 LAT:39.561 N LONG=86.415 W MAG= 0.6 m_d

STA	PHASE	ARRIVAL TIME	PHASE	ARRIVAL TIME
AN12	iP	10:53:34.2		
IN1	iP	10:53:16.2	S	10:53:30.5
IN3	iP	10:53:07.8	S	10:53:15.0

***** 24 JULY 1991 INDIANA *****

O.T.= 21:37:12.30 LAT:39.748 N LONG=84.587 W MAG= 1.0 m_d

STA	PHASE	ARRIVAL TIME	PHASE	ARRIVAL TIME
AN1	iP	21:37:26.5		
AN3	iP	21:37:30.0		
AN4	iP	21:37:24.7	S	21:37:33.9
AN7	iP	21:37:33.0		
AN8	iP	21:37:21.8	S	21:37:29.7
AN9	iP	21:37:29.1		
AN10	iP	21:37:24.8	S	21:37:35.1
AN11	iP	21:37:26.5	S	21:37:38.1
AN12	iP	21:37:33.4	S	21:37:49.4
BLO	iP	21:37:40.5	S	21:38:02.3
IN1	iP	21:37:33.8		
IN2	iP	21:37:41.1		
IN4	iP	21:37:18.0		

***** 11 NOVEMBER 1991 ILLINOIS *****

O.T.= 08:20:04.3 LAT:38.31 N LONG=88.99 W MAG= 3.8 $m_b L_g$

(Location from NEIS)

STA	PHASE	ARRIVAL TIME	PHASE	ARRIVAL TIME
AN7	iP	09:21:47.7	S	09:21:54.8
AN8	iP	09:21:42.4	S	09:21:49.5
AN9	iP	09:21:39.5	S	09:21:56.1

NRC FORM 335 (2-89) NRCM 1102, 3201, 3202

U.S. NUCLEAR REGULATORY COMMISSION

BIBLIOGRAPHIC DATA SHEET

(See instructions on the reverse)

1. REPORT NUMBER (Assigned by NRC, Add Vol., Supp., Rev., and Addendum Numbers, if any.)
NUREG/CR-3145,Vol. 10

2. TITLE AND SUBTITLE
Geophysical Investigations of the Western Ohio-Indiana Region
Final Report, October 1986-September 1992

3. DATE REPORT PUBLISHED
MONTH: February
YEAR: 1994

4. FIN OR GRANT NUMBER
D1695

5. AUTHOR(S)
L. Ruff, R. LaForge, R. Thorson, T. Wagner, F. Goudaen

6. TYPE OF REPORT
Final

7. PERIOD COVERED (Inclusive Dates)
Oct. 1986-Sept. 1992

8. PERFORMING ORGANIZATION – NAME AND ADDRESS (If NRC, provide Division, Office or Region, U.S. Nuclear Regulatory Commission, and mailing address; if contractor, provide name and mailing address.)
Department of Geological Sciences
The University of Michigan
Ann Arbor, MI 48109

9. SPONSORING ORGANIZATION – NAME AND ADDRESS (If NRC, type "Same as above"; if contractor, provide NRC Division, Office or Region, U.S. Nuclear Regulatory Commission, and mailing address.)
Division of Engineering
Office of Nuclear Regulatory Research
U.S. Nuclear Regulatory Commission
Washington, DC 20555 -0001

10. SUPPLEMENTARY NOTES

11. ABSTRACT (200 words or less)

Earthquake activity in the Western Ohio-Indiana region has been monitored with a seismograph network consisting of nine stations located in west-central Ohio and four stations located in Indiana. Six local and regional earthquakes have been recorded from October 1990 to September 1992 with magnitudes ranging from 0.6 to 5.0. A total of 36 local and regional earthquakes have been recorded in the past 6-year period (October 1986 to September 1992). Overall a total of 78 local and regional earthquakes have been recorded since the network went into operation in 1977. There was a peak in seismicity in 1986, including the July 12, 1986 St. Marys' event (mb=4.5), followed by an anomalously low level of seismicity for about 2 years. The most unusual feature of the seismicity in the past year is the occurrence of three earthquakes in Indiana. The locations of the felt earthquakes are scattered across central Indiana; an area that had been aseismic. Analysis of arrival time data accumulated over the past 14 years shows that the Anna region crustal structure is "slower" than the average mid-continent crustal structure. This implies that the proposed Keewenawan rift in the Anna region has a different structure than that of other Keewenawan rifts in the mid-continent.

12. KEY WORDS/DESCRIPTORS (List words or phrases that will assist researchers in locating the report.)
Anna, Ohio
Crustal Structure
Seismicity

13. AVAILABILITY STATEMENT
Unlimited

14. SECURITY CLASSIFICATION
(This Page)
Unclassified
(This Report)
Unclassified

15. NUMBER OF PAGES

16. PRICE

NRC FORM 335 (2-89)

Federal Recycling Program

UNITED STATES
NUCLEAR REGULATORY COMMISSION
WASHINGTON, D.C. 20555-0001

OFFICIAL BUSINESS
PENALTY FOR PRIVATE USE, $300

SPECIAL FOURTH-CLASS RATE
POSTAGE AND FEES PAID
USNRC
PERMIT NO. G-67